

Experimental evaluation and model development for analysis of pressure drop in the lungs
of children

by

Tyler James Paxman

A thesis submitted in partial fulfillment of the requirements for the degree of

Master of Science

Department of Mechanical Engineering
University of Alberta

© Tyler James Paxman, 2018

Abstract

Airway resistance describes the ratio between pressure drop and flow rate through the conducting respiratory airways. Analytical models of airway resistance for tracheobronchial airways have previously been developed and assessed without upper airways positioned upstream of the trachea. This work investigated pressure drop as a function of flow rate and gas properties for upper and central airway replicas of 10 child subjects, ages 4–8. Replica geometries were built based on computed tomography scan data and included airways from the nose through 3–5 distal branching airway generations. Pressure drop through the replicas was measured for constant inspiratory flows of air and heliox. For both the nose-throat and branching airways, the relationship between non-dimensional coefficient of friction, C_F , with Reynolds number, Re , was found to resemble the turbulent Blasius equation for pipe flow, where $C_F \propto Re^{-0.25}$. Additionally, pressure drop ratios between heliox and air were consistent with analytical predictions for turbulent flow. The presence of turbulence in the branching airways likely resulted from convection of turbulence produced upstream in the nose and throat. An airway resistance model based on the Blasius pipe friction correlation for turbulent flow was proposed for prediction of pressure drop through the branching bronchial airways downstream from the upper airway.

The modified-Blasius model was then incorporated into a model for estimating pressure drop across a single path through the tracheobronchial airways of children of ages 4 to 8. Analysis of model sensitivity to airway dimensions (age-related), flow rates (exertion level- and age-related) and gas properties was performed. To capture the convection and then dissipation of turbulence generated upstream in the nose-throat, the modified-Blasius model was used

for the first five tracheobronchial generations only, and the well-known Pedley model was used for more distal airway generations.

Gas properties had moderately larger impact on pressure drop at higher flow rates. The age-averaged pressure drop percent changes at tidal breathing (14 L/min) and heavy exertion (60 L/min), respectively, were -35% and -46% when changing air to He-O₂ (80/20), and 9.9% and 14% when changing air to N₂O-O₂ (50/50). He-O₂ (80/20) is shown to reduce pressure drop significantly whereas N₂O-O₂ (50/50) has less impact on pressure drop across the range of flow rates studied.

Single path tracheobronchial pressure drop results obtained using a combined model (with a transition generation of 6) were compared with usage of both pure models (modified-Blasius or Pedley). At typical tidal breathing flow rates (14 L/min), the combined model predicted higher values than either of the pure model cases when considering air and N₂O-O₂ (50/50), whereas similar values to those of the Pedley model were predicted for He-O₂ (80/20). At flow rates typical of heavy exertion (30–65 L/min), the combined model results were closest to the pure modified-Blasius model for air or N₂O-O₂ (50/50).

This combined pressure drop model incorporation of a modified-Blasius equation for analytical predictions in the first 5 generations of the conducting airways, in conjunction with the Pedley model in the more distal airways, provides an improvement for pressure drop prediction in the lungs of 4- to 8-year-old children.

Preface

This thesis contains some work that has been co-authored and submitted for publication as well as currently unpublished material. Chapter 2 was a co-authored manuscript (submitted for publication to Journal of Biomechanics, currently in review) for which I was the primary author. Co-author contributors were Dr. Michelle Noga, Warren Finlay and Andrew Martin. Printed replicas used in those experiments were derived from CT scan data provided by Dr. Noga, which were procured previously by Dr. Azadeh Borojeni. The process of converting CT scan geometries to physical replicas, as well as apparatus set-up were initialized by Fraser Bulbuc, which I later continued. I was responsible for building the experimental apparatus used to supply gases via nasal mask to the replicas. The analytical work in both Chapters 2 and 3 was completed chiefly in MATLAB using scripts created specifically for this work. Data on average branching airway dimensions used in the analytical predictions of Chapter 2 were prepared previously by Dr. Borojeni. The drafting of this manuscript was my responsibility, with significant editorial support, direction and contributions by Dr. Martin throughout the body of this thesis, as well as from the co-authors listed for Chapter 2.

For Jill, who makes it all worthwhile

Acknowledgements

I would like to express my gratitude to my exceptional supervisor, Dr. Andrew Martin, who gave me the opportunity to pursue graduate studies under his direction at the University of Alberta. It has been an absolute pleasure to research in his group and I have enjoyed the chance to constantly learn and discover new and interesting things. His extensive knowledge of respiratory mechanics, experimental techniques, scientific research, and a number of other areas has benefited me greatly and has made it possible for me to present this work. I also admire and appreciate his constant professionalism and consideration, which have made my graduate student experience enjoyable. I express my thanks to Dr. Warren Finlay for providing his guidance and extensive knowledge throughout the research process and for his contributions to this work.

I would also like to thank all those who assisted with the technical aspects of the experimental portion of this work. Dr. Michelle Noga, for not only providing the foundational CT scan data that made this research possible, but also taking time to help with the imaging of replicas, and to provide guidance on image processing. I am very thankful for Helena, who was eager to help with any problem I encountered along the way and would always recommend the perfect tool for the job. Her help with preparing the replicas was vital. Thanks to Fraser Bulbuc, for giving me a big head-start in terms of preparing replicas and laying the groundwork for the experimentation in this thesis and to everyone in the shop, including Tuula Hilvo, Marc Maccagno, and Roger Marchand, who and extended a helping hand whenever it was needed made the production process feel simple.

I am thankful for having a couple excellent lab-mates, Paul Moore and Kineshta Pillay, who have been good friends and have generously offered me advice, assistance, and even delicious food. I also appreciate our next-door neighbors, Milad, Scott, Conor, Alvin and John, who have been welcoming from the start, and have offered invaluable advice for a beginner in the world of graduate studies.

I am grateful for parents who have always preached the importance of education and who continually express interest in whatever area I find myself working. Thanks to my siblings, who ensure that life is never dull; I could not have picked a better family if I tried. Finally, I am especially grateful for my magnificent wife, Jill, for her unwavering support and infinite patience, especially throughout the process of preparing this work. Her encouragement and comfort have made all the difference. I am lucky to have her by my side.

This research was supported and funded by the Canadian Natural Sciences and Engineering Research Council (NSERC), and I express my thanks to them for providing means to accomplish the work.

Table of Contents

Abstract	ii
Preface	iv
Acknowledgements	vi
Table of Contents	viii
List of Tables	xi
List of Figures	xiii
Chapter 1:Introduction	1
1.1 Background.....	1
1.2 Objective	5
1.3 Thesis Structure	6
1.4 Chapter Citations	7
Chapter 2:Experimental evaluation of pressure drop for flows of air and heliox through upper and central conducting airway replicas of 4- to 8-year-old children	13
2.1 Introduction.....	13
2.2 Methods	15
2.2.1 Child airway replicas	15
2.2.2 Apparatus	18
2.2.3 Experimental procedure.....	19
2.2.4 Pressure drop dependence on Reynolds number	20
2.2.5 General analytical calculation of pressure drop.....	22
2.2.6 Analytical turbulent flow model determination	23
2.3 Results	25
2.3.1 Experimental pressure drop compared with Reynolds number.....	25
2.3.2 Analytical calculation of pressure drop and airway resistance.....	27
2.4 Discussion.....	29
2.4.1 Experimental pressure drop compared with Reynolds number.....	29
2.4.2 Analytical pressure drop prediction – Absolute values	34
2.5 Conclusions.....	35
2.6 Chapter Citations	35

Chapter 3:Application of pressure drop findings for development of a single path child airway model	39
3.1 Introduction.....	39
3.2 Methods	43
3.2.1 Single-path tracheobronchial airways model	43
3.2.2 Modelling of pediatric lung airway dimensions.....	45
3.2.3 Gas types and applications	46
3.2.4 Typical inhalation flow rates by age	47
3.2.5 Pressure drop models for flow regimes	49
3.2.6 Determining pressure drop sensitivity due to transition generation	52
3.2.7 Determination of turbulent-to-laminar transition generation.....	52
3.2.8 Entry length for laminar flow development	55
3.3 Results	56
3.3.1 Total tracheobronchial pressure drop as a function of transition generation ..	56
3.3.2 Laminar entry length comparison with airways length.....	60
3.3.3 Pressure drop calculations with selected transition generation, G_T	63
3.4 Discussion.....	67
3.4.1 Effects of inspiratory flow rate, gas type, and model transition generation on tracheobronchial pressure drop	67
3.4.2 Laminar entry length comparison with airway length	70
3.4.3 Relative impact of model transition generation and gas type.....	72
3.4.4 Pressure drop calculations with selected model transition generation	76
3.4.5 Tracheobronchial pressure drop relative to the upper airways	78
3.5 Conclusions.....	79
3.6 Chapter Citations	81
Chapter 4:Conclusions	87
4.1 Summary and Conclusions.....	87
4.2 Assumptions, Limitations and Future Work.....	89
4.3 Chapter Citations	91
Bibliography	94
Appendix – MATLAB Code	103
Chapter 2 Code.....	104

Main function	104
Experimental data.....	107
Analytical Data	108
Compute ideal coefficient for modified-Blasius equation.....	115
Chapter 3 Code.....	116
Import airway dimensions from Finlay et al. (2000).....	116
Calculate and tabulate pressure values for each flow rate, age, and gas type.....	117
Calls to plot each figure.....	120
General Sub-functions	124
Fluid flow and properties	124
Data manipulation	125
Data plotting	127

List of Tables

Table 2.1: Physical properties for each child subject.....	16
Table 2.2: Range of tracheal Reynolds numbers for each fluid and nominal flow rate	21
Table 2.3: β -Coefficient, α -exponent and R^2 values for each CF vs. Re plot.....	25
Table 2.4: Ideal C coefficient values for modified-Blasius equation described by Eq. (13)....	27
Table 2.5: Average pressure drop ratios of heliox vs. air for branching and nose-throat airways (calculated from ratios of fitted values, ranging from 5-45 L/min)	32
Table 3.1: Model dimensions of lung generations for 4-year-old, 8-year-old and adult geometries (reproduced from Finlay et al. (2000)).....	46
Table 3.2: Gas properties adapted from Katz et al. (2011a) where standard conditions are assumed (20°C, 1 atm).....	47
Table 3.3: Typical inspiratory flow rate approximations for children ages 4 and 8, calculated from age, height, breathing frequency, and tidal volume	48
Table 3.4: Inspiratory flow rates calculated based on minute volumes for ages 4 and 8 at various levels of activity (reproduced from Phalen et al. (1985)), and using a duty cycle of 0.435 (Finlay, 2001).....	49
Table 3.5: Contributions of viscosity and density to the pressure drop models, modified-Blasius and Pedley (described in Eqs. (27) and (28)), and their relative contributions compared with air.....	68
Table 3.6: Nominal inspiratory flow rate values at which total pressure drop from generation 0 to 23, calculated by the Pedley model, exceeds that of the modified-Blasius model.....	70

Table 3.7: Percent increase of total branching airways pressure drop comparing model switch generations (at constant flow rate of 14 L/min).....73

Table 3.8: Percent increase of total branching airways pressure drop comparing fluid types (at constant flow rate of 14 L/min and given a model transition generation of 6).....74

Table 3.9: Total branching airway single path pressure drop values at a constant flow rate of 14 L/min when using a purely Pedley model, a pure modified-Blasius model and a combination of both, with a transition to the Pedley model beginning at generation 6.....78

List of Figures

Figure 1.1: Schematic of human respiratory airways with corresponding generation classifications based on description given by Finlay (2001) 2

Figure 2.1: 3D-printed airway replicas of all child subjects (top row, left to right: subjects 2, 3, 5, 6, and 9; bottom row, left to right: subjects 10, 11, 12, 13, and 14).....17

Figure 2.2: Experimental apparatus schematic illustrating the measurement of pressure drop across child airway replicas19

Figure 2.3: Log-log plot of friction coefficient, CF , vs. Reynolds number, Re , for subject 10 in the (a) branching and (b) nose-throat airways. (Solid lines represent the best fit function indicated in the lower left corner of each plot. Error bars represent standard error. Where error bars are not visible the standard error is less than the size of the data symbol.)26

Figure 2.4: Branching airways pressure drop using the blasius equation vs. experimental pressure drop; (a) using an ideal C coefficient value for each subject measurements ($\rho c = 0.997$) and (b) using an average ideal C coefficient value ($\rho c = 0.909$)28

Figure 2.5: Pressure drop vs. flow rate for subject 10 in the (a) branching and (b) nose-throat airways with the pressure drop ratio for 5-45 L/min overlaid33

Figure 3.1: Reynolds number in each branch vs. generation number for (a) air, (b) He-O₂ (80/20), and (c) N₂O-O₂ (50/50), at ages 4 and 8 years old and flow rates of 5 and 20 L/min.54

Figure 3.2: Total single-path pressure drop (generations 0–23) vs. model transition generation (changing from the modified-Blasius to the Pedley et al. (1970) model) for ages and gas flow rates of (a) 4 years, 5 L/min, (b) 8 years, 5 L/min, (c) 4 years, 20 L/min, (d) 8 years, 20 L/min., (e) 4 years, 60 L/min, and (f) 8 years, 60 L/min, respectively58

Figure 3.3: Model transition generation (from modified-Blasius to Pedley) at which the maximum branching airway pressure drop occurs, as a function of nominal tracheal flow rate for ages (a) 4 and (b) 859

Figure 3.4: Ratio of length to laminar entry length at each airway generation for ages and flow rates of (a) 4 years and 5 L/min, (b) 8 years and 5 L/min, (c) 4 years and 15 L/min, (d) 8 years and 15 L/min, for air, He-O₂ (80/20), and N₂O-O₂ (50/50).....61

Figure 3.5: Generation of airway path where airway length, L , first exceeds laminar entry length, Le vs. flow rate for (a) 4-year-old and (b) 8-year-old models62

Figure 3.6: Total single-path pressure drop (generation 0–23) for low activity to light exertion (flow rates up to 20 L/min) for ages and gases (a) 4 years, air, (b) 8 years, air; (c) 4 years, He-O₂ (80/20); (d) 8 years, He-O₂ (80/20); (e) 4 years, N₂O-O₂ (50/50); and (f) 8 years, N₂O-O₂ (50/50), respectively. Total tracheobronchial pressure drops are calculated with a pure Pedley model, pure Modified-Blasius model, and a combination using Modified-Blasius before generation 6 and Pedley thereafter.....64

Figure 3.7: Total single-path pressure drop (generations 0–23) for light to heavy exertion level (flow rates 20–65 L/min) for ages and gases (a) 4 years, air; (b) 8 years, air; (c) 4 years, He-O₂ (80/20); (d) 8 years, He-O₂ (80/20); (e) 4 years, N₂O-O₂ (50/50); and (f) 8 years, N₂O-O₂ (50/50), respectively. Total tracheobronchial pressure drops are calculated with a pure Pedley model, pure Modified-Blasius model, and a combination using Modified-Blasius before generation 6 and Pedley thereafter.....65

Figure 3.8: Generational and cumulative tracheobronchial pressure drop (generations 0–23) for (a) age 4, air; (b) age 8, air; (c) age 4, He-O₂ (80/20); (d) age 8, He-O₂ (80/20); (e) age 4, N₂O-O₂ (50/50); (f) age 8, N₂O-O₂ (50/50 at a constant flow rate of 14 L/min66

Figure 3.9: Total tracheobronchial pressure drop percent increases vs. nominal inlet flow rate, compared between cases using (a) & (c) various gases for ages 4 and 8, respectively, and a constant transition generation of 6; (b) & (d) transition generations 10 and 6, for ages 4 and 8 respectively.75

Chapter 1: Introduction

1.1 Background

Respiratory disease is a prevalent issue among children. Diseases such as asthma, cystic fibrosis, and acute respiratory infections are widespread and problematic (Ferkol and Schraufnagel, 2014). The respiratory system (shown in Figure 1.1) comprises many structural segments beginning with the extrathoracic (upper) airways, passing through the larynx into the tracheobronchial region (lower airways), where the trachea conveys gas into multiple generations of branching bronchiolar airways and ultimately to the branching alveolar airways where gas exchange occurs (Finlay, 2001). An important quantity used for describing respiratory mechanics in the conducting airways (comprising both upper and lower airways) is airway resistance, the ratio between pressure drop and flow rate. Respiratory disease can cause imbalances in airway resistance between airways or lung regions, which can influence ventilation distribution and ultimately impact gas transport and exchange (Tgavalekos et al., 2007) and higher airway resistance can increase work of breathing in obstructive lung disease. Assessments of airway resistance play a role in diagnosing, as well as evaluating progression and treatment of such diseases; thus, development of appropriate airway resistance models is a useful tool in these applications.

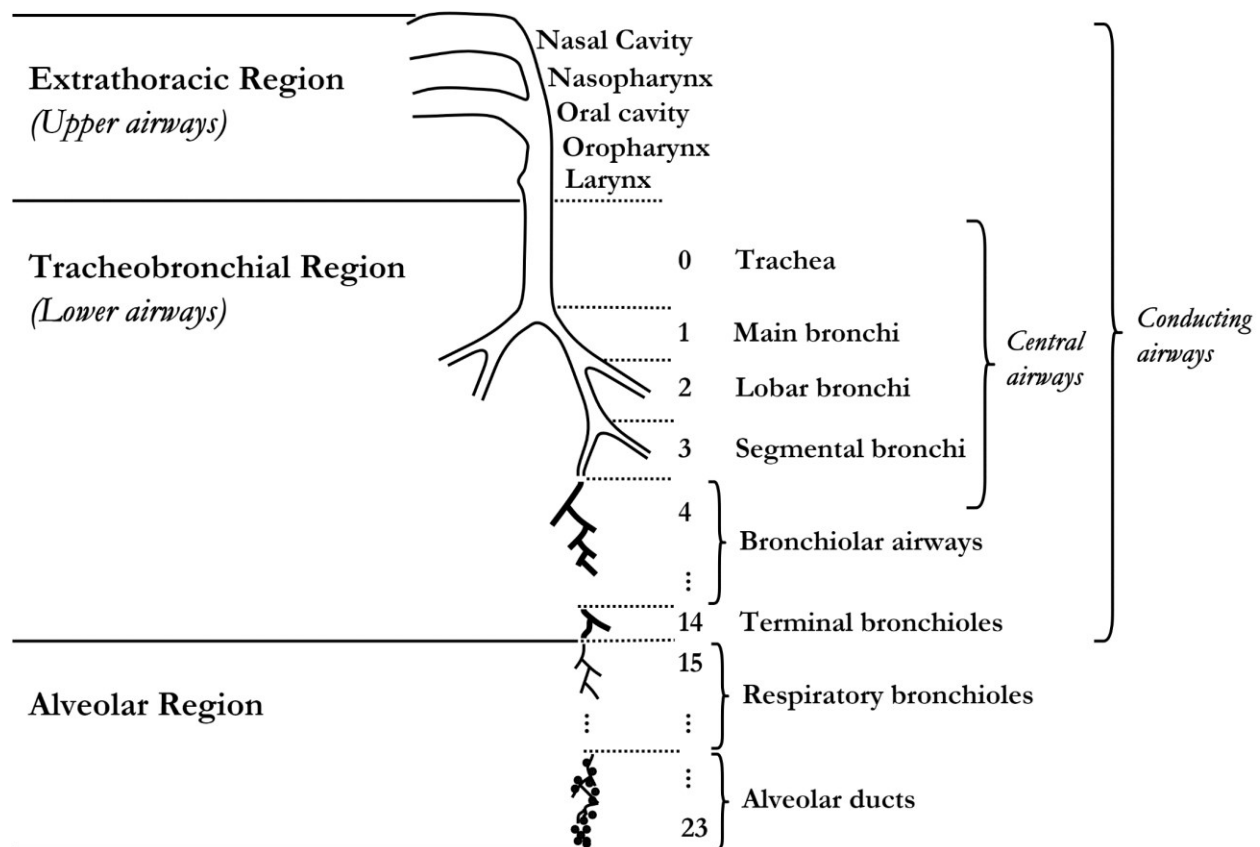


Figure 1.1: Schematic of human respiratory airways with corresponding generation classifications based on description given by Finlay (2001)

Analytical airway resistance models have been proposed for prediction of pressure distribution (Gemci et al., 2008; Katz et al., 2012; Katz et al., 2011b; Litwin et al., 2017), assessment of ventilation distribution effects (Pozin et al., 2017; Swan et al., 2012; Wongviriyawong et al., 2012), and prediction of alveolar pressure with mechanical ventilation (Damanhuri et al., 2014). Additionally, analytical airway resistance models have been proposed for predicting pressure drop due to viscous energy dissipation in the bifurcating airways as a function of airway dimensions, gas properties, and flow rate. Pedley et al. (1970) proposed a model using a correction to the Hagen-Poiseuille equation and later van Ertbruggen et al. (2005) proposed modified coefficients for the Pedley et al. (1970) equation,

based on pressure drop simulations of an adult tracheobronchial airway tree. Borojeni et al. (2015) compared predictions of these models to pressure drop measured experimentally through adult and child conducting airway replicas and found that the van Ertbruggen et al. (2005) model predictions were in reasonable agreement with measurements for adults, while for children, the original Pedley model most closely matched (although under-predicted) experimental pressure drop measurements. However, neither model was optimized for children, as previous airway resistance modelling has largely focused on adults. Another limitation of the work done by Pedley et al. (1970), van Ertbruggen et al. (2005) and Borojeni et al. (2015) is the omission of an upper airway. These models assume that flows in the branching airways are non-turbulent (i.e. disturbed laminar flow). However, computational studies have shown that turbulence generated in the upper airway can influence flow patterns in the trachea and bronchi (Calmet et al., 2016; Koullapis et al., 2018; Lin et al., 2007; Xi et al., 2008). The constriction of the larynx produces the “laryngeal jet,” which generates turbulent flow patterns in the trachea (Martonen et al., 1993). This raises a question of whether existing airway resistance models are suitable for pressure drop prediction in conducting airways of children when a realistic upper airway is present upstream.

Airway pressure drop modelling is expected to depend primarily on airway dimensions (a function of age), fluid density and viscosity (dependent on gas type) and flow rates (related to both activity level and age), such as shown in the (Pedley et al., 1970) model. Because airways increase in size with age and at different rates dependent on lung region, accurate lung dimensions for young children cannot be derived simply by direct uniform scaling of adult models (Hofmann et al., 1989; Reid, 1977). More suitable scaling practices were demonstrated by Finlay et al. (2000) who used a combination of models from Phillips et al.

(1994) and Haefeli-Bleuer and Weibel (1988) and then scaled them with methods described by Hofmann et al. (1989) for children 4 and 8 years old. There are various gases employed in pediatric medical applications which warrant inclusion in airway resistance modelling. For example, a mixture of 80% helium and 20% oxygen—i.e. He-O₂ (80/20) or “Heliox”—has been shown to lessen resistance in branching airways largely due to its low density in comparison with air (Valli et al., 2016). It has shown potential for lessening work of breathing for certain asthmatic patients (Pozin et al., 2017) and assisting with inhaled pharmaceuticals by facilitating delivery to more distal airways (Darquenne and Prisk, 2004). Other experiments indicate beneficial use of He-O₂ (80/20) in pediatric treatments (Frazier and Cheifetz, 2010) such as upper airway obstructions (Duncan, 1979), infant bronchiolitis (Cambonie et al., 2006), work of breathing assistance for asthmatics (Kudukis et al., 1997) and drug delivery given severe lower airway obstructions (Piva et al., 2002). Another medical gas in use is a 50% nitrous oxide and 50% oxygen mixture—i.e. N₂O-O₂ (50/50), “Entonox” (Praxair, Inc.), or Kalinox (Air Liquide)—which has been used effectively as a pediatric analgesic (Faddy and Garlick, 2005; Lyratzopoulos and Blain, 2003; Pedersen et al., 2013) and an anxiety-reducing sedative in pediatric dentistry (Holroyd, 2008). It has been recommended that its use should be avoided when asthma or airway obstructions are present (Douglas et al., 1974) and is contraindicated in cases of severe asthma (Agah et al., 2014), indicating the importance of considering its airway resistance effects.

Proper modelling of pressure drop across a single path (from the trachea to an alveolar sac) requires assumptions about how far turbulent flow is expected to propagate into the branching airways, which is uncertain. Although certain models assume that turbulence in any given generation is governed purely by its local Reynolds number, and take $Re > 2000$ to be the criterion for turbulence (Gouinaud et al., 2015; Katz et al., 2011b), it has been

suggested that this criterion alone does not fully characterize flow regimes in branching airways and has been experimentally observed to be much less where upper airways are present (Cohen et al., 1993; Dekker, 1961). Unstable flows extending up until the segmental bronchi have been predicted and observed (Olson et al., 1973; Owen, 1969). Airway length relative to laminar entry length has also been shown to have an impact on flow regime at lower Reynolds numbers (Cohen et al., 1993; Olson et al., 1970). In general, previous work in this regard has indicated that appropriate modelling of airway resistance in children will require knowledge of how far into the branching airways turbulent flow may extend, as well as an understanding of the pressure drop resulting from various fluids, inlet flow rates, and airway dimensions. An investigation of the appropriate parameters for such a model is done in this thesis.

1.2 Objective

The central focus of this work is to add to the current literature on airway resistance modelling to develop more accurate ways to predict pressure drop in the lungs of children. One objective was to build on the work of Borojeni et al. (2015) to address the question of how the addition of an upper airway would influence pressure drop in the branching airways. By measuring pressure drop across the upper and central airways of 10 replicas of children, ages 4 to 8, with both air and heliox, a functional form of an appropriate pressure drop model could be determined. Comparisons of Reynolds number and a dimensionless friction factor were done to obtain insight into the functional form. It will be shown that the central airway replicas exhibited behavior described best by a modified form of the turbulent Blasius formulation, rather than the Pedley model.

The second objective of this thesis was to develop a model to describe pressure drop across a single path in the tracheobronchial airways of children of ages 4 to 8, by incorporating the modified-Blasius pressure drop formulation obtained from the first objective. The developed model was then used to make predictions for various ages, flow rates and gases. This involved firstly an investigation of the effects of airway dimensions (a function of age), inhalation flow rates (a function of exertion level and age) and gas properties on the total tracheobronchial pressure drop. Secondly, this required a determination of the generation where a transition from a modified-Blasius model to the Pedley et al. (1970) model should occur to capture the dissipation of the turbulent flow patterns generated upstream in the nose-throat, which are assumed to dissipate to a laminar flow pattern in the more distal generations.

The overall intent is to further the development of airway resistance models for children, and more accurately describe pressure drop in the conducting airways. It is intended that the results will provide valuable information for modelling pressure drop in the lungs of children, thereby aiding in prediction and understanding of the impact of age, gas type, and inspiratory flow rates on airway resistance.

1.3 Thesis Structure

The content of this thesis is presented in four chapters, where this initial chapter describes background details about the motivation of the research topic and the main objectives of the work. Chapter 2 is a description of experimental pressure drop measurements done with upper and central airway replicas of children, ages 4 to 8. Pressure drop was recorded for in vitro experiments with 3-D printed replicas of child replicas from the nose to the 5th branching generation, on average. Using both air and heliox, these experiments provided a means to

investigate the functional behavior of pressure drop in the lungs for future modelling. Chapter 3 describes the investigation of total tracheobronchial pressure drop across an entire single path of a simplified airway. It includes an analytical analysis of the effects of various airway dimensions, gas types, and inspiratory flow rates on pressure drop. It also discusses which airway generations for which the model proposed in the previous chapter would be most applicable. Chapter 4 is a summary of the main findings and describes potential research topics for future work in this area.

1.4 Chapter Citations

Agah, J., Baghani, R., Tali, S., Hossein, S., & Tabarraei, Y. (2014). Effects of continuous use of Entonox in comparison with intermittent method on obstetric outcomes: a randomized clinical trial. *Journal of pregnancy*, 2014.

Borojeni, A. A., Noga, M. L., Martin, A. R., & Finlay, W. H. (2015). Validation of airway resistance models for predicting pressure loss through anatomically realistic conducting airway replicas of adults and children. *Journal of Biomechanics*, 48(10), 1988-1996. doi:10.1016/j.jbiomech.2015.03.035

Calmet, H., Gambaruto, A. M., Bates, A. J., Vázquez, M., Houzeaux, G., & Doorly, D. J. (2016). Large-scale CFD simulations of the transitional and turbulent regime for the large human airways during rapid inhalation. *Computers in Biology and Medicine*, 69, 166-180. doi:<https://doi.org/10.1016/j.compbimed.2015.12.003>

Cambonie, G., Milési, C., Fournier-Favre, S., Counil, F., Jaber, S., Picaud, J.-C., & Matecki, S. (2006). Clinical effects of heliox administration for acute bronchiolitis in young infants. *Chest*, 129(3), 676-682.

- Cohen, B. S., Sussman, R. G., & Lippmann, M. (1993). Factors affecting distribution of airflow in a human tracheobronchial cast. *Respiration Physiology*, *93*(3), 261-278. doi:[https://doi.org/10.1016/0034-5687\(93\)90073-J](https://doi.org/10.1016/0034-5687(93)90073-J)
- Damanhuri, N. S., Docherty, P. D., Chiew, Y. S., van Drunen, E. J., Desai, T., & Chase, J. G. (2014). A patient-specific airway branching model for mechanically ventilated patients. *Computational and mathematical methods in medicine*, *2014*.
- Darquenne, C., & Prisk, G. K. (2004). Aerosol deposition in the human respiratory tract breathing air and 80: 20 heliox. *Journal of Aerosol Medicine*, *17*(3), 278-285.
- Dekker, E. (1961). Transition between laminar and turbulent flow in human trachea. *Journal of Applied Physiology*, *16*(6), 1060-1064.
- Douglas, R. B., Brown, P., Knight, K., Mills, G., & Wilson, G. (1974). Letter: Effects of entonox on respiratory function. *British Medical Journal*, *2*(5913), 277-277.
- Duncan, P. G. (1979). Efficacy of helium — oxygen mixtures in the management of severe viral and post-intubation croup. *Canadian Anaesthetists' Society Journal*, *26*(3), 206-212. doi:10.1007/bf03006983
- Faddy, S. C., & Garlick, S. R. (2005). A systematic review of the safety of analgesia with 50% nitrous oxide: can lay responders use analgesic gases in the prehospital setting? *Emergency Medicine Journal*, *22*(12), 901.
- Ferkol, T., & Schraufnagel, D. (2014). The Global Burden of Respiratory Disease. *Annals of the American Thoracic Society*, *11*(3), 404-406. doi:10.1513/AnnalsATS.201311-405PS
- Finlay, W. H. (2001). *The Mechanics of Inhaled Pharmaceutical Aerosols*.
- Finlay, W. H., Lange, C. F., King, M., & Speert, D. P. (2000). Lung delivery of aerosolized dextran. *Am J Respir Crit Care Med*, *161*(1), 91-97. doi:10.1164/ajrccm.161.1.9812094

- Frazier, M. D., & Cheifetz, I. M. (2010). The Role of Heliox in Paediatric Respiratory Disease. *Paediatric Respiratory Reviews*, *11*(1), 46-53. doi:10.1016/j.prrv.2009.10.008
- Gemci, T., Ponyavin, V., Chen, Y., Chen, H., & Collins, R. (2008). Computational model of airflow in upper 17 generations of human respiratory tract. *Journal of Biomechanics*, *41*(9), 2047-2054. doi:10.1016/j.jbiomech.2007.12.019
- Gouinaud, L., Katz, I., Martin, A., Hazebroucq, J., Texereau, J., & Caillibotte, G. (2015). Inhalation pressure distributions for medical gas mixtures calculated in an infant airway morphology model. *Computer Methods in Biomechanics and Biomedical Engineering*, *18*(12), 1358-1366. doi:10.1080/10255842.2014.903932
- Haefeli-Bleuer, B., & Weibel, E. R. (1988). Morphometry of the human pulmonary acinus. *The Anatomical Record*, *220*(4), 401-414.
- Hofmann, W., Martonen, T., & Graham, R. (1989). Predicted deposition of nonhygroscopic aerosols in the human lung as a function of subject age. *Journal of Aerosol Medicine*, *2*(1), 49-68.
- Holroyd, I. (2008). Conscious sedation in pediatric dentistry. A short review of the current UK guidelines and the technique of inhalational sedation with nitrous oxide. *Pediatric anesthesia*, *18*(1), 13-17.
- Katz, I. M., Martin, A. R., Feng, C.-H., Majoral, C., Caillibotte, G., Marx, T., . . . Daviet, C. (2012). Airway pressure distribution during xenon anesthesia: the insufflation phase at constant flow (volume controlled mode). *Appl Cardiopulm Pathophysiol*, *16*(5).
- Katz, I. M., Martin, A. R., Muller, P. A., Terzibachi, K., Feng, C. H., Caillibotte, G., . . . Texereau, J. (2011b). The ventilation distribution of helium-oxygen mixtures and the role of inertial losses in the presence of heterogeneous airway obstructions. *Journal of Biomechanics*, *44*(6), 1137-1143. doi:10.1016/j.jbiomech.2011.01.022

- Koullapis, P. G., Nicolaou, L., & Kassinos, S. C. (2018). In silico assessment of mouth-throat effects on regional deposition in the upper tracheobronchial airways. *Journal of Aerosol Science*, *117*, 164-188. doi:10.1016/j.jaerosci.2017.12.001
- Kudukis, T. M., Manthous, C. A., Schmidt, G. A., Hall, J. B., & Wylam, M. E. (1997). Inhaled helium-oxygen revisited: effect of inhaled helium-oxygen during the treatment of status asthmaticus in children. *The Journal of pediatrics*, *130*(2), 217-224.
- Lin, C.-L., Tawhai, M. H., McLennan, G., & Hoffman, E. A. (2007). Characteristics of the turbulent laryngeal jet and its effect on airflow in the human intra-thoracic airways. *Respiratory physiology & neurobiology*, *157*(2), 295-309.
- Litwin, P. D., Reis Dib, A. L., Chen, J., Noga, M., Finlay, W. H., & Martin, A. R. (2017). Theoretical and experimental evaluation of the effects of an argon gas mixture on the pressure drop through adult tracheobronchial airway replicas. *Journal of Biomechanics*, *58*, 217-221. doi:<https://doi.org/10.1016/j.jbiomech.2017.04.002>
- Lyratzopoulos, G., & Blain, K. (2003). Inhalation sedation with nitrous oxide as an alternative to dental general anaesthesia for children. *Journal of Public Health*, *25*(4), 303-312.
- Martonen, T. B., Zhang, Z., & Lessmann, R. C. (1993). Fluid Dynamics of the Human Larynx and Upper Tracheobronchial Airways. *Aerosol Science and Technology*, *19*(2), 133-156. doi:10.1080/02786829308959627
- Olson, D. E., Dart, G. A., & Filley, G. F. (1970). Pressure drop and fluid flow regime of air inspired into the human lung. *Journal of Applied Physiology*, *28*(4), 482-494. doi:10.1152/jappl.1970.28.4.482
- Olson, D. E., Sudlow, M. F., Horsfield, K., & Filley, G. F. (1973). Convective patterns of flow during inspiration. *Archives of internal medicine*, *131*(1), 51-57.

- Owen, P. (1969). Turbulent flow and particle deposition in the trachea. *Circulatory and Respiratory Mass Transport*, 236-252.
- Pedersen, R. S., Bayat, A., Steen, N. P., & Jacobsson, M.-L. B. (2013). Nitrous oxide provides safe and effective analgesia for minor paediatric procedures—a systematic review. *children*, 9, 11.
- Pedley, T. J., Schroter, R. C., & Sudlow, M. F. (1970). Energy losses and pressure drop in models of human airways. *Respiration Physiology*, 9(October 1969), 371-386. doi:10.1016/0034-5687(70)90093-9
- Phillips, C. G., Kaye, S. R., & Schroter, R. C. (1994). A diameter-based reconstruction of the branching pattern of the human bronchial tree Part I. Description and application. *Respiration Physiology*, 98(2), 193-217. doi:[https://doi.org/10.1016/0034-5687\(94\)00042-5](https://doi.org/10.1016/0034-5687(94)00042-5)
- Piva, J. P., Barreto, S. S. M., Zelmanovitz, F., Amantéa, S., & Cox, P. (2002). Heliox versus oxygen for nebulized aerosol therapy in children with lower airway obstruction. *Pediatric Critical Care Medicine*, 3(1), 6-10.
- Pozin, N., Montesantos, S., Katz, I., Pichelin, M., Grandmont, C., & Vignon-Clementel, I. (2017). Calculated ventilation and effort distribution as a measure of respiratory disease and Heliox effectiveness. *J Biomech*, 60, 100-109. doi:10.1016/j.jbiomech.2017.06.009
- Reid, L. (1977). 1976 Edward BD Neuhauser lecture: the lung: growth and remodeling in health and disease. *American Journal of Roentgenology*, 129(5), 777-788.
- Swan, A. J., Clark, A. R., & Tawhai, M. H. (2012). A computational model of the topographic distribution of ventilation in healthy human lungs. *Journal of Theoretical Biology*, 300, 222-231.

- Tgavalekos, N. T., Musch, G., Harris, R., Melo, M. V., Winkler, T., Schroeder, T., . . . Venegas, J. (2007). Relationship between airway narrowing, patchy ventilation and lung mechanics in asthmatics. *European Respiratory Journal*, *29*(6), 1174-1181.
- Valli, G., Paoletti, P., Savi, D., Martolini, D., & Palange, P. (2016). Clinical use of Heliox in asthma and COPD. *Monaldi archives for chest disease*, *67*(3).
- van Ertbruggen, C., Hirsch, C., & Paiva, M. (2005). Anatomically based three-dimensional model of airways to simulate flow and particle transport using computational fluid dynamics. *J. Appl. Physiol.*, *98*(3), 970-980. doi:10.1152/jappphysiol.00795.2004.
- Wongviriyawong, C., Harris, R. S., Greenblatt, E., Winkler, T., & Venegas, J. G. (2012). Peripheral resistance: a link between global airflow obstruction and regional ventilation distribution. *Journal of Applied Physiology*, *114*(4), 504-514.
- Xi, J., Longest, P. W., & Martonen, T. B. (2008). Effects of the laryngeal jet on nano-and microparticle transport and deposition in an approximate model of the upper tracheobronchial airways. *Journal of Applied Physiology*, *104*(6), 1761-1777.

Chapter 2: Experimental evaluation of pressure drop for flows of air and heliox through upper and central conducting airway replicas of 4- to 8-year-old children

A version of this chapter has been submitted for publication to Journal of Biomechanics (currently in review).

2.1 Introduction

Airway resistance, the ratio between pressure drop and flow rate through the conducting airways, is an important quantity used in describing respiratory mechanics. Assessment of airway resistance is used in diagnosis of respiratory diseases, and in evaluation of their progression and treatment. Increased airway resistance contributes to increased work of breathing in obstructive lung disease. Variation in airway resistance between airways or lung regions can influence ventilation distribution, which in turn affects regional gas transport and exchange (Tgavalekos et al., 2007). Analytical models of airway resistance have been used to predict the pressure distribution through the conducting airways as a function of flow rate and gas properties (Gemci et al., 2008; Katz et al., 2012; Katz et al., 2011b; Litwin et al., 2017), to assess the contribution of heterogeneous airway resistance to ventilation distribution (Pozin et al., 2017; Swan et al., 2012; Wongviriyawong et al., 2012), and to optimize algorithms predicting alveolar pressure during mechanical ventilation (Damanhuri et al., 2014).

Development and validation of analytical airway resistance models has focused primarily on adults. Pedley et al. (1970) proposed a correction to the Hagen-Poiseuille equation to estimate pressure drop due to viscous energy dissipation through bifurcating airways as a function of airway dimensions, gas properties, and flow rate. van Ertbruggen et al. (2005) simulated pressure drop through an adult tracheobronchial airway tree, and proposed modified coefficients for the Pedley et al. (1970) equation. Recent work was done by Borojeni et al. (2015) to compare predictions of these models to pressure drop measured experimentally through adult and child conducting airway replicas. Borojeni et al. (2015) found the predictions of the van Ertbruggen et al. (2005) model were in reasonable agreement with measurements for adults, while for children, the original Pedley model most closely matched experimental data, though with a tendency to under predict measured pressure drop.

A limitation of the experiments done by Borojeni et al. (2015), and in the work of Pedley et al. (1970) and van Ertbruggen et al. (2005), is the omission of an upper airway upstream from the trachea. In computational studies, turbulence generated in the upper airway has been observed to influence flow patterns in the trachea and bronchi (Calmet et al., 2016; Koullapis et al., 2018; Lin et al., 2007; Xi et al., 2008). The suitability of existing airway resistance models for predicting pressure drop through conducting airways downstream from realistic upper airways is therefore not known.

In the work reported here, pressure drop was measured for varying gas flow rates through realistic conducting airway replicas that included the nose-throat airway, trachea, and bronchial airways terminating, on average, between generations 3 and 5. Replicas were based on computed tomography (CT) scans of 10 child subjects, between 4- and 8-years old.

Experiments were conducted with both air and a helium/oxygen mixture (heliox). A dimensionless friction coefficient (Slutsky et al., 1980) was analysed as a function of tracheal Reynolds number to investigate the functional form of the pressure drop behaviour through the tracheobronchial airways. An airway resistance model based on the Blasius pipe friction correlation (White, 2016) is proposed for prediction of pressure drop through the bifurcating bronchial airways downstream from the upper airway.

2.2 Methods

2.2.1 Child airway replicas

The airway replicas were created from CT scan data of the same 10 child subjects studied by Borojeni et al. (2015). The details of the extraction of data from the CT scans to create 3D model (STL) files are described in previous work (Borojeni et al., 2014). In the present work, new models were built from the same CT scan source data for 10 child subjects, with the upper airway of the nose and throat included. Demographic and geometric data are listed in Table 2.1.

Table 2.1: Physical properties for each child subject

Subject Number	Tracheal Length (mm)	Tracheal Diameter (mm)	Age	Sex	Height (m)	Weight (kg)
2	62	7.1	5	M	1.17	22.9
3	66	8.0	5	M	1.12	20.0
5	56	8.0	6	F	1.12	18.0
6	59	8.5	6	F	1.18	21.5
9	60	7.6	5	M	1.13	20.0
10	52	7.2	4	F	0.99	16.0
11	64	10	8	M	1.25	24.5
12	74	7.4	6	F	1.24	24.0
13	63	9.8	7	F	1.21	20.0
14	59	7.2	4	F	1.00	16.0

The replicas were produced with a 3D printer (Objet Eden 350V, Stratasys Ltd., MN, USA), using a rigid opaque photopolymer material (VeroGray, Stratasys Ltd., MN, USA). The printing of each replica was done in three parts, where the top and middle pieces comprised the airways from the nasal inlet to the end of the trachea, and the bottom piece consisted of all branching airways (up to an average of 3–5 generations, depending on the subject replica). These three pieces were fastened to create a single airway geometry. This modular printing facilitated removal of support material after printing, and allowed for measurements with the bottom branching airways either attached or detached.

After printing, support material was removed manually, assisted by using a sonic bath. To verify that the support material was removed from the internal airways, the printed models were scanned using CT (SOMATOM Definition Flash CT Scanner, Siemens, Munich, Germany), converted to a 3D model, and then compared with original 3D models using CAD software (3-matic, Materialise, Leuven, Belgium). It was concluded that negligible amounts

of support material remained in the main air passages of the replicas. Support material did remain in the sinus cavities; however, this was assumed to have no influence on airflow through the replicas. The printed replicas are shown in Figure 2.1.

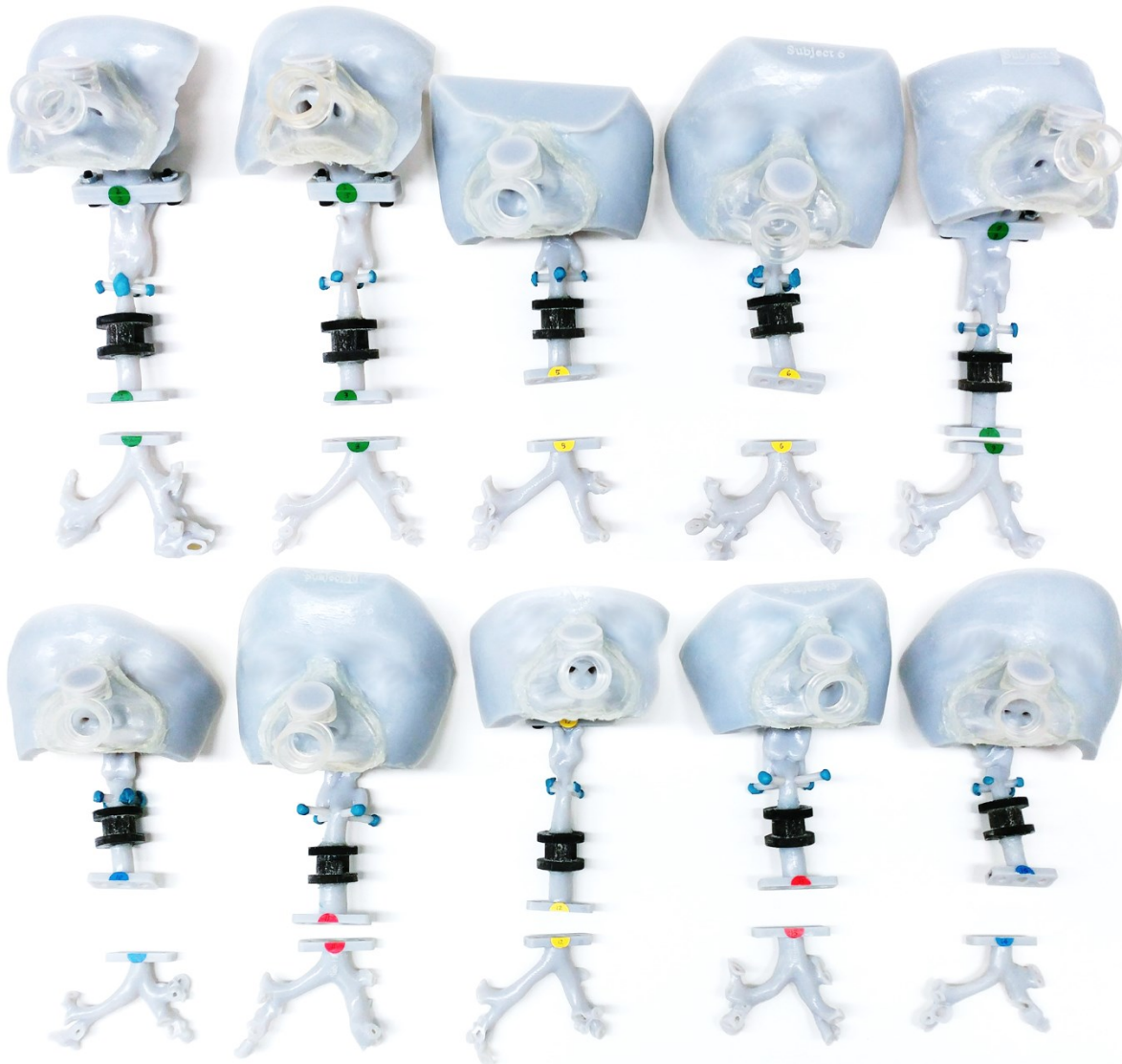


Figure 2.1: 3D-printed airway replicas of all child subjects (top row, left to right: subjects 2, 3, 5, 6, and 9; bottom row, left to right: subjects 10, 11, 12, 13, and 14)

2.2.2 Apparatus

A rotary vane vacuum pump (Gast Model 0523, Gast Manufacturing, MI, USA) was used to draw unidirectional airflow through the replica, with a needle valve and mass flow meter (TSI Model 4043; TSI; MN, USA) used to set the flow rate. A cylindrical plastic chamber housed the airway replica. For each test, the airway replica was placed in the chamber, suspended and sealed midway around the trachea, such that branching airways were contained within the sealed chamber, with the nasal inlet outside the chamber.

Both room air and heliox (80/20 helium/oxygen mixture, by volume) were used in the experimental procedure. Each replica was fitted with a mask (Infant Pocket Mask, nSpire Health Inc., CO, USA) sealed to the face with silicone, as visible in Figure 2.1. For heliox, a Douglas Bag (1196 Series, VacuMed, CA, USA) was filled from a compressed cylinder and connected to the mask via large-bore tubing. For air, the mask was left open to the room air. Preliminary tests drawing air from the room versus the Douglas bag produced indistinguishable results. Pressure drop across the replicas was measured using a digital manometer (HHP-103, Omega Engineering, CT, USA). A schematic of the experimental apparatus is shown in Figure 2.2.

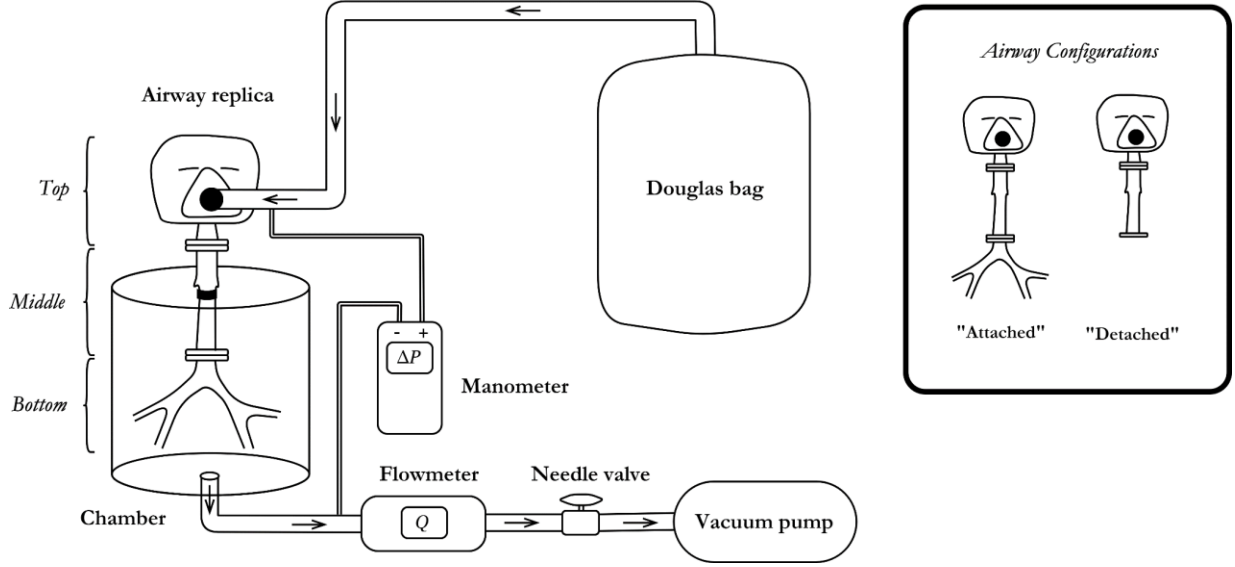


Figure 2.2: Experimental apparatus schematic illustrating the measurement of pressure drop across child airway replicas

2.2.3 Experimental procedure

After installing a replica into the chamber, pressure drop (ΔP) was recorded for standard flow rates of 5, 10, 15, and 30 L/min for air, and 7, 14, 23, and 46 L/min for heliox. This was repeated for each replica, in two configurations: with the branching airway segment (bottom) either attached or detached (yielding ΔP_{attach} and ΔP_{detach} , respectively). These two measurements were used to obtain values for the pressure drop over the branching and nose-throat airways ($\Delta P_{Branches}$ and ΔP_{NT} , respectively), using the following formulae:

$$\Delta P_{NT} = \Delta P_{detach} - \Delta P_{SE} - \Delta P_{open} \quad (1)$$

$$\Delta P_{Branches} = \Delta P_{attach} - \Delta P_{detach} + \Delta P_{SE} \quad (2)$$

ΔP_{SE} is the sudden expansion pressure loss, which accounts for the losses occurring when the gas exits the trachea and expands into the plenum when in the detached-configuration:

$$\Delta P_{SE} = \frac{1}{2} \rho K_{SE} v_{exit}^2 \quad (3)$$

where v_{exit} is the velocity at the exit, and K_{SE} is the sudden expansion coefficient—set as 1 in all cases. ΔP_{open} is the pressure drop recorded across the chamber in the absence of any replica, and accounts for the losses in the short outlet connection between the chamber and pressure tap. Measurements were made in triplicate for each unique experimental arrangement (i.e. for a given flow rate, gas type, and replica configuration).

2.2.4 Pressure drop dependence on Reynolds number

The Reynolds number was defined using tracheal diameter as follows:

$$Re = \frac{\rho v d_{trachea}}{\mu} = \frac{4\rho Q}{\pi \mu d_{trachea}} \quad (4)$$

where μ and ρ are the fluid viscosity and density, respectively, $d_{trachea}$ is the tracheal diameter, and v and Q are fluid velocity and flow rate, respectively. The maximum, minimum, and mean Reynolds numbers for the ten subjects are listed in Table 2.2 for each fluid and flow rate.

Table 2.2: Range of tracheal Reynolds numbers for each fluid and nominal flow rate

	Nominal Q (L/min)	Re_{max}	Re_{min}	Re_{mean}
Air	5	998	671	882
	10	1995	1343	1764
	15	2992	2012	2646
	30	5988	4021	5262
Heliox	7	386	259	341
	14	810	544	716
	23	1276	859	1129
	46	2547	1711	2251

The non-dimensional coefficient of friction (C_F) defined by Slutsky et al. (1980) is:

$$C_F = \frac{\Delta P}{1/2 \rho (Q^2/A^2)} \quad (5)$$

where ΔP is the pressure drop across the branching airways and A is the tracheal cross-sectional area. This friction coefficient may be related to Reynolds number using an alternate form of the Weisbach equation (White, 2016):

$$C_F = \beta Re^{-\alpha} \quad (6)$$

where α depends on the flow regime and β is some constant related to the airway geometry. From the definition of the Darcy friction factor, it follows that $\alpha = 1$ signifies laminar Poiseuille flow, while $\alpha = 0.25$ denotes turbulent flow, based on the Blasius turbulent equation (Blasius, 1911). By taking the log of Eq. (6), α can be readily extracted from the slope of the line of best fit in the resultant expression:

$$\log(C_F) = \log(\beta) - \alpha \log(Re) \quad (7)$$

2.2.5 General analytical calculation of pressure drop

An iterative procedure for the calculation of pressure drop in a bifurcating network was adapted from Borojeni et al. (2015). For the calculation, a resistance ratio incorporating pressure drop, fluid density, and the square of flow rate through an individual airway was used:

$$R = \frac{\Delta P}{\rho Q^2} \quad (8)$$

In the present experiments, gas flows from the nasal inlet to the branching airways where it empties into a plenum; as such, the pressure drop through every path in the model must be the same. With this constraint, a system of equations can be derived where each branch is assigned an equivalent resistance, which can be determined as a function of its own resistance and the resistances of all its daughter branches:

$$R_{eq,p} = R_p + \left(R_{eq,a}^{-1/2} + R_{eq,b}^{-1/2} \right)^{-2} \quad (9)$$

where p denotes any parent airway branch, and a and b refer to its daughter branches.

This creates a recursive series of equivalent resistance calculations, where the ultimate branch values (i.e. final generation) are known resistances, defined as $R_{eq,p} = R_p$. The resulting system of non-linear equations is solvable in an iterative procedure, where total pressure drop values across each path ultimately converge to a single value. Flow rates in

each branch are initialized assuming equal flow division at each bifurcation. Equivalent resistances are then calculated, beginning with the most distal airways and moving to the trachea, using Eq. (9). Each branch flow rate is then updated as follows, beginning with the trachea and moving distally through the branching airways:

$$Q_a^{i+1} = \left(\frac{R_{eq,b}^{1/2}}{R_{eq,a}^{1/2} + R_{eq,b}^{1/2}} \right)^i Q_{inlet}^{i+1} \quad (10)$$

$$Q_b^{i+1} = Q_{inlet}^{i+1} - Q_a^{i+1} \quad (11)$$

where Q_{inlet} is the flow rate of the parent of branches a and b .

The convergence criterion was defined as the difference of the maximum and minimum pressure drop values across each path, divided by the tracheal pressure drop. A value of less than 10^{-8} was accepted as fully converged, as changes to the difference in pressure drop between paths were found to be negligible below this value.

Comparisons of the predictions of this analytical model with the experimental values were done using the concordance correlation coefficient, ρ_c , developed by Lawrence and Lin (1989). This coefficient ranges from 0 to 1, with a higher value indicating better agreement between experimental measurements and analytical predictions.

2.2.6 Analytical turbulent flow model determination

Based on analysis presented below of C_F and Re in Eqs. (6) and (7), the following equation was defined:

$$f = C_F \frac{d}{L} = C Re_d^{-0.25} \quad (12)$$

where f is the Darcy friction factor, L and d are the length and diameter of an airway segment, and C is a constant. Standard conditions were assumed for gas properties (20°C, 1 atm). Density and viscosity values used, respectively, were 1.206 kg/m³ and 1.820 × 10⁻⁵ Pa·s for air, and 0.399 kg/m³ and 2.147 × 10⁻⁵ Pa·s for heliox (Katz et al., 2011a).

A modified-Blasius model for pressure drop can be constructed by combining the Weisbach equation (White, 2016) with Eq. (12), as follows:

$$\Delta P = f \frac{L}{d} \frac{\rho v^2}{2} = \frac{C}{Re^{0.25}} \frac{L}{d} \frac{\rho v^2}{2} \quad (13)$$

To determine a value for C , pressure drop was calculated analytically using the modified-Blasius equation in Eq. (13) to define the resistance in Eq. (8), and beginning with an arbitrary initial guess for C . For a given subject, the resultant pressure drop values were then compared with their corresponding experimental pressure drop measurements using the concordance correlation coefficient (ρ_c) to assess their agreement. Iterative adjustments were made to C to optimize ρ_c to a value of 1, indicating equivalence between analytical and experimental data. This process was applied to each subject separately, to obtain an optimal, subject-specific coefficient value for the modified-Blasius model, defined as C_{ideal} .

2.3 Results

2.3.1 Experimental pressure drop compared with Reynolds number

Calculations of C_F versus Re using nose-throat and branching pressure drop values were used to fit Eq. (7) where the coefficient, β , exponent, α , and R^2 value are shown in Table 2.3. Exemplary log-log plots of C_F vs. Re in Subject 10, for both branching and nose-throat airways, are shown with lines of best fit in Figure 2.3.

Table 2.3: β -Coefficient, α -exponent and R^2 values for each C_F vs. Re plot

Subject Number	Branching Airways			NT Airways		
	β (coef.)	α (exponent)	R^2	β (coef.)	α (exponent)	R^2
2	14.68	0.261	0.896	34.64	0.207	0.696
3	12.05	0.183	0.886	64.21	0.261	0.776
5	17.38	0.256	0.829	69.01	0.254	0.773
6	18.93	0.259	0.981	57.29	0.206	0.926
9	20.91	0.225	0.798	67.44	0.116	0.434
10	18.30	0.206	0.903	36.02	0.258	0.870
11	20.45	0.247	0.891	101.94	0.147	0.520
12	28.76	0.251	0.970	100.35	0.222	0.952
13	22.03	0.277	0.844	40.63	0.207	0.583
14	14.02	0.212	0.896	62.00	0.297	0.794

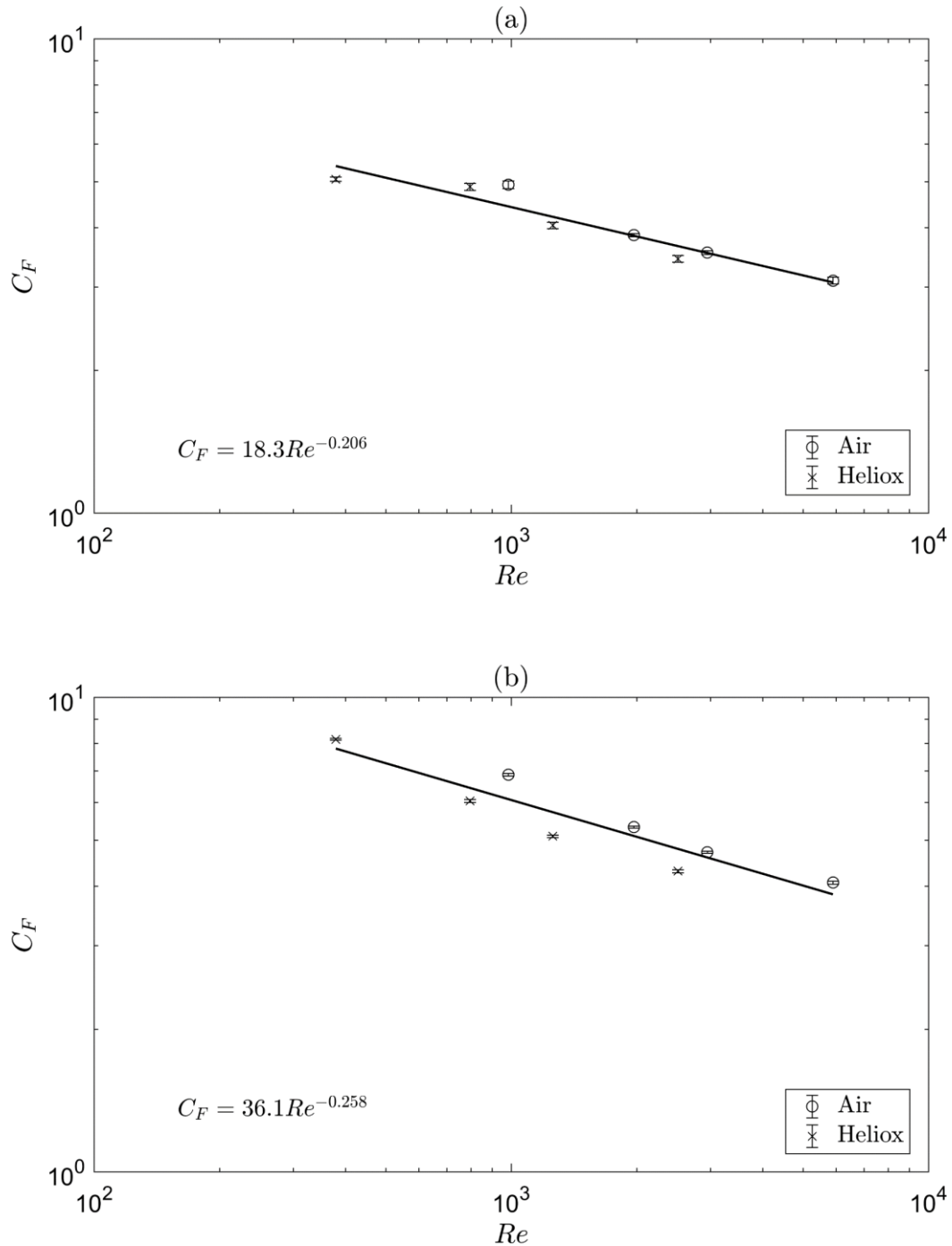


Figure 2.3: Log-log plot of friction coefficient, C_F , vs. Reynolds number, Re , for subject 10 in the (a) branching and (b) nose-throat airways. (Solid lines represent the best fit function indicated in the lower left corner of each plot. Error bars represent standard error. Where error bars are not visible the standard error is less than the size of the data symbol.)

2.3.2 Analytical calculation of pressure drop and airway resistance

Subject-specific coefficients, C_{ideal} , for the modified-Blasius model are shown in Table 2.4.

Table 2.4: Ideal C coefficient values for modified-Blasius equation described by Eq. (13)

Subject Number	Modified-Blasius, C_{ideal}
2	2.59
3	2.16
5	2.01
6	3.44
9	3.53
10	2.01
11	4.98
12	1.97
13	3.65
14	3.41
Average	2.98

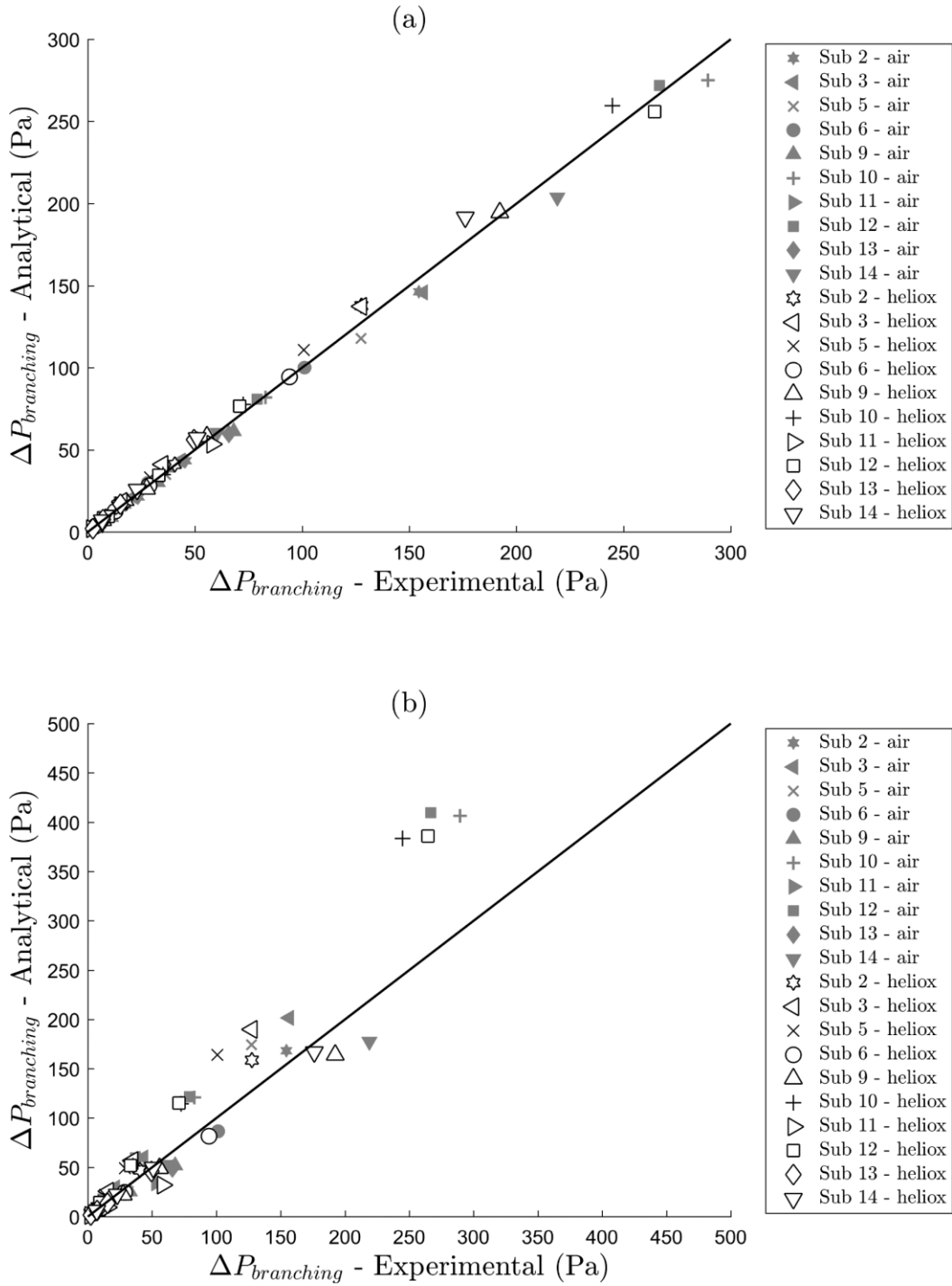


Figure 2.4: Branching airways pressure drop using the blasius equation vs. experimental pressure drop; (a) using an ideal C coefficient value for each subject measurements ($\rho_c = 0.997$) and (b) using an average ideal C coefficient value ($\rho_c = 0.909$)

Analytical calculations for pressure drop were done for each subject using C_{ideal} in the modified-Blasius formulation, Eq. (13). Analytical vs. experimental pressure drop in the branching airways for all subjects is shown in Figure 2.4a. Figure 2.4b shows a similar comparison, instead using the average of all subject-specific C_{ideal} values, such that $C_{avg} = 2.98$ for all subjects.

2.4 Discussion

2.4.1 Experimental pressure drop compared with Reynolds number

The aim of this work was to experimentally assess pressure drop behavior in the upper and central airways of children. In particular, pressure drop was assessed in the central branching airways with the anatomically accurate boundary condition of a nose-throat airway upstream from the trachea. The relationship between C_F and Re was evaluated in both the nose-throat and branching airways.

NOSE-THROAT

The average of all fitted α values in Eq. (6) for the nose-throat airways was 0.218. By comparing Eq. (6) with the Blasius equation for pipe friction at low turbulent Re , it may be shown that turbulent flow is characterized by $\alpha = 0.25$. The reasonably close agreement between these values is indicative of turbulent flow within the nose-throat airways. Past work in adult nasal airway replicas by Garcia et al. (2009) described pressure drop with an expression analogous to Eq. (6): $\Delta P = aQ^b$, where a and b are constants. From Eqs. (4) and (5), it can be shown that $b = 2 - \alpha$; thus, a value of $\alpha = 0.25$ corresponds to $b = 1.75$. Garcia et al. (2009) determined a range of b values of 1.76–1.85 for four adult replicas at 30–75 L/min

flow rates. The range of experimentally determined b values in the present work was 1.70–1.88 (derived from Table 2.3), showing a notably similar range to that seen by Garcia et al. (2009) and suggesting similar Re -dependent flow behavior in their adult and our child nasal airway replicas.

BRANCHING AIRWAYS

The relationship between C_F and Re in the branching airways was investigated in the same manner, where the average α value was found to be 0.238. This α value suggests that turbulence is present in flow through the central branching airways. Much previous work done to model branching airway pressure drop has used the Pedley et al. (1970) equation, for which $\alpha = 0.5$, under the assumption of disturbed laminar flow through branching airways. However, computational fluid dynamics (CFD) studies have indicated that turbulence generated in the upper airways is convected downstream through the central branching airways. For example, a direct numerical simulation (DNS) conducted by Lin et al. (2007) using a realistic adult geometry showed that for a tracheal flow rate of 19.2 L/min ($Re = 1700$) turbulence produced downstream of the glottis constriction influenced flow patterns in the intra-thoracic airways. Similarly, simulations in adult airway geometries performed by Xi et al. (2008), Calmet et al. (2016), and Koullapis et al. (2018) demonstrated that turbulence generated in the upper airways influences flow downstream in the branching airways. The results of the present work in airway replicas of children (aged 4–8 years) appear to be consistent with these simulations, in that the relationship between C_F and Re indicates the presence of turbulence in the branching airways. Given the tracheal Reynolds number range studied (671–5988 for air and 259–2547 for heliox; Table 2.2), and increase in total airway cross-section (and hence decrease in Re) with each bifurcation, we attribute turbulence in the branching airways mainly to convection of turbulence produced upstream in the upper

airway, as opposed to turbulence production in the branching airways, which is also supported by an analysis of turbulent production versus dissipation (Finlay, 2001).

COMPARISONS OF PRESSURE DROP FOR HELIOX VS. AIR

Obtaining pressure drop measurements with both air and heliox provided means for an additional method for evaluating flow regime, and defining a model accordingly. Litwin et al. (2017) found the ratio of expected pressure drop at a given flow rate between two fluids is dependent on ρ , μ , and α only. The ratio between pressure drop predicted using the modified-Blasius model in Eq. (13), where $\alpha = 0.25$, for heliox versus air is:

$$\frac{\Delta P_{heliox}}{\Delta P_{air}} = \frac{\left(C Re^{-0.25} \frac{L}{d} \frac{\rho v^2}{2} \right)_{heliox}}{\left(C Re^{-0.25} \frac{L}{d} \frac{\rho v^2}{2} \right)_{air}} = \frac{(\rho^{0.75} \mu^{0.25})_{heliox}}{(\rho^{0.75} \mu^{0.25})_{air}} \quad (14)$$

Thus, based on gas fluid properties described in the methods, the expected pressure drop ratio between heliox and air ($\Delta P_{heliox}/\Delta P_{air}$) is 0.455. The average pressure drop ratio was calculated for each subject, for both branching and nose-throat airways (Table 2.5). The overall mean ratios of all subjects and the corresponding standard deviations (representing variation between subjects) are 0.43 ± 0.03 and 0.39 ± 0.03 for branching and nose-throat airways, respectively. The average for each subject was calculated from the pressure drop ratios of the fitted ΔP vs. Q curves for 5–45 L/min (for example, see Figure 2.5). Agreement with the ratio of 0.455 predicted analytically is particularly close for the branching airways. In contrast, the ratio predicted by the Pedley et al. (1970) model is 0.625. This provides evidence that the dependence of branching airway pressure drop on gas properties is better predicted using a modified-Blasius turbulent model than using the Pedley et al. (1970) model for the replicas studied here.

Table 2.5: Average pressure drop ratios of heliox vs. air for branching and nose-throat airways (calculated from ratios of fitted values, ranging from 5-45 L/min)

Subject Number	Branching Airways	NT Airways
2	0.42	0.37
3	0.39	0.39
5	0.42	0.39
6	0.47	0.42
9	0.42	0.34
10	0.41	0.41
11	0.50	0.34
12	0.46	0.42
13	0.42	0.36
14	0.40	0.41

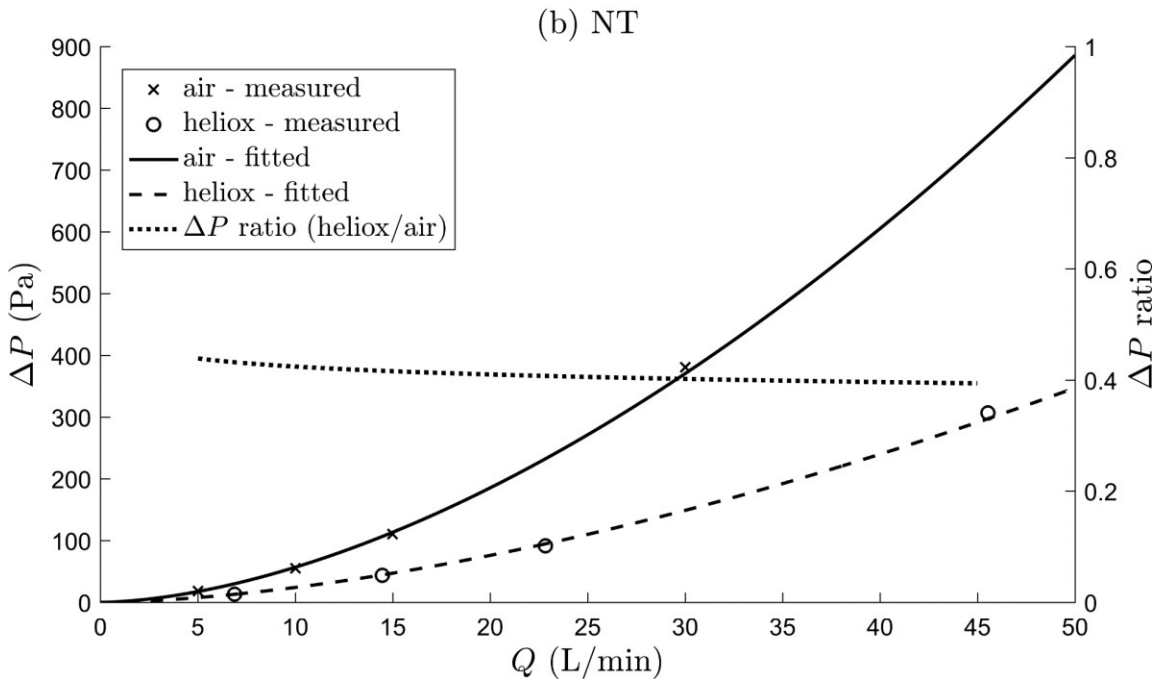
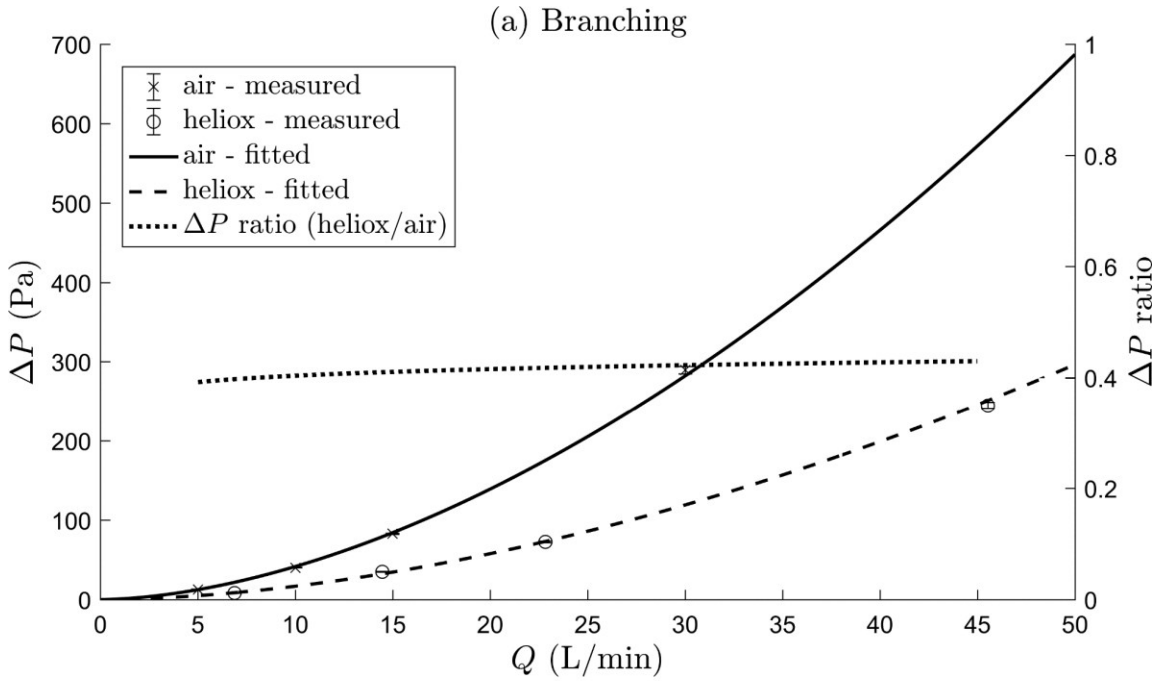


Figure 2.5: Pressure drop vs. flow rate for subject 10 in the (a) branching and (b) nose-throat airways with the pressure drop ratio for 5-45 L/min overlaid

2.4.2 Analytical pressure drop prediction – Absolute values

With the suitability of the modified-Blasius formulation established, an additional aim of the present work was to explore its use in predicting absolute pressure drop values in individual child airways. To fully define the modified-Blasius formulation in Eq. (13), a value for constant C was needed. Initially, subject-specific values, C_{ideal} , were obtained by fitting the experimental data; that is, by optimizing ρ_c as described in the methods. Analytical pressure drop values calculated using C_{ideal} for each subject (Table 2.4) are compared with the experimental data in Figure 2.4a. The strong correlation ($\rho_c = 0.997$) demonstrates that pressure drop can be accurately predicted using a modified-Blasius formulation, with a single, but subject-specific, coefficient used in each airway segment, and with a constant α value of 0.25. However, it must be emphasized that in the present analysis C_{ideal} was a fit parameter, and no clear correlation between C_{ideal} and subject age, height, weight, trachea length or diameter could be established. It is likely that different values of C_{ideal} for different subjects arise from intersubject variability in more complex features of airway geometry (e.g. branching angles, parent-to-child diameter ratios, asymmetric bifurcations) that are not captured with the parameters listed above.

As an alternative approximation, an average of all C_{ideal} values was calculated as $C_{avg} = 2.98$ (Table 2.4). Analytical predictions of pressure drop made for all replicas with this single value were considerably less accurate, showing a correlation of $\rho_c = 0.909$ (Figure 2.4). Estimation of absolute values of pressure drop through central conducting airways of individual subjects made using the modified-Blasius equation with $C_{avg} = 2.98$ should therefore be done with caution. However, calculation of absolute values of pressure drop for

archetypal subjects within the age range studied (4- to 8-years old) may be done so long as airway lengths and diameters are defined.

2.5 Conclusions

Pressure drop through the nose-throat and central branching airways was measured in airway replicas based on computed tomography (CT) scans of 10 child subjects, between 4- and 8-years old. The relationship between the coefficient of friction, C_F (Slutsky et al., 1980), and Reynolds number, Re , was indicative of turbulent flow for both the nose-throat and for the branching airways. The ratio of pressure drop through the branching airways between heliox and air flow was also consistent with predictions made for turbulent flow. The presence of turbulence in the branching airways likely resulted from convection of turbulence produced upstream in the nose and throat. An airway resistance model based on the Blasius pipe friction correlation for turbulent flow was proposed for prediction of pressure drop through the bifurcating bronchial airways downstream from the upper airway.

2.6 Chapter Citations

Blasius, H. (1911). The similarity law in friction processes. *Physikalische Zeitschrift*, 12, 1175-1177.

Borojeni, A. A., Noga, M. L., Martin, A. R., & Finlay, W. H. (2015). Validation of airway resistance models for predicting pressure loss through anatomically realistic conducting airway replicas of adults and children. *Journal of Biomechanics*, 48(10), 1988-1996. doi:10.1016/j.jbiomech.2015.03.035

- Borojeni, A. A. T., Noga, M. L., Vehring, R., & Finlay, W. H. (2014). Measurements of total aerosol deposition in intrathoracic conducting airway replicas of children. *Journal of Aerosol Science*, *73*, 39-47. doi:10.1016/j.jaerosci.2014.03.005
- Calmet, H., Gambaruto, A. M., Bates, A. J., Vázquez, M., Houzeaux, G., & Doorly, D. J. (2016). Large-scale CFD simulations of the transitional and turbulent regime for the large human airways during rapid inhalation. *Computers in Biology and Medicine*, *69*, 166-180. doi:<https://doi.org/10.1016/j.compbio.2015.12.003>
- Damanhuri, N. S., Docherty, P. D., Chiew, Y. S., van Drunen, E. J., Desai, T., & Chase, J. G. (2014). A patient-specific airway branching model for mechanically ventilated patients. *Computational and mathematical methods in medicine*, *2014*.
- Finlay, W. H. (2001). *The Mechanics of Inhaled Pharmaceutical Aerosols*.
- Garcia, G. J. M., Tewksbury, E. W., Wong, B. A., & Kimbell, J. S. (2009). Interindividual Variability in Nasal Filtration as a Function of Nasal Cavity Geometry. *Journal of Aerosol Medicine and Pulmonary Drug Delivery*, *22*(2), 139-156. doi:10.1089/jamp.2008.0713
- Gemci, T., Ponyavin, V., Chen, Y., Chen, H., & Collins, R. (2008). Computational model of airflow in upper 17 generations of human respiratory tract. *Journal of Biomechanics*, *41*(9), 2047-2054. doi:10.1016/j.jbiomech.2007.12.019
- Katz, I., Caillibotte, G., Martin, A. R., & Arpentinier, P. (2011a). Property value estimation for inhaled therapeutic binary gas mixtures: He, Xe, N₂O, and N₂ with O₂. *Medical Gas Research*, *1*, 28-28. doi:10.1186/2045-9912-1-28
- Katz, I. M., Martin, A. R., Feng, C.-H., Majoral, C., Caillibotte, G., Marx, T., . . . Daviet, C. (2012). Airway pressure distribution during xenon anesthesia: the insufflation phase at constant flow (volume controlled mode). *Appl Cardiopulm Pathophysiol*, *16*(5).

- Katz, I. M., Martin, A. R., Muller, P. A., Terzibachi, K., Feng, C. H., Caillibotte, G., . . . Texereau, J. (2011b). The ventilation distribution of helium-oxygen mixtures and the role of inertial losses in the presence of heterogeneous airway obstructions. *Journal of Biomechanics*, *44*(6), 1137-1143. doi:10.1016/j.jbiomech.2011.01.022
- Koullapis, P. G., Nicolaou, L., & Kassinos, S. C. (2018). In silico assessment of mouth-throat effects on regional deposition in the upper tracheobronchial airways. *Journal of Aerosol Science*, *117*, 164-188. doi:10.1016/j.jaerosci.2017.12.001
- Lawrence, I., & Lin, K. (1989). A concordance correlation coefficient to evaluate reproducibility. *Biometrics*, 255-268.
- Lin, C.-L., Tawhai, M. H., McLennan, G., & Hoffman, E. A. (2007). Characteristics of the turbulent laryngeal jet and its effect on airflow in the human intra-thoracic airways. *Respiratory physiology & neurobiology*, *157*(2), 295-309.
- Litwin, P. D., Reis Dib, A. L., Chen, J., Noga, M., Finlay, W. H., & Martin, A. R. (2017). Theoretical and experimental evaluation of the effects of an argon gas mixture on the pressure drop through adult tracheobronchial airway replicas. *Journal of Biomechanics*, *58*, 217-221. doi:<https://doi.org/10.1016/j.jbiomech.2017.04.002>
- Pedley, T. J., Schroter, R. C., & Sudlow, M. F. (1970). Energy losses and pressure drop in models of human airways. *Respiration Physiology*, *9*(October 1969), 371-386. doi:10.1016/0034-5687(70)90093-9
- Pozin, N., Montesantos, S., Katz, I., Pichelin, M., Grandmont, C., & Vignon-Clementel, I. (2017). Calculated ventilation and effort distribution as a measure of respiratory disease and Heliox effectiveness. *J Biomech*, *60*, 100-109. doi:10.1016/j.jbiomech.2017.06.009
- Slutsky, A. S., Berdine, G. G., & Drazen, J. M. (1980). Steady flow in a model of human central airways. *J Appl Physiol Respir Environ Exerc Physiol*, *49*(3), 417-423.

- Swan, A. J., Clark, A. R., & Tawhai, M. H. (2012). A computational model of the topographic distribution of ventilation in healthy human lungs. *Journal of Theoretical Biology*, *300*, 222-231.
- Tgavalekos, N. T., Musch, G., Harris, R., Melo, M. V., Winkler, T., Schroeder, T., . . . Venegas, J. (2007). Relationship between airway narrowing, patchy ventilation and lung mechanics in asthmatics. *European Respiratory Journal*, *29*(6), 1174-1181.
- van Ertbruggen, C., Hirsch, C., & Paiva, M. (2005). Anatomically based three-dimensional model of airways to simulate flow and particle transport using computational fluid dynamics. *J. Appl. Physiol.*, *98*(3), 970-980. doi:10.1152/jappphysiol.00795.2004.
- White, F. M. (2016). *Fluid Mechanics* (8 ed.): McGraw-Hill, New York.
- Wongviriyawong, C., Harris, R. S., Greenblatt, E., Winkler, T., & Venegas, J. G. (2012). Peripheral resistance: a link between global airflow obstruction and regional ventilation distribution. *Journal of Applied Physiology*, *114*(4), 504-514.
- Xi, J., Longest, P. W., & Martonen, T. B. (2008). Effects of the laryngeal jet on nano-and microparticle transport and deposition in an approximate model of the upper tracheobronchial airways. *Journal of Applied Physiology*, *104*(6), 1761-1777.

Chapter 3: Application of pressure drop findings for development of a single path child airway model

3.1 Introduction

Airway resistance is of interest in respiratory medicine, as it is important in diagnosis and treatment of respiratory disease. Analytical models for pressure drop through the airways, as described in the previous chapter, indicate that airway diameters and lengths are important factors in determining pressure drop (and therefore airway resistance); thus, age is expected to play a role in appropriate modelling. Likewise, the pressure drop is known to have a functional dependence on both gas density and viscosity, indicating that inhaled gas type will affect pressure drop predictions. In general, proper modelling of airway pressure drop is expected to depend on airway dimensions (i.e. age), fluid properties (i.e. the type of gas used) and flow rates (related to activity level and age).

Consideration of gas type is a necessary component of airway resistance modelling as various gases are employed in pediatric medical applications. For example, a mixture of 80% helium and 20% oxygen (i.e. He-O₂ (80/20), commonly described as “Heliox”) has been shown to lessen resistance in branching airways due to its density being significantly lower and viscosity only slightly higher than air (Valli et al., 2016). A case study of simulations of airway flow indicated the potential for reduction of work of breathing in certain asthmatic conditions (Pozin et al., 2017). It has also been suggested that low gas density reduces deposition of inhaled pharmaceuticals in the upper respiratory tract, allowing increased drug delivery to

more distal airways (Darquenne and Prisk, 2004). Various other investigative experiments have indicated potential benefits of He-O₂ (80/20) in pediatric treatments (Frazier and Cheifetz, 2010) including cases of upper airway obstructive croup, ultimately obviating the need for intubation (Duncan, 1979), some cases of infant bronchiolitis (Cambonie et al., 2006), and asthma treatments such as assistance with work of breathing (Kudukis et al., 1997) and drug delivery where lower airway obstruction is severe (Piva et al., 2002).

Another commonly used medical gas mixture is composed of 50% nitrous oxide and 50% oxygen (i.e. N₂O-O₂ (50/50), marketed as Entonox (Praxair, Inc.) and Kalinox (Air Liquide), for example). N₂O-O₂ (50/50) gas has been shown to serve as an efficacious analgesic in various applications. In pediatric dentistry, it has been used for patient sedation to reduce anxiety (Holroyd, 2008) and was found to be an effective alternative to general anesthetic treatments (Lyratzopoulos and Blain, 2003). Additionally, N₂O-O₂ (50/50) has been recommended for pain treatment of hospitalized children undergoing small procedures (Pedersen et al., 2013), as well as for prehospital treatments involving severe pain (Faddy and Garlick, 2005). In the present work, both of these gas mixtures, in addition to air, have been used in assessing the influence of gas properties on airway resistance in children. Previous work has suggested that effects of N₂O-O₂ (50/50) on airway resistance warrant avoiding its use when treating patients who are asthmatic or otherwise have airway obstructions (Douglas et al., 1974) and severe asthma has been described as one of its contraindications (Agah et al., 2014). This suggests that a better understanding of its effects on airway resistance are pertinent to medical treatments.

As determined in the previous chapter, airway resistance models commonly employed for branching airways (Pedley et al., 1970; van Ertbruggen et al., 2005) may not accurately

predict pressure drop through the bifurcating bronchial airways downstream from the upper airway. Analysis of C_F vs. Re in the branching airways showed that $C_F \propto Re^{-0.25}$, having resemblance to the turbulent Blasius equation, and suggesting turbulent flow through these airways. However, given that Re decreases by several orders of magnitude moving from the trachea down to the distal generation of the lung, it may be assumed that laminar flows develop after a certain number of generations. Modelling pressure drop across a single path, from the trachea to the final lung generation (i.e. an alveolar sac), requires an assumption of how far the turbulent flow extends and where laminar flow begins.

Some models have assumed that turbulence in each generation is governed purely by the Reynolds number value at that location, and take $Re > 2000$ to be the criterion for turbulence (Gouinaud et al., 2015; Katz et al., 2011b). The previous chapter suggests that turbulence generated in the extra-thoracic airways is convected into the branching airways, despite Reynolds numbers less than this turbulent criterion. This is consistent with available literature (Calmet et al., 2016; Cohen et al., 1990).

According to Cohen et al. (1993), in bifurcating lung trees the consideration of the typical Reynolds number criterion of approximately 2000 used for pipe flow is, on its own, an incomplete indicator of flow regime. It has been observed that unstable flows can persist at Reynolds numbers less than 2000. Dekker (1961) performed water flow experiments in upper airway casts, showing that the larynx had a substantial effect on the Reynolds number criteria for the appearance of turbulence, lowering the typical Reynolds number criterion by up to 3 or 4 times (Cohen et al., 1993). Olson et al. (1973) found that instabilities in the flow of air existed up to the segmental bronchi (generation 3) in mouth-to-subsegmental bronchi replicas. Similarly, Owen (1969) assessed the rate of turbulence decay and saw that turbulent

fluctuations were only half dissipated in the segmental bronchi. Olson et al. (1970) and Cohen et al. (1993) discussed the effects of airway properties such as cross sectional area, airway length, and branching angle, noting that the short length of the airways, in comparison to the laminar entrance length required to establish fully-developed laminar flow, has a large impact on the flow regimes even at lower Reynolds numbers.

Given that the Reynolds number criteria that were developed specifically for fully-developed pipe flow (e.g. $Re > 2000$) may not be a proper indicator of flow regime in various generations of branching airways, it follows that the location of transition from turbulent to laminar flow must be determined by some other means for modelling purposes. The distance of the persisting turbulence in the lung is uncertain. According to Hardin and Patterson (1979), flow within the human lung is mainly laminar apart from the trachea and first few generations of bronchi. Xi et al. (2008) observed turbulence generated from the larynx in simulations of air through simplified adult replicas extending to generations 3 and 6 at flow rates of 15 and 30 L/min, respectively. CFD studies by Calmet et al. (2016) on an anatomically accurate upper and central airways model of an adult at $Re \approx 5000$ showed turbulence dissipating by about generation 3.

In addition to the selection of appropriate pressure drop models, choosing appropriate airway dimensions is critical for modelling airway resistance in children. Various methods have been employed to estimate the length and diameters of airways of children (Crawford, 1982; Finlay et al., 2000; Hofmann et al., 1989; Longest et al., 2006; Xu and Yu, 1986). It is known that airways in the lung grow in generation number and individual dimensions with increased age, and that growth patterns vary in different lung regions (Reid, 1977). As such, accurate lung dimensions for young children cannot be derived simply by direct uniform

scaling of adult models (such as the well-known Weibel (1963) (“Weibel A”) model) to a smaller size (Hofmann et al., 1989). Longest et al. (2006) used values from Hofmann et al. (1989) for a 4-year-old. Finlay et al. (2000) used a combination of models from Phillips et al. (1994) and Haefeli-Bleuer and Weibel (1988) and then scaled them with methods described by Hofmann et al. (1989) for children 4 and 8 years old.

The main focus of this study is an investigation of the modelling of each generation of a single path in child airways, to find the relationship of pressure drop to age, gas properties, flow rate, and flow model. An investigation of commonly used gases in medical applications is done and contrasted with results for air. Dependence on flow rate is also assessed, given a range of flow rates typical for children ages 4 to 8 over a range of exertion levels. The selection of appropriate model parameters, such as the generation where a transition from a modified-Blasius to a Pedley et al. (1970) model may be used, are detailed in this chapter. Predictions of total and generational pressure drop are made based on the defined model.

3.2 Methods

3.2.1 Single-path tracheobronchial airways model

One aim of this work is to determine the total tracheobronchial pressure drop across a single path, beginning at the trachea (generation 0) and extending to an ultimate alveolar airway (generation 23). The approach was adapted from Katz et al. (2011b), and can be shown as an energy balance along the entire path:

$$\Sigma(\Delta P_{G0-G23}) = \left(P + a \frac{\rho v^2}{2} + \rho g z \right)_{G0} - \left(P + a \frac{\rho v^2}{2} + \rho g z \right)_{G23} \quad (15)$$

where P is pressure, a is a constant that depends on velocity profile, and z is elevation ($G0$ and $G23$ denote generations 0 and 23, respectively). It is assumed that changes in velocity and elevation both have negligible influence. By a rough calculation of kinetic energy differences and elevation differences (where a z difference of 10 cm is considered) at a flow rate of 14 L/min, the magnitude of the contributions of kinetic energy and elevation differences are 3% of the total tracheobronchial pressure difference. Considering those terms to be negligible, Eq. (15) can be simplified to:

$$\Sigma(\Delta P_{G0-G23}) = P_{G0} - P_{G23} \quad (16)$$

Thus, the tracheobronchial pressure drop across a single path in the lung can be described as a sum of individual values of pressure drop due to frictional losses through each airway segment along that path. For convenience, this can be defined as:

$$\Sigma(\Delta P_{G0-G23}) = \sum_{i=0}^{23} (\Delta P_i) \quad (17)$$

where ΔP_i is the pressure drop across generation, i , which ranges from 0 to a maximum of 23 generations in adults. Therefore, the sum term represents total pressure drop through the trachea and all branching airways on a single path.

3.2.2 Modelling of pediatric lung airway dimensions

As the subjects studied in the previous chapter ranged from 4 to 8 years old, the pressure drop model developed in this chapter is intended to apply to the same range. Scaled model airway dimensions for ages 4 and 8 were determined by Finlay et al. (2000), which account for the growth and changes in lungs during development. These were determined using a combination of models from Phillips et al. (1994) and Haefeli-Bleuer and Weibel (1988) and then scaled using methods described by Hofmann et al. (1989) for children 4 and 8 years. A table of the diameters and lengths at each generation is shown in Table 3.1, reproduced from Finlay et al. (2000).

Table 3.1: Model dimensions of lung generations for 4-year-old, 8-year-old and adult geometries (reproduced from Finlay et al. (2000))

Generation	Age 4		Age 8		Adult	
	Length (cm)	Diameter (cm)	Length (cm)	Diameter (cm)	Length (cm)	Diameter (cm)
0	5.330	1.105	6.560	1.351	12.456	1.810
1	2.544	0.803	2.987	0.973	3.614	1.414
2	0.971	0.575	1.143	0.688	2.862	1.115
3	0.673	0.436	0.804	0.517	2.281	0.885
4	0.559	0.276	0.645	0.318	1.780	0.706
5	0.455	0.216	0.536	0.251	1.126	0.565
6	0.340	0.178	0.394	0.208	0.897	0.454
7	0.268	0.122	0.300	0.139	0.828	0.364
8	0.235	0.091	0.255	0.101	0.745	0.286
9	0.261	0.082	0.287	0.090	0.653	0.218
10	0.236	0.071	0.256	0.076	0.555	0.162
11	0.221	0.058	0.239	0.061	0.454	0.121
12	0.207	0.056	0.221	0.058	0.357	0.092
13	0.192	0.052	0.204	0.053	0.277	0.073
14	0.178	0.048	0.187	0.049	0.219	0.061
15	0.080	0.029	0.099	0.036	0.134	0.049
16	0.065	0.029	0.081	0.035	0.109	0.048
17	0.054	0.023	0.067	0.029	0.091	0.039
18	0.048	0.022	0.060	0.027	0.081	0.037
19	0.040	0.021	0.050	0.026	0.068	0.035
20	0.040	0.020	0.050	0.024	0.068	0.033
21	0.040	0.018	0.050	0.022	0.068	0.030
22	0.039	0.017	0.048	0.021	0.065	0.028
23	—	—	0.054	0.018	0.073	0.024

3.2.3 Gas types and applications

Various gas types that are common in medical applications have been included in this work as part of the model. In addition to air, calculations for an 80% helium-20% oxygen (“heliox”) mixture and a 50% nitrous oxide-50% oxygen mixture were also examined (He-O₂ (80/20) and N₂O-O₂ (50/50), respectively). These gases were chosen based on their use in pediatric

medical treatments, as outlined in the introduction. Gas properties used to model air and He-O₂ (80/20) are the same as used in the previous chapter (Section 2.2.6), taken from Katz et al. (2011a). Additionally, N₂O-O₂ (50/50) fluid properties are similarly obtained from the same source. All gas properties are summarized in Table 3.2.

Table 3.2: Gas properties adapted from Katz et al. (2011a) where standard conditions are assumed (20°C, 1 atm).

Fluid	Density, ρ (kg/m³)	Dynamic Viscosity, μ (Pa·s)
Air	1.206	1.820×10^{-5}
He-O ₂ (80/20)	0.399	2.147×10^{-5}
N ₂ O-O ₂ (50/50)	1.580	1.580×10^{-5}

3.2.4 Typical inhalation flow rates by age

An approximation for average inhalation flow rate can be determined by:

$$Q_{inhale} = \frac{V_T}{t_i} \quad (18)$$

where V_T is the tidal volume in litres and t_i is the inspiratory time in a breath. When the breathing frequency, f , is known, Eq. (18) can be expressed as:

$$Q_{inhale} = \frac{V_T \cdot f}{c_d} \quad (19)$$

where c_d is the duty cycle, which is a ratio of t_i to the total breath period (Amirav et al., 2015). Data for tidal breathing and breathing frequency in children between 3 months and 6 years

old was used to develop empirical correlations found by Taussig et al. (1977). Expressions for both f and V_T are provided:

$$f = 31.61 - 0.09m \quad (20)$$

$$V_T = (-186.83 + 3.91h) \times 10^{-3} \quad (21)$$

where m is age in months, and h is height in cm, resulting in f and V_T in breaths/min and litres, respectively. As an approximation for height, the averages of the subjects in the previous chapter, at ages 4 and 8 (Table 2.1), were used in Eq. (21). A duty cycle value for inspiratory flow was taken to be a constant of 0.435 (Finlay, 2001). The approximate values for inspiratory flow rate from Eq. (19) are given in Table 3.3.

Table 3.3: Typical inspiratory flow rate approximations for children ages 4 and 8, calculated from age, height, breathing frequency, and tidal volume

Age (yr.)	Inspiratory Flow Rate, Q_{inhale} (L/min)	Breathing frequency, f (min ⁻¹)	Tidal volume, V_T (L)
4	12.7	27.3	0.20
8	15.8	23.0	0.30

These approximations indicate that a typical tidal flow rate for the age range in question would tend to fall between 12 and 16 L/min. For the results where flow rate dependence is of interest, this general range is included in the presented range. Where values calculated at a constant flow rate are investigated, a flow rate of 14 L/min is used.

To determine the extremes of flow rates that would be visible in the given age range, similar data tabulated by Phalen et al. (1985) was used. This shows a range of minute ventilations

for various ages from 0 to 18 years of age, and different levels of activity. Minute volume is defined as:

$$V_m = V_T \cdot f \quad (22)$$

Thus, combining Eq. (19) and (22) allows for calculation of approximate inhalation flow rate given values of minute volume, which are tabulated in Table 3.4

Table 3.4: Inspiratory flow rates calculated based on minute volumes for ages 4 and 8 at various levels of activity (reproduced from Phalen et al. (1985)), and using a duty cycle of 0.435 (Finlay, 2001)

Activity state	Age (yr.)	Height (cm)	Minute volume (L/min)	Inspiratory flow rate (L/min)
Low activity	4	104	3.18	7.3
Light exertion	4	104	6.34	14.6
Heavy exertion	4	104	19	43.7
Low activity	8	127	4.53	10.4
Light exertion	8	127	9.05	20.8
Heavy exertion	8	127	27.1	62.3

Thus, the range of approximate inhalation flow rates encompasses flows of about 5–45 L/min for age 4 and 10–65 L/min for age 8. Assessments of flow rates for both ages were made by examining a range of 5–65 L/min.

3.2.5 Pressure drop models for flow regimes

For this model, the flow division is assumed to be symmetrical at each transition, as the model developed by Finlay et al. (2000) is also symmetrical. Thus, each generation in the

path has half the flow rate of its parent branch, which can be determined at any generation, i , as:

$$Q_i = \frac{Q_0}{2^i} \quad (23)$$

where Q_i is the flow at generation i , and Q_0 is the tracheal inlet flow rate.

Reynolds number for a generation is defined as (White, 2016):

$$Re = \frac{4\rho Q}{\pi\mu d} \quad (24)$$

For disturbed laminar flow, the Pedley et al. (1970) model is well-known for airway resistance calculations:

$$\Delta P_{Pedley} = Z \cdot \Delta P_{HP} = \left[\frac{1.85}{4\sqrt{2}} \left(Re \frac{d}{L} \right)^{0.5} \right] \left[\frac{128\mu L Q}{\pi d^4} \right] \quad (25)$$

where ΔP_{HP} is the Hagen-Poiseuille fully-developed flow equation and Z is a ratio of actual pressure drop vs. the value given by pure fully-developed Hagen-Poiseuille flow. Additionally, L is the length and d is the diameter of the airway, Re is the Reynolds number, ρ is the fluid density, v is the fluid velocity, and ΔP is the pressure drop across the airway. For the equation to remain physical, the ratio Z must be greater than or equal to one, such that at very low Reynolds numbers Eq. (25) simplifies to ΔP_{HP} .

For turbulent flow, the modified-Blasius model from the previous chapter is used, which employs the average coefficient found experimentally for 10 subjects between ages 4 and 8, i.e. $C = 2.98$:

$$\Delta P_{Mod-Blasius} = \frac{2.98}{Re^{0.25}} \frac{L \rho v^2}{d^2} \quad (26)$$

The models can also be expressed as functions of L , d , ρ , Q (flow rate), and μ (dynamic viscosity):

$$\Delta P_{Mod-Blasius} = (2.98 \cdot 2^{2.5} \pi^{-1.75}) (\mu^{0.25} \rho^{0.75}) (L d^{-4.75}) (Q^{1.75}) \quad (27)$$

$$\Delta P_{Pedley} = (118.4 \cdot 2^{-0.5} \pi^{-1.5}) (\mu^{0.5} \rho^{0.5}) (L^{0.5} d^{-4}) (Q^{1.5}) \quad (28)$$

It has been determined that the first few generations of the branching airways exhibit turbulent flow behavior, as seen in the previous chapter. Eventually turbulence is expected to dissipate moving downstream through the airway tree. A simple pressure drop model can be developed where the most proximal airways are calculated using the modified-Blasius model and distal generations (beginning at a transitional generation denoted as G_T) are calculated with the Pedley et al. (1970) model. To represent this, the sum term in Eq. (17) can be further divided as follows:

$$\Sigma(\Delta P_{G0-G23}) = \sum_{i=0}^{G_T-1} (\Delta P_i^{Mod-Blasius}) + \sum_{i=G_T}^{23} (\Delta P_i^{Pedley}) \quad (29)$$

3.2.6 Determining pressure drop sensitivity due to transition generation

To assess how critical the selection of the transition generation is in determining tracheobronchial pressure drop through the airways, a sensitivity study was done. By comparing total single path pressure drop with the generation at which the pressure drop model transitions from the modified-Blasius to Pedley model, the rates of change of the pressure drop at each generation can be seen. This gives an indication of the relative impact a transition would have at each generation. Similarly, using either a purely Pedley et al. (1970) or turbulent flow model to calculate pressure drop at each individual generation from 0 to 23 shows which generations contribute the most to the overall pressure drop across a single path. As described previously, the Pedley model becomes equivalent to the Hagen-Poiseuille equation as Re becomes small, thus pressure drop in distal generations with small Re are effectively calculated with the Hagen-Poiseuille equation.

To show the relationship between pressure drop and model transition generation, tracheobronchial path pressure drop was calculated using Eq. (29) for every value of G_T , i.e. from 0 to 23. This was done for flow rates encompassing that of normal tidal volumes. The determination of the transition generation at which pressure drop is a maximum was also calculated and plotted as a function of flow rate, age and fluid.

3.2.7 Determination of turbulent-to-laminar transition generation

In some previous airway models, a Reynolds number of approximately 2000 has been suggested for demarcating the transition value above which flow begins to transition to turbulence (Katz et al., 2011b). Figure 3.1 shows the Reynolds numbers at each airway generation, calculated with Eq. (24). Each panel corresponds to a gas and shows both ages

(4 and 8 years) at a flow rates below and above the normal inspiratory flow rate (5 and 20 L/min, respectively). Figure 3.1 indicates that such a criterion (turbulence when $Re \geq 2000$) would limit turbulent flow to at most 2 generations in some fluid cases. However, the previous results (Chapter 2) using the airway replicas shows that turbulence may be convected to more distal generations at the same flow rate, when an anatomically correct nasal airway was included. This generation of turbulence at lower Reynolds numbers than 2000 has been attributed to the laryngeal jet, and has been shown to propagate through multiple airway generations (Darquenne, 2012; Dekker, 1961; Xi et al., 2008). Thus, the presence of turbulence is not necessarily purely based on Reynolds number. The figure also shows that Reynolds number decreases significantly with each generation.

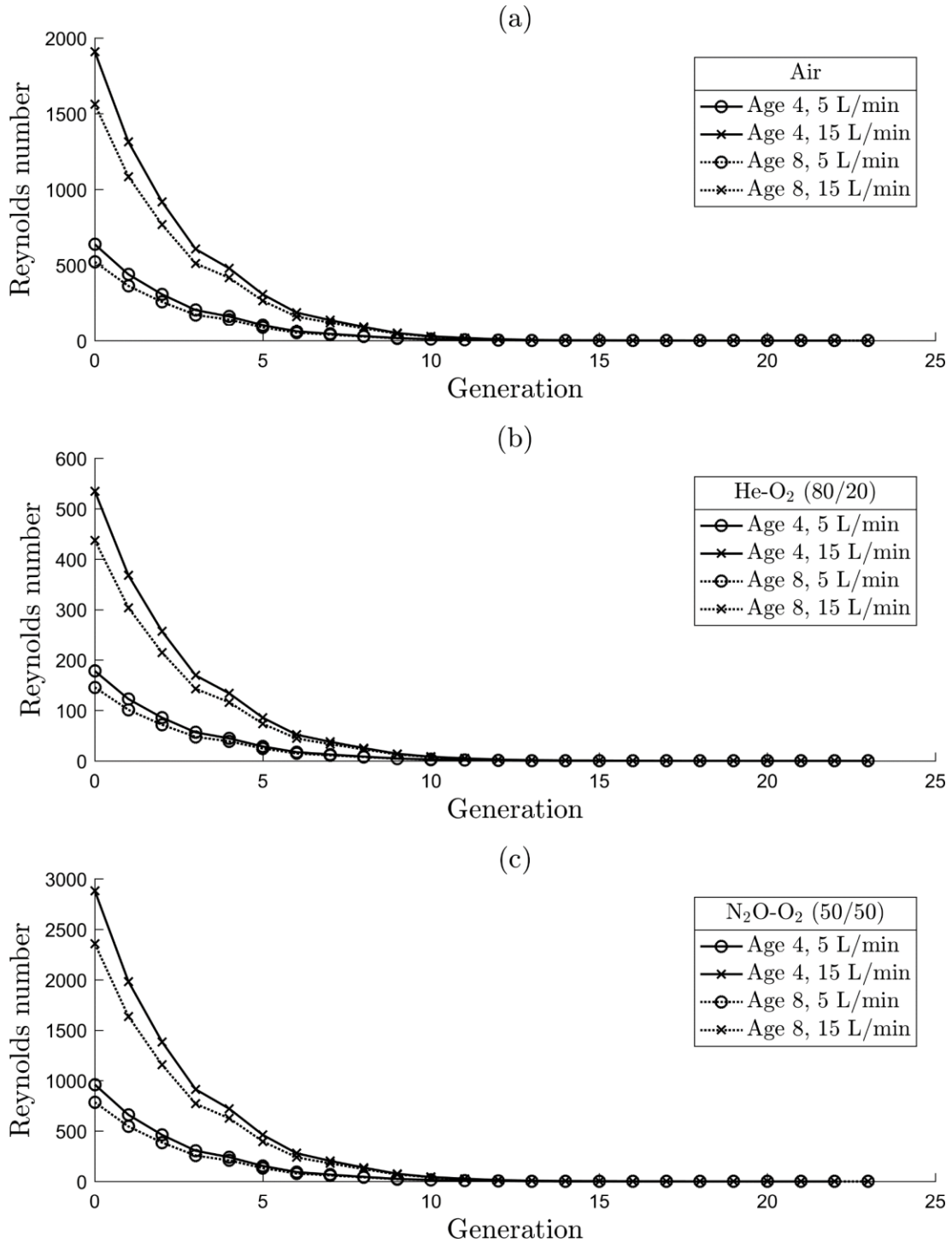


Figure 3.1: Reynolds number in each branch vs. generation number for (a) air, (b) He-O₂ (80/20), and (c) N₂O-O₂ (50/50), at ages 4 and 8 years old and flow rates of 5 and 20 L/min.

It follows that the determination of the transition generation must be done by including other factors, in addition to Reynolds number. Potential candidates for appropriate transition generations were investigated taking into account the following previous work:

1. Results from Chapter 2, where paths extended on average to generation 5 and produced pressure drop results that indicated turbulence, implying that a value of $G_T = 6$ may be considered.
2. Comparison of laminar entry length vs. airway length, as described in the following section. ($G_T = 10$)
3. Purely Pedley et al. (1970) model, assuming disturbed laminar flow throughout ($G_T = 0$).
4. Purely Modified-Blasius model, assuming no transition from turbulent to laminar flow at any generation ($G_T = \infty$).

In the current chapter, pressure drop calculations were made using various model transition generation numbers (G_T) to determine the best representation of physical behavior.

3.2.8 Entry length for laminar flow development

The entry length of a circular tube where flow becomes fully-developed and laminar is defined by White (2016) as:

$$L_e = 0.06 \cdot Re \cdot d \quad (30)$$

According to Cohen et al. (1993), for laminar flow development to occur, the criterion $L \geq L_e$ must be satisfied. This comparison of each airway length to its corresponding entry length

can indicate the generation where laminar flow may develop for a given flow rate and gas. From Eqs. (4) and (30) the criteria for sufficient length for laminar flow development is:

$$\frac{\pi\mu L}{0.24\rho Q} \geq 1 \quad (31)$$

That is, at the generation where this equation is satisfied, the flow is expected to be fully developed by the time it exits the generation. As the criterion is a description of the length required for disturbed laminar flow to become fully laminar, its use is not directly correlated with predictions of turbulence, but may be used as an approximate indicator for predicting the potential number of generations that it may propagate. Similar approximations have been done by Olson et al. (1970) who showed that the short lengths in the airway branches cause the friction of the flow regime to remain high. Also, Cohen et al. (1993) observed that the crossover point for satisfying Eq. (31) occurred between generations 5 and 10 at a flow rate of 7.5 L/min. Thus, a candidate for an approximate G_T value might be chosen at the first generation where Eq. (31) holds true.

3.3 Results

3.3.1 Total tracheobronchial pressure drop as a function of transition generation

Figure 3.2 shows the tracheobronchial pressure drop (i.e. all branching airways for a single path from generation 0 to 23 for ages 4 and 8, and flow rates of 5, 20, and 60 L/min, to illustrate the behavior of the models with the extremes of flow rates considered (from low activity to heavy exertion as described in Table 3.4). A transition generation of zero

corresponds to all branch pressure drop values being calculated purely using the Pedley et al. (1970) model; conversely, $G_T = 23$ denotes use of the modified-Blasius model in all airways. Common among all plots in Figure 3.2 is that as the transition to the Pedley model occurs further into the lung, the total pressure drop increases to a maximum and subsequently decreases as the transition generation is chosen at higher generations. The transition generations at which these maximums occur are shown in Figure 3.3 as a function of flow rate. Additionally, as G_T increases and more generations are modelled with the modified-Blasius formulation, the effects of the gas type become more prominent. This can be readily seen when comparing Eqs. (27) and (28), where the density of the former (modified-Blasius model) has a higher exponent than that of the latter (Pedley model).

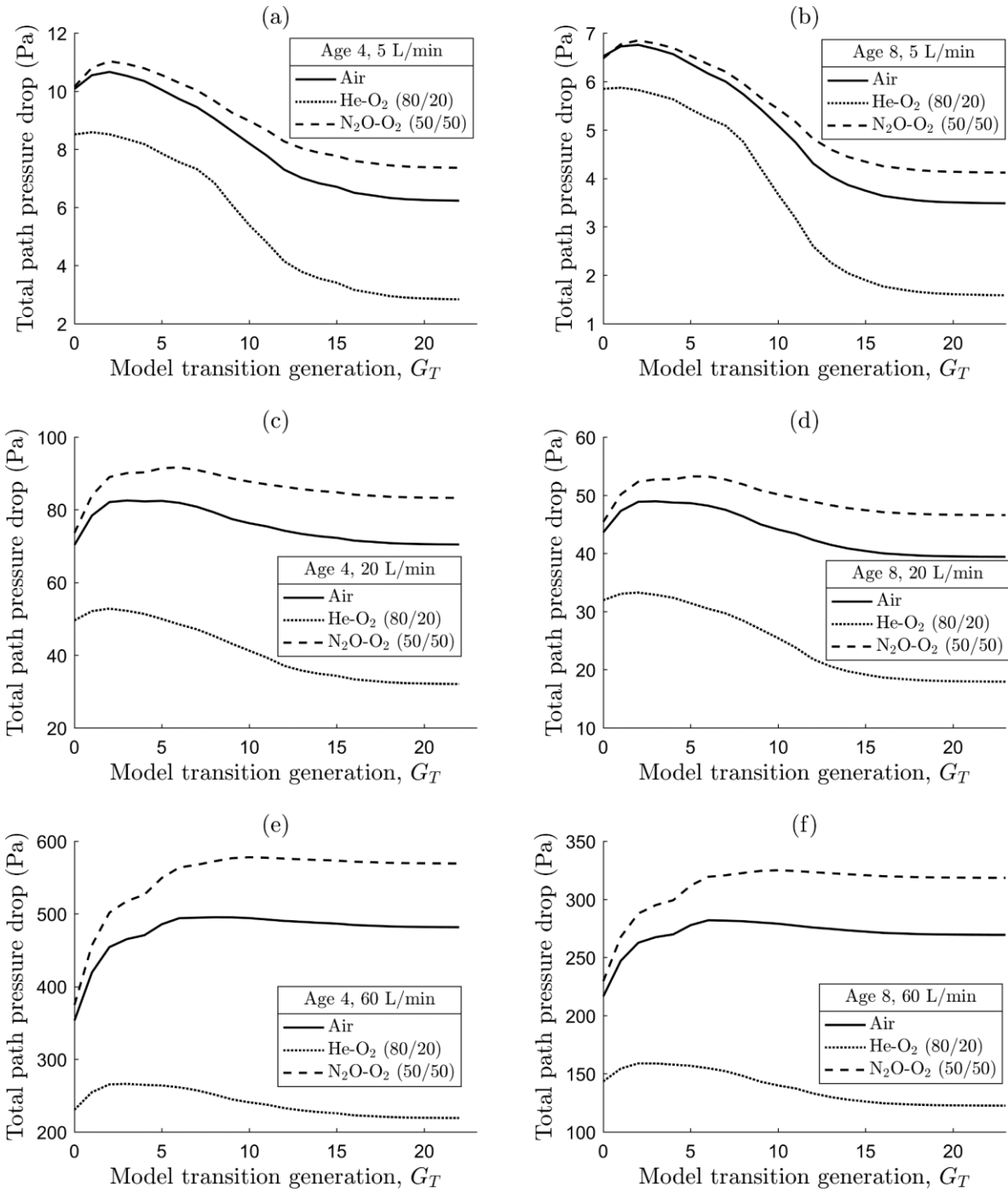


Figure 3.2: Total single-path pressure drop (generations 0–23) vs. model transition generation (changing from the modified-Blasius to the Pedley et al. (1970) model) for ages and gas flow rates of (a) 4 years, 5 L/min, (b) 8 years, 5 L/min, (c) 4 years, 20 L/min, (d) 8 years, 20 L/min, (e) 4 years, 60 L/min, and (f) 8 years, 60 L/min, respectively

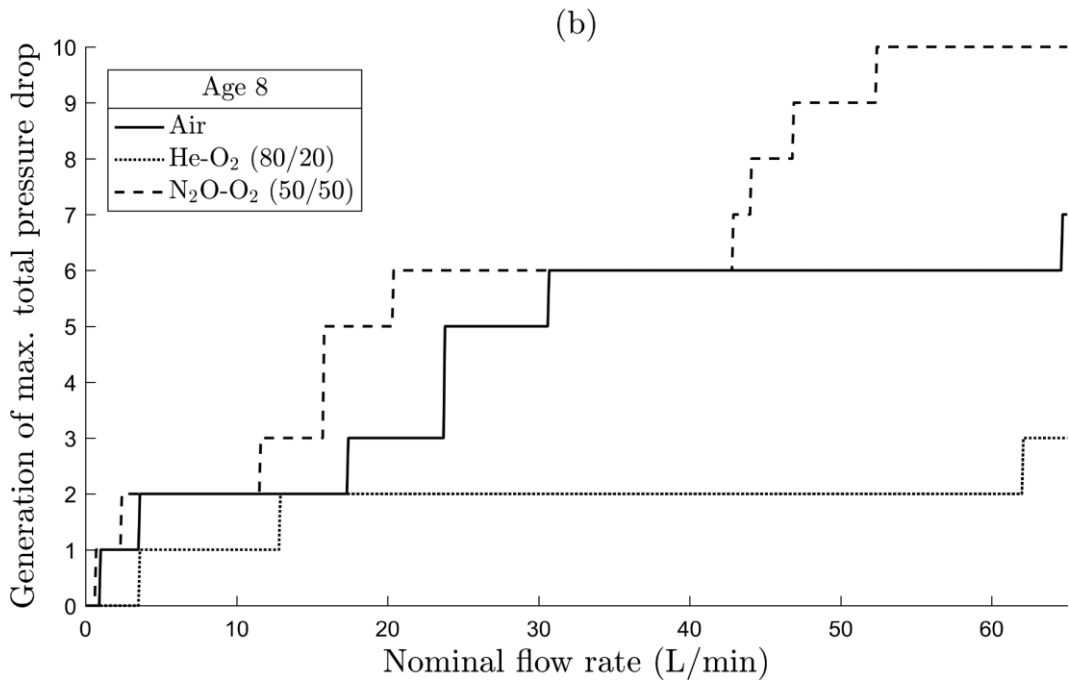
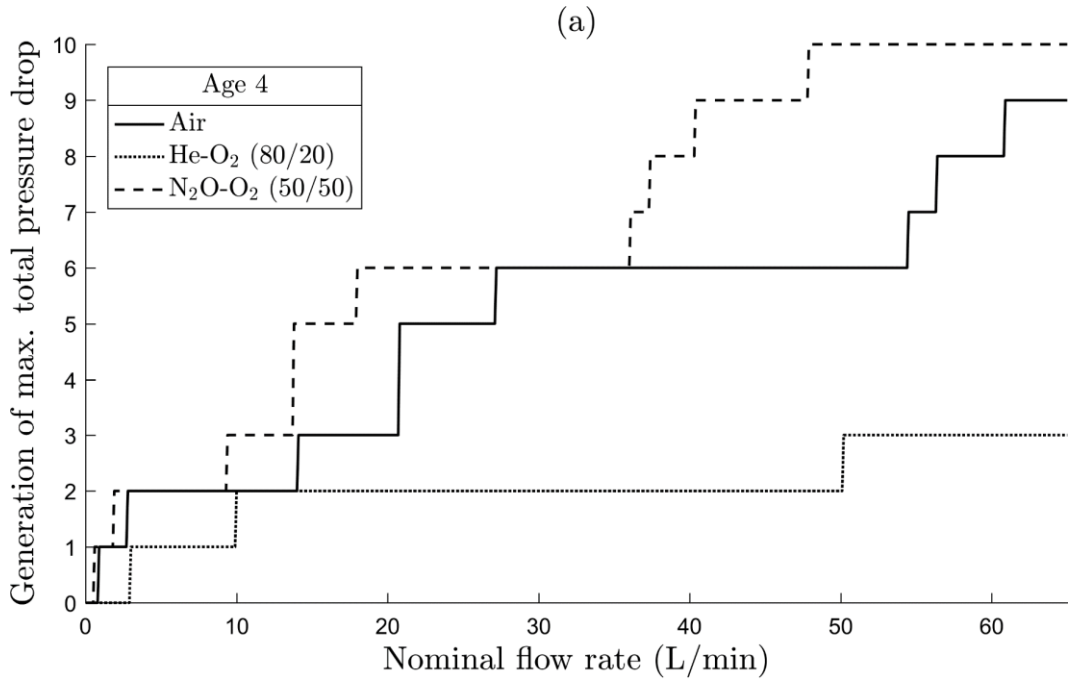


Figure 3.3: Model transition generation (from modified-Blasius to Pedley) at which the maximum branching airway pressure drop occurs, as a function of nominal tracheal flow rate for ages (a) 4 and (b) 8

3.3.2 Laminar entry length comparison with airways length

Figure 3.4 shows the ratio of airway length to laminar entry length vs. generation number. The lengths are from Table 3.1 (Finlay et al., 2000) and laminar entrance lengths are calculated with Eq. (30). A reference line at a ratio of one indicates the value above which airway length exceeds the calculated laminar entry length, such that Eq. (31) is satisfied. The first airway generation where this value exceeds 1, are shown in Figure 3.5 (i.e. where $L > L_e$).

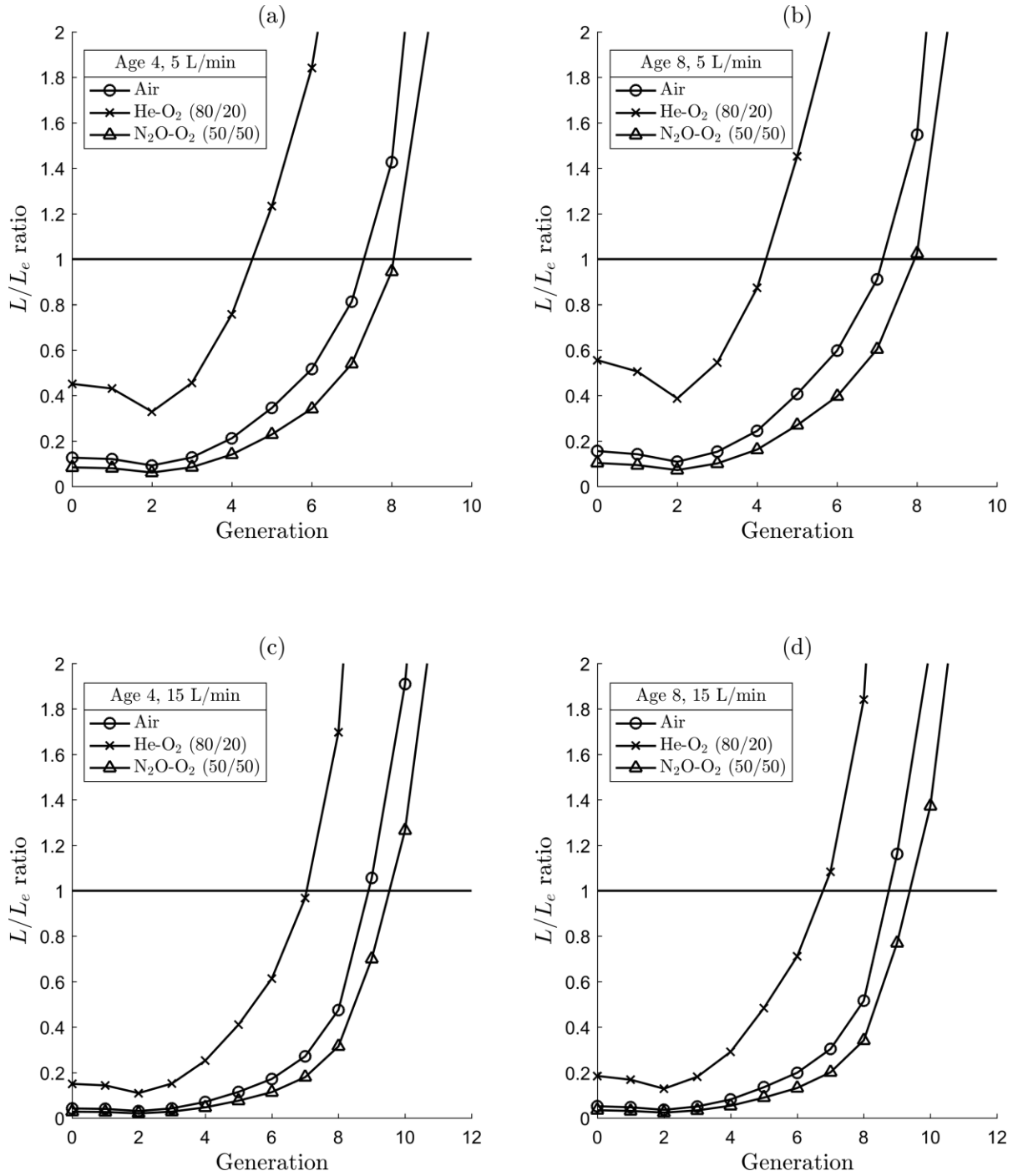


Figure 3.4: Ratio of length to laminar entry length at each airway generation for ages and flow rates of (a) 4 years and 5 L/min, (b) 8 years and 5 L/min, (c) 4 years and 15 L/min, (d) 8 years and 15 L/min, for air, He-O₂(80/20), and N₂O-O₂ (50/50).

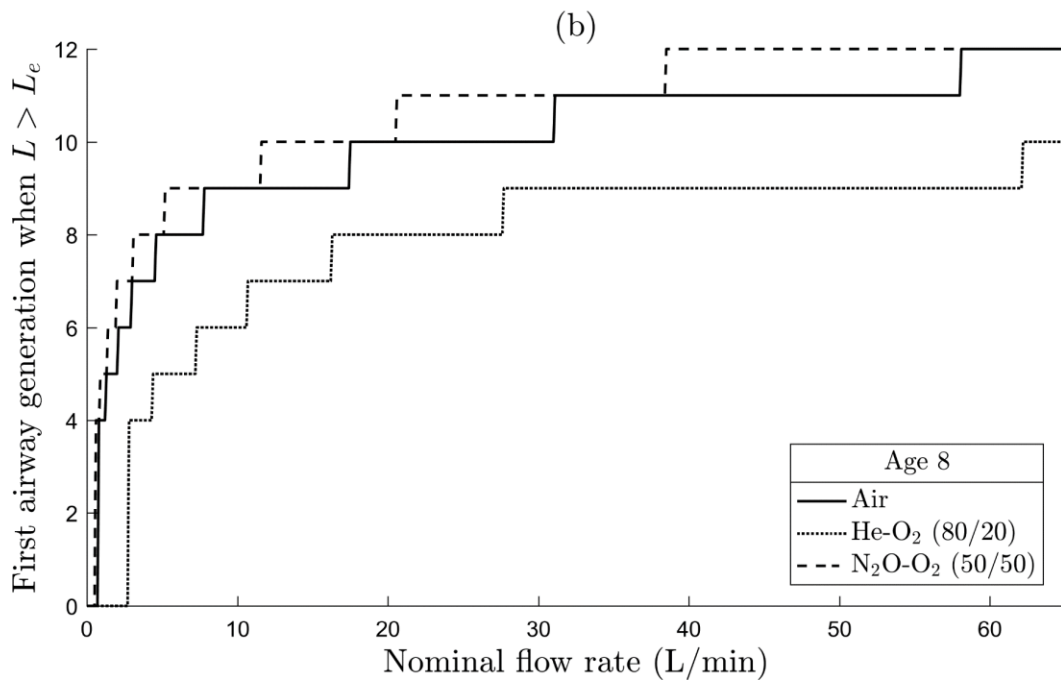
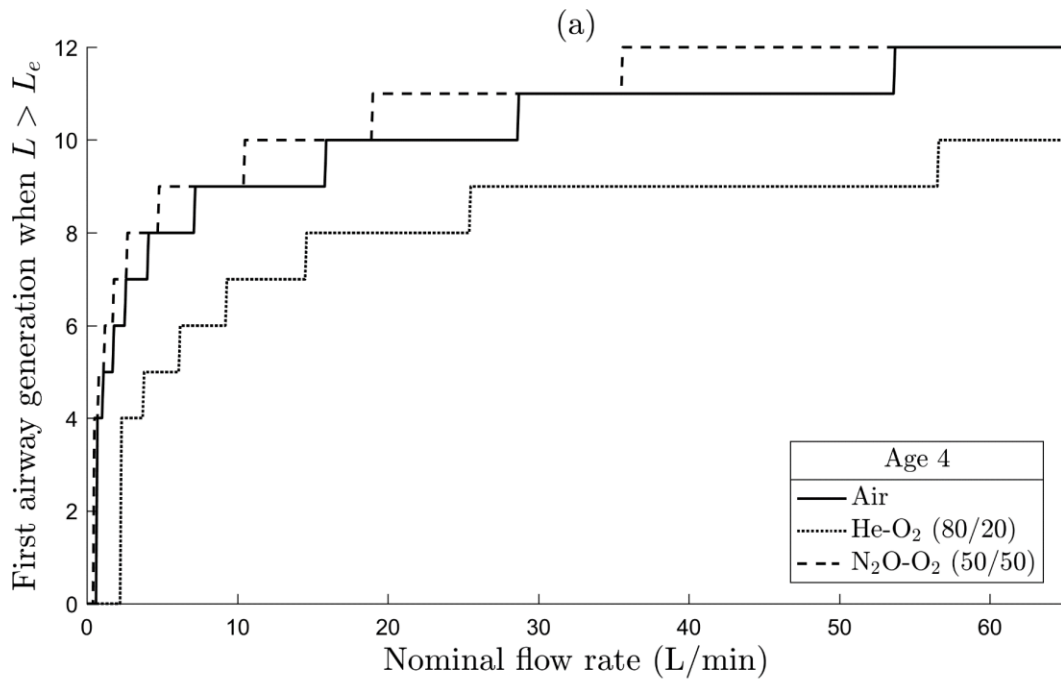


Figure 3.5: Generation of airway path where airway length, L , first exceeds laminar entry length, L_e vs. flow rate for (a) 4-year-old and (b) 8-year-old models

3.3.3 Pressure drop calculations with selected transition generation, G_T

The pressure drop vs flow rate is shown where it was calculated with three different model transition generations: (1) pure Modified-Blasius ($G_T = \infty$), (2) pure Pedley et al. (1970) ($G_T = 0$), and (3) a combination of both models, where pressure drop is calculated using the modified-Blasius model until generation 5, and uses the Pedley et al. (1970) model thereafter ($G_T = 6$). These scenarios are shown in Figure 3.6 for cases of low activity to light exertion. Figure 3.7 shows the same relationship in range of flow rates from light to heavy exertion.

Figure 3.8 shows pressure drop values by generation using a combination of Pedley and modified-Blasius models, respectively, at a constant flow rate of 14 L/min. Pressure drop values at a given generation are shown with the bar graphs while the line plot shows the corresponding cumulative value at the given generation. Panels are shown for each combination of age (4 and 8 years) and gas (air, He-O₂ (80/20), and N₂O-O₂ (50/50)).

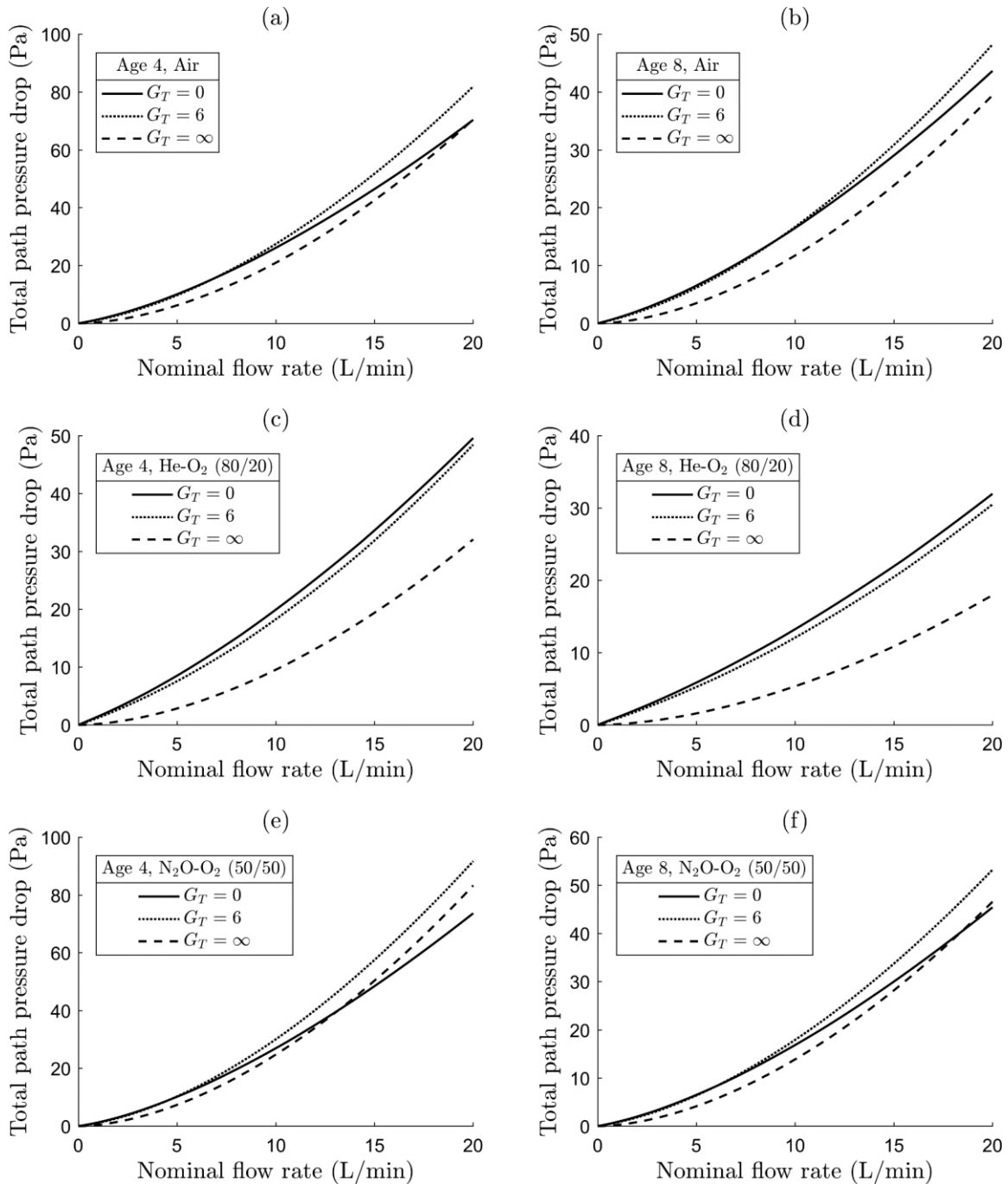


Figure 3.6: Total single-path pressure drop (generation 0–23) for low activity to light exertion (flow rates up to 20 L/min) for ages and gases (a) 4 years, air, (b) 8 years, air; (c) 4 years, He-O₂(80/20); (d) 8 years, He-O₂(80/20); (e) 4 years, N₂O-O₂(50/50); and (f) 8 years, N₂O-O₂(50/50), respectively. Total tracheobronchial pressure drops are calculated with a pure Pedley model, pure Modified-Blasius model, and a combination using Modified-Blasius before generation 6 and Pedley thereafter.

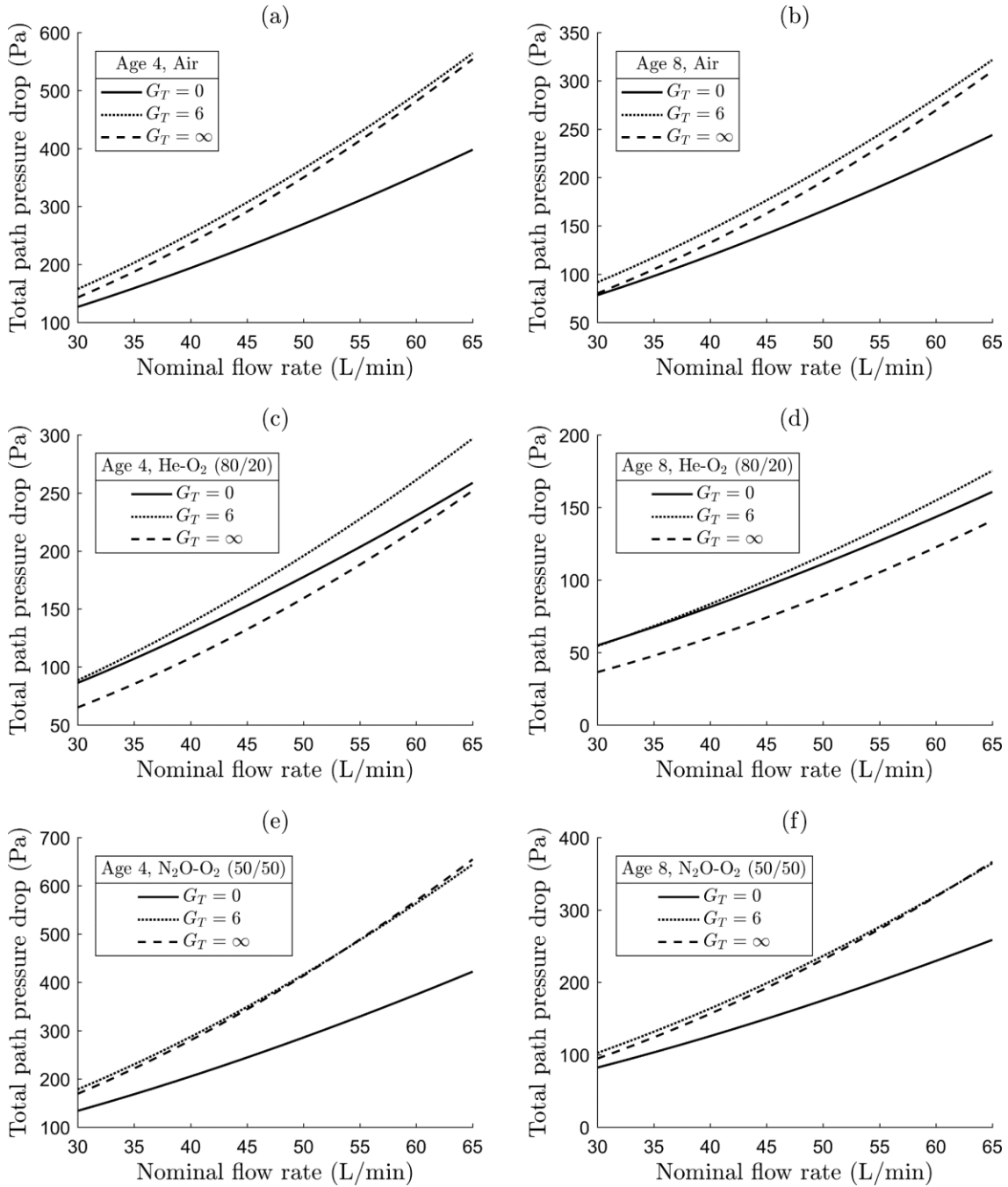


Figure 3.7: Total single-path pressure drop (generations 0–23) for light to heavy exertion level (flow rates 20–65 L/min) for ages and gases (a) 4 years, air; (b) 8 years, air; (c) 4 years, He-O₂ (80/20); (d) 8 years, He-O₂ (80/20); (e) 4 years, N₂O-O₂ (50/50); and (f) 8 years, N₂O-O₂ (50/50), respectively. Total tracheobronchial pressure drops are calculated with a pure Pedley model, pure Modified-Blasius model, and a combination using Modified-Blasius before generation 6 and Pedley thereafter.

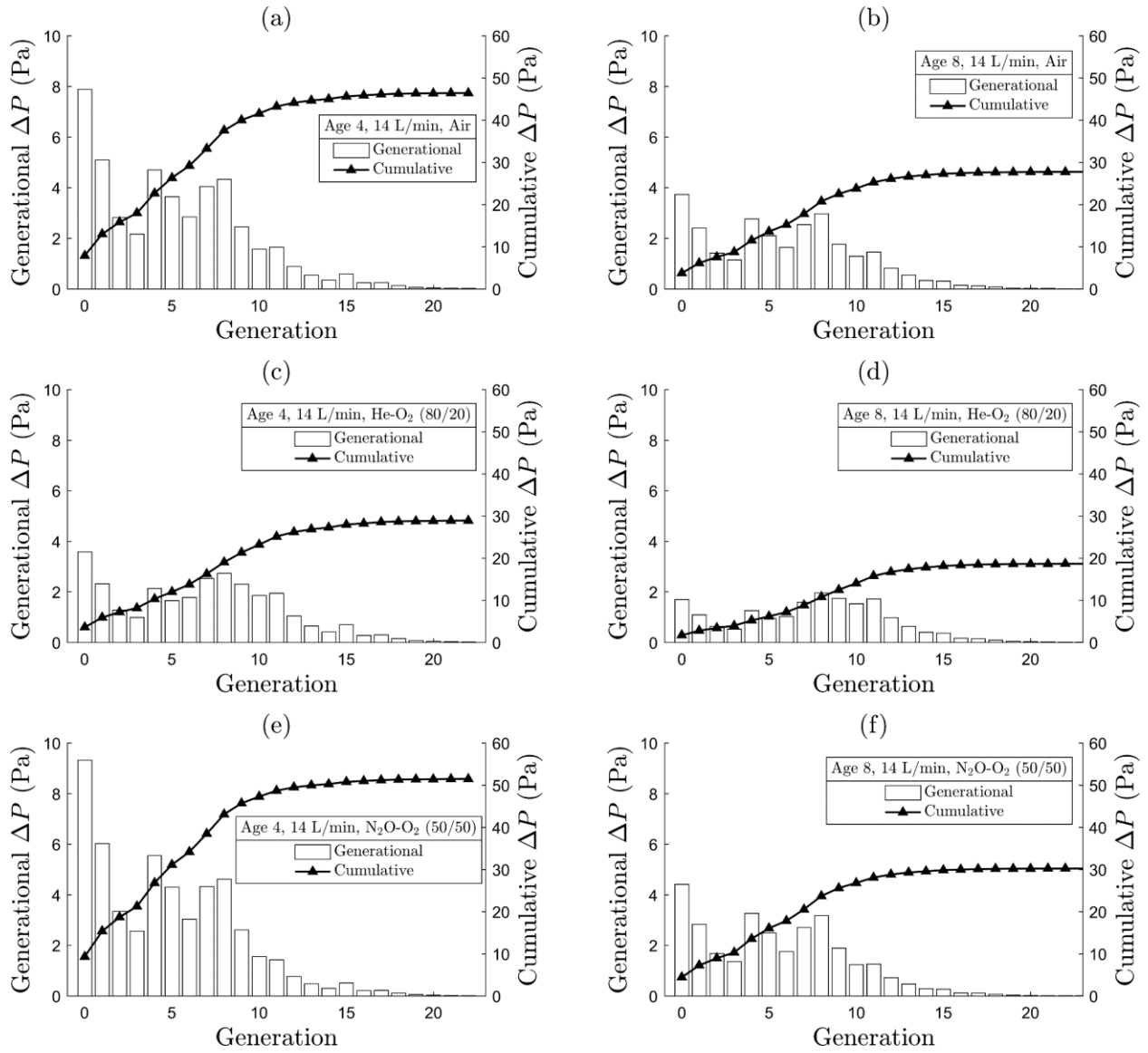


Figure 3.8: Generational and cumulative tracheobronchial pressure drop (generations 0–23) for (a) age 4, air; (b) age 8, air; (c) age 4, He-O₂ (80/20); (d) age 8, He-O₂ (80/20); (e) age 4, N₂O-O₂ (50/50); (f) age 8, N₂O-O₂ (50/50) at a constant flow rate of 14 L/min

3.4 Discussion

3.4.1 Effects of inspiratory flow rate, gas type, and model transition generation on tracheobronchial pressure drop

A main focus of the current chapter was to investigate the effects of inspiratory flow rate, gas type and model transition generation on tracheobronchial pressure drop in children ages 4–8, corresponding with the replicas studied in the previous chapter. The total prediction of tracheobronchial pressure drop will be dependent on the combination of all these variables; however, the relative effects of variables can be briefly described in isolation:

AIRWAY DIMENSIONS

The airway dimensions chosen for the model were adapted from Finlay et al. (2000) for ages 4 and 8 years old. The pressure drop dependence on age is manifested through the airway length and diameter values, which increase on average with age. It can be seen from Eqs. (27) and (28) that pressure drop is increased as airway length increases, but is decreased at a much greater rate as diameter becomes larger, thus the model pressure drop in the 4-year-old airways will be higher than that of the 8-year-old, all else being equal.

FLUID PROPERTIES

In addition to air, gas mixtures used in medical applications were studied here, namely He-O₂ (80/20) and N₂O-O₂ (50/50). In Eqs. (27) and (28), the effect of gas properties is readily visible in the contributions of viscosity and density. The isolated effects of the gas properties for each of the gases studied here is shown in Table 3.5. These were calculated using the values described in Table 3.2.

Table 3.5: Contributions of viscosity and density to the pressure drop models, modified-Blasius and Pedley (described in Eqs. (27) and (28)), and their relative contributions compared with air

Fluid	Factor of viscosity and density contributed by gas to ΔP model		Contribution to ΔP model relative to air	
	Modified-Blasius ($\mu^{0.25} \rho^{0.75}$)	Pedley ($\mu^{0.5} \rho^{0.5}$)	Modified-Blasius	Pedley
Air	0.075	0.0047	—	—
He-O ₂ (80/20)	0.034	0.0029	0.455	0.625
N ₂ O-O ₂ (50/50)	0.089	0.0050	1.18	1.07

This shows that the pressure drop in a given airway with He-O₂ (80/20) gas is expected to be 45.5% or 62.5% of that calculated by air (using a modified-Blasius or Pedley model, respectively), thus, significantly less pressure drop is expected in this case. Conversely, using N₂O-O₂ (50/50) gas, the pressure drop is expected to increase slightly above that found with air (118% or 107% of the air pressure drop, for modified-Blasius or Pedley model, respectively).

INSPIRATORY FLOW RATE

Flow rates are a function of activity level, which increase with the amount of exertion. These were found to range between 7 and 44 L/min for 4-year-olds or 10 and 63 L/min for 8-year-olds. For a single airway, the pressure drop increases faster with flow rate for the modified-Blasius model, compared to the Pedley model according to the relative magnitudes of the coefficients of Q visible in Eqs. (27) and (28).

MODEL TRANSITION GENERATION (G_T)

The total tracheobronchial pressure drop will vary based on a combination of gas properties, airway dimensions, flow rates, and pressure drop model used. A combination of the modified-Blasius and Pedley model is needed in addition to these other properties. As Reynolds numbers decrease significantly with branching generation number (Figure 3.1), a transition from turbulent flow to a disturbed laminar flow model is expected to occur at some point along each path, at the transitional generation, G_T , as represented in Eq. (29). Tracheobronchial pressure drop (across airways from generation 0 to 23) for each age and fluid was calculated analytically with a combination of the modified-Blasius model for the most proximal airways and the Pedley model in the more distal airways for all values of G_T shown in Figure 3.2. The effect of transition generation on the tracheobronchial pressure drop is most significant in the most proximal airways, as its rate of change is highest in the first few generations (i.e. roughly before generation 10). Tracheobronchial pressure drop depends less on transitions to the Pedley model in the more distal regions. This establishes the importance of the choice of model for these airways. Increasing values of transition generation also cause a magnification of the effects due to gas type. This can be seen from Eqs. (27) and (28), where the gas density in the modified-Blasius equation has a larger exponent than that of the Pedley model equation.

At lower flow rates, the Pedley model tends to predict a higher pressure drop than the modified-Blasius model. At high flow rates, the trend is reversed. The flow rates above which the modified-Blasius model begins to predict a higher tracheobronchial pressure drop are shown for each gas and age in Table 3.6. For air and N₂O-O₂ (50/50), these crossover flow rates are in the range of 16.5–23.6 L/min and 10.9–15.6 L/min, respectively, which fall close to and within the range of typical inspiratory flows, respectively. In the case of He-O₂ (80/20),

the range is much higher (58.8–84.1 L/min) and outside the range of typical inspiratory flows for the age range. This indicates that for typical flow rates, the Pedley model will nearly always predict higher pressure drop for He-O₂ (80/20). Comparing across ages for each of the described cases, the crossover flow rates are higher for age 8 than for age 4.

Table 3.6: Nominal inspiratory flow rate values at which total pressure drop from generation 0 to 23, calculated by the Pedley model, exceeds that of the modified-Blasius model

Fluid	Q (L/min) 4-year-old	Q (L/min) 8-year-old
Air	16.5	23.6
He-O ₂ (80/20)	58.8	84.1
N ₂ O-O ₂ (50/50)	10.9	15.6

Figure 3.3 shows that the maximum pressure drop value for all fluids in the range of low activity to light exertion always occurs before generation 6. This maximum is bracketed by the values of the greatest rate of change, supporting the conclusion drawn from the previous figures that the choice of model in these generations is important. However, when N₂O-O₂ (50/50) is considered at high exertion flow rates, the maximum can occur at as high as 10 generations. This indicates that pressure drop is still increasing as a function of G_T before this point.

3.4.2 Laminar entry length comparison with airway length

Laminar entry lengths were calculated for each generation and compared with airway length. The ratio of airway length, L , to entry length, L_e , (Eq. (30)) is plotted against generation for ages 4 and 8 years and flow rates in the range of typical tidal flow rates in children (Figure 3.4). A reference line at a ratio of one demarcates the point at which the airway length for a

given generation is longer than the corresponding entry length, as described in Eq. (31). In the theory discussed in Section 3.2.8, it is described that the airway length must be greater than the laminar entry length for laminar flow to develop (Cohen et al., 1993). Figure 3.4 shows that $L > L_e$ occurs at a more proximal generation for lower flow rates (e.g. for air, at generation 9 for a tracheal flow rate of 5 L/min, compared with generation 10 when flow is 15 L/min). For gases, heliox reaches the crossover point ($L > L_e$) at a lower generation than air, followed by N₂O-O₂ (50/50).

Figure 3.5 shows the first generation where $L > L_e$ as a function of flow rate. It can be seen that this crossover point is affected by flow rate and by fluid, and to a lesser extent by age (airway dimensions). Taking flow rate to be a typical tidal flow rate value of 14 L/min, the generation of crossover falls between 6 and 10. This gives an idea as to a potential choice for the generation to choose for the pressure drop model transition. It is noted that this is only an approximation, as this formula is a description of the length required for disturbed laminar flows to transition to purely laminar. This approach has been discussed in other work investigating turbulence in branching airways (Cohen et al., 1993; Olson et al., 1970). The results from the previous chapter indicated that the Modified-Blasius model appears to predict pressure drop in experimental cases in the given age range up to on average generation 5, as this is the average extent of a path in the experimental replicas. As such, a reasonable selection for the model transition generation would be generation 6. Although the entry length analysis indicates that this transition generation may be even higher, when viewed as an approximation it does support that the transition could happen in this range.

3.4.3 Relative impact of model transition generation and gas type

MODEL TRANSITION GENERATION (G_T)

Given the range of candidates for a model transition generation, it is then pertinent to understand the significance of choosing generation 6 as the model transition vs. generation 10. A test of the percent increase can be done as follows:

$$\text{Percent Increase} = \frac{\Delta P_{G_T=10} - \Delta P_{G_T=6}}{\Delta P_{G_T=6}} \times 100\% \quad (32)$$

where $\Delta P_{G_T=6}$ and $\Delta P_{G_T=10}$ are the tracheobronchial pressure drop across all branching airways, given a transition generation of 6 or 10, respectively. A calculation is done at a value of 14 L/min for each fluid and age, shown in Table 3.7. This indicates that the average percent change of the tracheobronchial path pressure drop, due to a selection of generation 10 rather than 6 for G_T is a decrease of approximately 12%. Therefore, the effect of the selection for generation of model switch between these candidate values is low, suggesting that a model transition generation of $G_T = 6$ would be appropriate and would provide results within approximately 12% of those obtained using $G_T = 10$ at typical tidal breathing flow rates.

Table 3.7: Percent increase of total branching airways pressure drop comparing model switch generations (at constant flow rate of 14 L/min)

Age (years)	Gas Type	Percent increase of tracheobronchial ΔP (G_T of 10 vs. 6)
4	Air	-9.0%
	He-O ₂ (80/20)	-17%
	N ₂ O-O ₂ (50/50)	-6.5%
8	Air	-11%
	He-O ₂ (80/20)	-19%
	N ₂ O-O ₂ (50/50)	-8.1%
<i>Average</i>		<i>-12%</i>

GAS TYPE

By selecting a value of 6 for G_T , the tracheobronchial pressure drop percent change resulting from a change of fluid can also be analysed. Pressure drop obtained when using both medical gases were compared to those obtained with air (Table 3.8). The switch from air to He-O₂ (80/20) results in substantial decreases in tracheobronchial pressure drop (38% or 33% decrease for ages 4 and 8, respectively), indicating that the employment of heliox in applications where pressure drop reduction is intended has a significant effect. When gas is changed from air to N₂O-O₂ (50/50), an increase in pressure drop is predicted (11% or 9.0% for ages 4 and 8, respectively). This increase in pressure drop is relatively low compared with the magnitude of decrease produced by He-O₂ (80/20), suggesting that negative effects on airway resistance, and subsequently work of breathing, may not be severe.

Table 3.8: Percent increase of total branching airways pressure drop comparing fluid types (at constant flow rate of 14 L/min and given a model transition generation of 6)

Age (years)	Percent increase of tracheobronchial ΔP (He-O ₂ (80/20) vs. air)	Percent increase of tracheobronchial ΔP (N ₂ O-O ₂ (50/50) vs. air)
4	-38%	11%
8	-33%	9.0%
<i>Average</i>	<i>-35%</i>	<i>9.9%</i>

COMPARISON OF CHANGING TRANSITION GENERATION VS. CHANGING GAS TYPE

Percent increase of tracheobronchial pressure drop for changing of transition generation and gas type are plotted in Figure 3.9 for a range of flow rates that encompass light activity to heavy exertion. It shows that the percentage increase due to changing gas type becomes more substantial as flow rate increases. The effects of changing to He-O₂ (80/20), however, are more pronounced than those of N₂O-O₂ (50/50). The resultant He-O₂ (80/20) percentage change is -35% at 14 L/min and goes to -46% at 60 L/min (combined averages of ages 4 and 8). In comparison, switching to N₂O-O₂ (50/50) causes percent changes of 9.9% at 14 L/min and 14% at 60 L/min. This suggests that airway resistance is at most increased by 14% during heavy exertion.

In contrast, the differences caused by changing model transition generation choice from 6 to 10 become less pronounced at higher flow rates. For flow rates of 14 L/min and 60 L/min, the respective percentage changes with a G_T of 10 rather than 6 are -9.8% and -0.5% for air, -18% and -8.7% for He-O₂ (80/20), and -7.3% and 2.1% for N₂O-O₂ (50/50), or -12% to -2.4% on

average for all fluids. This indicates that, compared to the effect of changing the fluid, a selection of $G_T = 10$ instead of 6 would be small, particularly as flow rate is increased.

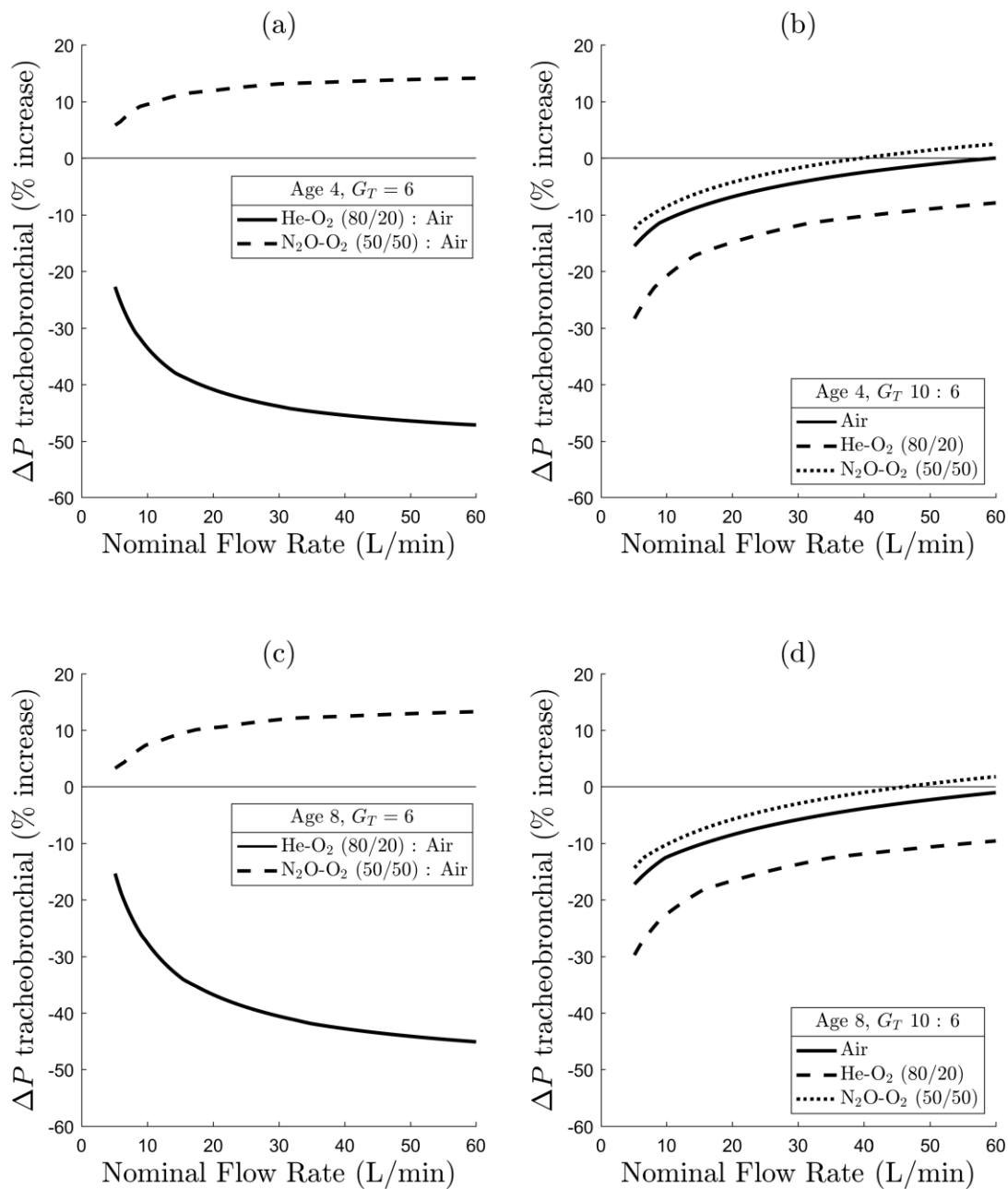


Figure 3.9: Total tracheobronchial pressure drop percent increases vs. nominal inlet flow rate, compared between cases using (a) & (c) various gases for ages 4 and 8, respectively, and a constant transition generation of 6; (b) & (d) transition generations 10 and 6, for ages 4 and 8 respectively.

3.4.4 Pressure drop calculations with selected model transition generation

Figure 3.6 shows total pressure drop from generation 0 to 23 vs. nominal flow rates for low activity to light exertion. It demonstrates how the pressure drop predicted with the Pedley et al. (1970) model is higher than the modified-Blasius model at lower flow rates, and the relationship is inverted as flow rate increases. In addition to the pure Pedley and pure modified-Blasius tracheobronchial pressure drops, it also shows the predicted value where the laminar transition occurs after generation 5 (chosen to correspond with the observations from the previous chapter where turbulent flow was seen in up to 5 generations on average). For air (Figure 3.6a, b), the combined-model tracheobronchial pressure drop is close to that of the pure Pedley model with lower flowrates (less than 10 L/min, approximately). Ultimately, at higher flow rates, nearing 20 L/min, the pressure drop exceeds both pure models. In the case of He-O₂ (80/20) (Figure 3.6c, d), for flow rates less than 20 L/min, the combined model prediction is much closer to that of the Pedley model, both of which are higher than the modified-Blasius model prediction. When N₂O-O₂ (50/50) is analyzed (Figure 3.6e, f), the combined model results resemble the pure Pedley model at flow rates less than approximately 5 L/min and then exceed both pure models at 20 L/min.

A visualization of tracheobronchial pressure drop predicted at higher flow rates corresponding to light to heavy exertion are shown in Figure 3.7. At these higher inhalation flow rates, the pressure drop predicted by the model has a different relative relationship to both pure models. For air, (Figure 3.7a, b) the combined model predicts only slightly above the pressure drop values expected with a pure modified-Blasius model, both of which are substantially higher than the corresponding pure Pedley model prediction. For He-O₂ (80/20) (Figure 3.7c, d) the combined model pressure drop prediction diverges from the pure Pedley

model prediction as flow rate increases; thus, the approximation described for the low activity flow is not applicable in this range. Figure 3.7e, f describe N₂O-O₂ (50/50) pressure drop for each scenario. This appears to show that in the higher flow rate range of low to high exertion, the combined model prediction resembles much more closely the modified-Blasius model than the Pedley model. Gas properties are therefore important for proper predictions of tracheobronchial pressure drop. The importance of the transition generation, G_T is also evident, as the pressure drop cannot be properly predicted for these gases in certain flow rate ranges by using a simple pure model.

A summary of the pressure drop values at a flow rate of 14 L/min is shown in Table 3.9. This shows that for air the combination model predicts pressure drop similar to that of the pure Pedley model (albeit slightly higher). For He-O₂ (80/20), the combined model predicts a lower pressure drop than either of the models on their own, while the pure models predict comparable values. In the case of N₂O-O₂ (50/50), the combined model predicts slightly less pressure drop than the pure models on their own, but is much closer to the Pedley prediction than in the case of He-O₂ (80/20). It should be noted, that the total tracheobronchial pressure drop at a flow rate of 14 L/min is most sensitive in the N₂O-O₂ (50/50) case, as 14 L/min falls in the general range of the point of crossover where the Pedley model prediction for pressure drop exceeds that of the modified-Blasius equation. (This occurs at flow rates of 10.9 and 15.6 L/min for ages 4 and 8, respectively (Table 3.6).)

Table 3.9: Total branching airway single path pressure drop values at a constant flow rate of 14 L/min when using a purely Pedley model, a pure modified-Blasius model and a combination of both, with a transition to the Pedley model beginning at generation 6

Age (years)	Gas Type	Pure Pedley model (Pa)	Pure Modified-Blasius model (Pa)	Combination of models (switch to Pedley at gen. 6) (Pa)
4	Air	42.1	37.7	46.4
	He-O ₂ (80/20)	30.7	17.2	28.9
	N ₂ O-O ₂ (50/50)	43.8	44.6	51.5
8	Air	26.3	21.1	27.7
	He-O ₂ (80/20)	20.1	9.6	18.7
	N ₂ O-O ₂ (50/50)	27.2	25.0	30.2

The result of the model in generational and cumulative pressure drops is shown in Figure 3.8, where a combination of the Modified-Blasius model for generations 0–5 and the Pedley model for generations 6–23 is employed. Based on the cumulative flow predictions, it is shown that the contribution of pressure drop by generations higher than approximately 15 is negligible to the total tracheobronchial pressure drop. This trend holds generally for each examined age (4 or 8 years) and for each gas. Total tracheobronchial pressure drop is highest for N₂O-O₂ (50/50), closely followed by air. For He-O₂ (80/20) the value is lower in each case. Overall, the tracheobronchial pressure drop values for all branching airways and trachea range from approximately 20 to 50 Pa. In terms of generational pressure drop, the range of maximum values is approximately 2 to 10 Pa, which is a significant portion of the overall pressure drop.

3.4.5 Tracheobronchial pressure drop relative to the upper airways

The results of tracheobronchial pressure drop have been the focus of the preceding assessments. Such a focus on these airways in the model is useful for those applications

where gas is supplied to the inlet of the trachea, as when endotracheal tubes are used. Similarly, cases where high flow gas is supplied obviate the need to consider the effects of the nasal inlet on the work of breathing of a patient, for example. However, in applications where gas is supplied at the nose, consideration of the nasal pressure drop would be important. It is thus pertinent to show a comparison of the model predictions of the current chapter with values of pressure drop that are expected to occur within the nasal airway. The experimental pressure drop measurements recorded in the previous chapter provided values of pressure drop in the nose-throat section of each replica (ΔP_{NT}), which range from 60.3 to 533.5 Pa at a near tidal breathing flow rate of 15 L/min. These values show agreement with pressure drop predicted by others at the same flow rate, such as Zhou et al. (2014), who predict 52.9 Pa in a 5 year old replica for the nostrils to larynx and Cheng et al. (1995) who predict 523.6 Pa in a replica of the nostril to nasopharynx junction of a 4 year old. In comparison, analytical branching airway pressure drop values range from 30.8 to 51.7 Pa for ages 8 and 4, respectively. This shows that nasal airway pressure drop generally outweighs that of all branching airways, in some cases by multiple factors. This contribution thus cannot be ignored in cases where nasal pressure drop affects work of breathing, such as in the nasal mask case.

3.5 Conclusions

A single path pressure drop model was developed for the branching airways of children ages 4 to 8. Various factors of influence were considered, including airway dimensions (determined by age), inhalation flow rates (a function of age and exertion levels), and fluid properties (gas type), and their impact on pressure drop was determined. A combination of the modified-Blasius model from the previous chapter and the Pedley et al. (1970) model were

used for calculating pressure drop in each airway generation. Analysis of the change in tracheobronchial pressure drop as a function of model transition generation showed that the impact of transition generation was significant in generations lower than generation 10. It was then determined that a good choice for the generation where the pressure drop model switches was at generation 6, as the replicas tested in the previous chapter had on average up to 5 branching generations per path and were shown to be described well with the modified-Blasius description. By comparing laminar entry region lengths with airway lengths, it was shown that another potential choice for the model transition generation could be generation 10. Comparison between the results obtained with a model transition generation of both 6 and 10 showed that the average tracheobronchial pressure drop change of ages 4 and 8 ranged between -7.3% and -18% during typical tidal breathing (14 L/min) and between -0.52% and -8.7% for heavy exertion (60 L/min). This indicated that a change between transition generations 6 and 10 can be considered small, especially at higher flow rates, such that generation 6 is an appropriate choice. Pressure drop changes due to changing between fluid types were also determined, showing average (across ages) pressure drop percent changes of -35% to -46% for He-O₂ (80/20) and 9.9% to 14% for N₂O-O₂ (50/50) at tidal breathing (14 L/min) and heavy exertion (60 L/min) respectively. In general, the effects of changing fluid were more pronounced at higher flow rates. He-O₂ (80/20) appears to significantly reduce pressure drop in this model. N₂O-O₂ (50/50) has a significantly smaller impact on pressure drop compared to He-O₂ (80/20) across this range of flow rates.

Using a transition generation of 6, the tracheobronchial pressure drop results were calculated and compared with flow rate. At an inspiratory flow rate typical of tidal breathing of approximately 14 L/min, it was shown that the combined model predicts higher pressure drop for air and for N₂O-O₂ (50/50) than either of the pure model cases. For He-O₂ (80/20), it was

seen that the Pedley model and combined model predicted very similar results, with the values being slightly higher in the Pedley model case. This indicates that the Pedley model is a good approximation for this gas, but that proper estimation of pressure drop at typical inspiratory flows for air would be better predicted with the combined model. At flow rates corresponding to heavy exertion (approximately 30–65 L/min), the pure modified-Blasius model may be a good approximation for total tracheobronchial pressure drop when considering air or N₂O-O₂ (50/50), but neither pure model will accurately predict for He-O₂ (80/20) at these flow rates.

3.6 Chapter Citations

Agah, J., Baghani, R., Tali, S., Hossein, S., & Tabarraei, Y. (2014). Effects of continuous use of Entonox in comparison with intermittent method on obstetric outcomes: a randomized clinical trial. *Journal of pregnancy*, 2014.

Amirav, I., Borojeni, A. A. T., Halamish, A., Newhouse, M. T., & Golshahi, L. (2015). Nasal Versus Oral Aerosol Delivery to the "Lungs" in Infants and Toddlers. *Pediatric pulmonology*, 50(3), 276-283. doi:10.1002/ppul.22999

Calmet, H., Gambaruto, A. M., Bates, A. J., Vázquez, M., Houzeaux, G., & Doorly, D. J. (2016). Large-scale CFD simulations of the transitional and turbulent regime for the large human airways during rapid inhalation. *Computers in Biology and Medicine*, 69, 166-180. doi:<https://doi.org/10.1016/j.compbimed.2015.12.003>

Cambonie, G., Milési, C., Fournier-Favre, S., Counil, F., Jaber, S., Picaud, J.-C., & Matecki, S. (2006). Clinical effects of heliox administration for acute bronchiolitis in young infants. *Chest*, 129(3), 676-682.

- Cheng, Y. S., Smith, S. M., Yeh, H. C., Kim, D. B., Cheng, K. H., & Swift, D. L. (1995). Deposition of ultrafine aerosols and thoron progeny in replicas of nasal airways of young children. *Aerosol Science and Technology*, 23(4), 541-552. doi:10.1080/02786829508965336
- Cohen, B. S., Sussman, R. G., & Lippmann, M. (1990). Ultrafine Particle Deposition in a Human Tracheobronchial Cast. *Aerosol Science and Technology*, 12(4), 1082-1091. doi:10.1080/02786829008959418
- Cohen, B. S., Sussman, R. G., & Lippmann, M. (1993). Factors affecting distribution of airflow in a human tracheobronchial cast. *Respiration Physiology*, 93(3), 261-278. doi:[https://doi.org/10.1016/0034-5687\(93\)90073-J](https://doi.org/10.1016/0034-5687(93)90073-J)
- Crawford, D. J. (1982). Identifying critical human subpopulations by age groups: radioactivity and the lung. *Physics in Medicine & Biology*, 27(4), 539.
- Darquenne, C. (2012). Aerosol deposition in health and disease. *Journal of Aerosol Medicine and Pulmonary Drug Delivery*, 25(3), 140-147.
- Darquenne, C., & Prisk, G. K. (2004). Aerosol deposition in the human respiratory tract breathing air and 80: 20 heliox. *Journal of Aerosol Medicine*, 17(3), 278-285.
- Dekker, E. (1961). Transition between laminar and turbulent flow in human trachea. *Journal of Applied Physiology*, 16(6), 1060-1064.
- Douglas, R. B., Brown, P., Knight, K., Mills, G., & Wilson, G. (1974). Letter: Effects of entonox on respiratory function. *British Medical Journal*, 2(5913), 277-277.
- Duncan, P. G. (1979). Efficacy of helium — oxygen mixtures in the management of severe viral and post-intubation croup. *Canadian Anaesthetists' Society Journal*, 26(3), 206-212. doi:10.1007/bf03006983

- Faddy, S. C., & Garlick, S. R. (2005). A systematic review of the safety of analgesia with 50% nitrous oxide: can lay responders use analgesic gases in the prehospital setting? *Emergency Medicine Journal*, *22*(12), 901.
- Finlay, W. H. (2001). *The Mechanics of Inhaled Pharmaceutical Aerosols*.
- Finlay, W. H., Lange, C. F., King, M., & Speert, D. P. (2000). Lung delivery of aerosolized dextran. *Am J Respir Crit Care Med*, *161*(1), 91-97. doi:10.1164/ajrccm.161.1.9812094
- Frazier, M. D., & Cheifetz, I. M. (2010). The Role of Heliox in Paediatric Respiratory Disease. *Paediatric Respiratory Reviews*, *11*(1), 46-53. doi:10.1016/j.prrv.2009.10.008
- Gouinaud, L., Katz, I., Martin, A., Hazebroucq, J., Texereau, J., & Caillibotte, G. (2015). Inhalation pressure distributions for medical gas mixtures calculated in an infant airway morphology model. *Computer Methods in Biomechanics and Biomedical Engineering*, *18*(12), 1358-1366. doi:10.1080/10255842.2014.903932
- Haefeli-Bleuer, B., & Weibel, E. R. (1988). Morphometry of the human pulmonary acinus. *The Anatomical Record*, *220*(4), 401-414.
- Hardin, J. C., & Patterson, J. L. (1979). Monitoring the state of the human airways by analysis of respiratory sound. *Acta Astronautica*, *6*(9), 1137-1151. doi:[https://doi.org/10.1016/0094-5765\(79\)90061-4](https://doi.org/10.1016/0094-5765(79)90061-4)
- Hofmann, W., Martonen, T., & Graham, R. (1989). Predicted deposition of nonhygroscopic aerosols in the human lung as a function of subject age. *Journal of Aerosol Medicine*, *2*(1), 49-68.
- Holroyd, I. (2008). Conscious sedation in pediatric dentistry. A short review of the current UK guidelines and the technique of inhalational sedation with nitrous oxide. *Pediatric anaesthesia*, *18*(1), 13-17.

- Katz, I., Caillibotte, G., Martin, A. R., & Arpentinier, P. (2011a). Property value estimation for inhaled therapeutic binary gas mixtures: He, Xe, N₂O, and N₂ with O₂. *Medical Gas Research*, 1, 28-28. doi:10.1186/2045-9912-1-28
- Katz, I. M., Martin, A. R., Muller, P. A., Terzibachi, K., Feng, C. H., Caillibotte, G., . . . Texereau, J. (2011b). The ventilation distribution of helium-oxygen mixtures and the role of inertial losses in the presence of heterogeneous airway obstructions. *Journal of Biomechanics*, 44(6), 1137-1143. doi:10.1016/j.jbiomech.2011.01.022
- Kudukis, T. M., Manthous, C. A., Schmidt, G. A., Hall, J. B., & Wylam, M. E. (1997). Inhaled helium-oxygen revisited: effect of inhaled helium-oxygen during the treatment of status asthmaticus in children. *The Journal of pediatrics*, 130(2), 217-224.
- Longest, P. W., Vinchurkar, S., & Martonen, T. (2006). Transport and deposition of respiratory aerosols in models of childhood asthma. *Journal of Aerosol Science*, 37(10), 1234-1257. doi:10.1016/j.jaerosci.2006.01.011
- Lyratzopoulos, G., & Blain, K. (2003). Inhalation sedation with nitrous oxide as an alternative to dental general anaesthesia for children. *Journal of Public Health*, 25(4), 303-312.
- Olson, D. E., Dart, G. A., & Filley, G. F. (1970). Pressure drop and fluid flow regime of air inspired into the human lung. *Journal of Applied Physiology*, 28(4), 482-494. doi:10.1152/jappl.1970.28.4.482
- Olson, D. E., Sudlow, M. F., Horsfield, K., & Filley, G. F. (1973). Convective patterns of flow during inspiration. *Archives of internal medicine*, 131(1), 51-57.
- Owen, P. (1969). Turbulent flow and particle deposition in the trachea. *Circulatory and Respiratory Mass Transport*, 236-252.

- Pedersen, R. S., Bayat, A., Steen, N. P., & Jacobsson, M.-L. B. (2013). Nitrous oxide provides safe and effective analgesia for minor paediatric procedures—a systematic review. *children*, 9, 11.
- Pedley, T. J., Schroter, R. C., & Sudlow, M. F. (1970). Energy losses and pressure drop in models of human airways. *Respiration Physiology*, 9(October 1969), 371-386. doi:10.1016/0034-5687(70)90093-9
- Phalen, R. F., Oldham, M. J., Beaucage, C. B., Crocker, T. T., & Mortensen, J. (1985). Postnatal enlargement of human tracheobronchial airways and implications for particle deposition. *The Anatomical Record*, 212(4), 368-380.
- Phillips, C. G., Kaye, S. R., & Schroter, R. C. (1994). A diameter-based reconstruction of the branching pattern of the human bronchial tree Part I. Description and application. *Respiration Physiology*, 98(2), 193-217. doi:[https://doi.org/10.1016/0034-5687\(94\)00042-5](https://doi.org/10.1016/0034-5687(94)00042-5)
- Piva, J. P., Barreto, S. S. M., Zelmanovitz, F., Amantéa, S., & Cox, P. (2002). Heliox versus oxygen for nebulized aerosol therapy in children with lower airway obstruction. *Pediatric Critical Care Medicine*, 3(1), 6-10.
- Pozin, N., Montesantos, S., Katz, I., Pichelin, M., Grandmont, C., & Vignon-Clementel, I. (2017). Calculated ventilation and effort distribution as a measure of respiratory disease and Heliox effectiveness. *J Biomech*, 60, 100-109. doi:10.1016/j.jbiomech.2017.06.009
- Reid, L. (1977). 1976 Edward BD Neuhauser lecture: the lung: growth and remodeling in health and disease. *American Journal of Roentgenology*, 129(5), 777-788.
- Taussig, L. M., Harris, T. R., & Lebowitz, M. D. (1977). Lung function in infants and young children: functional residual capacity, tidal volume, and respiratory rate. *American Review of Respiratory Disease*, 116(2), 233-239.

- Valli, G., Paoletti, P., Savi, D., Martolini, D., & Palange, P. (2016). Clinical use of Heliox in asthma and COPD. *Monaldi archives for chest disease*, 67(3).
- van Ertbruggen, C., Hirsch, C., & Paiva, M. (2005). Anatomically based three-dimensional model of airways to simulate flow and particle transport using computational fluid dynamics. *J. Appl. Physiol.*, 98(3), 970-980. doi:10.1152/jappphysiol.00795.2004.
- Weibel, E. R. (1963). Geometric and Dimensional Airway Models of Conductive, Transitory and Respiratory Zones of the Human Lung. In (pp. 136-142). Berlin, Heidelberg: Springer Berlin Heidelberg.
- White, F. M. (2016). *Fluid Mechanics* (8 ed.): McGraw-Hill, New York.
- Xi, J., Longest, P. W., & Martonen, T. B. (2008). Effects of the laryngeal jet on nano-and microparticle transport and deposition in an approximate model of the upper tracheobronchial airways. *Journal of Applied Physiology*, 104(6), 1761-1777.
- Xu, G. B., & Yu, C. P. (1986). Effects of Age on Deposition of Inhaled Aerosols in the Human Lung. *Aerosol Science and Technology*, 5(3), 349-357. doi:10.1080/02786828608959099
- Zhou, Y., Guo, M., Xi, J., Irshad, H., & Cheng, Y.-S. (2014). Nasal deposition in infants and children. *Journal of Aerosol Medicine and Pulmonary Drug Delivery*, 27(2), 110-116. doi:10.1089/jamp.2013.1039

Chapter 4: Conclusions

4.1 Summary and Conclusions

One objective of this thesis was to continue the work of Borojeni et al. (2015) to determine what effect the addition of an upper airway would have on pressure drop downstream in the branching airways. Pressure drop through the nose-throat and central branching airways was measured in 10 child replicas formed from CT scans data, ages 4 to 8. By comparing the coefficient of friction, C_F (Slutsky et al., 1980) with Reynolds number, Re , the functional correlation was found to be representative of turbulent flow for both the nose-throat and for the branching airways. Additionally, the pressure drop ratio of heliox and air in the branching airways indicated the presence of turbulent flow. Turbulence in the branching airways is likely a result of turbulence produced in the nose and throat and convected downstream. A “modified-Blasius model” for airway resistance, derived from the Blasius pipe friction correlation for turbulent flow, was proposed for pressure drop prediction through the bifurcating bronchial airways downstream from the upper airway.

The second objective of this thesis was to apply the modified-Blasius formulation to a single path pressure drop model in the tracheobronchial airways of children of ages 4 to 8 to determine: (a) the effects of airway dimensions, inhalation flow rates and gas properties on total tracheobronchial pressure drop and (b) the generation where a transition from a modified-Blasius model to a Pedley et al. (1970) model should occur. A combination of the modified-Blasius model in the more proximal airways and the model in more distal airways was used for calculating pressure drop in each tracheobronchial generation.

Analysis of tracheobronchial pressure drop as a function of model transition generation showed that the selection of transition generation was significant in generations lower than generation 10. It was determined that generation 6 is an appropriate choice for the transition from the modified-Blasius model to the Pedley model based on the average path length of 5 generations in the replicas, wherein pressure drop was shown to be best described with the modified-Blasius formulation. Assessment of laminar development lengths in all airways suggested an alternative transition generation of 10. However, switching models at generation 10 instead of 6 resulted in changes in tracheobronchial pressure drop ranging between -7.3% and -18% for typical tidal breathing (14 L/min) and -0.52% and -8.7% for heavy exertion (60 L/min), indicating that a transition generation of 6 remains an appropriate choice, with comparatively low impact versus generation 10. The pressure drop effects of changing air to another fluid were percent changes of -35% to -46% for He-O₂ (80/20) and 9.9% to 14% for N₂O-O₂ (50/50) at tidal breathing (14 L/min) and heavy exertion (60 L/min) respectively (age-averaged). Changing fluid has more impact at higher flow rates. He-O₂ (80/20) is shown to reduce pressure drop significantly while N₂O-O₂ (50/50) has less impact on pressure drop across this range of flow rates.

Defining the model with a transition generation of 6, the tracheobronchial pressure drop results were calculated. At typical tidal breathing flow rates (14 L/min), the combined model predicted higher pressure drop with air and N₂O-O₂ (50/50) than either of the pure model cases. With He-O₂ (80/20), the Pedley model and combined model predicted very similar results (although slightly higher in the Pedley model case) indicating that the Pedley model is a good approximation of pressure drop for this gas at typical inspiratory flows, but better predictions would result from the combined model. At flow rates nearing heavy exertion (30–65 L/min), total tracheobronchial pressure drop is reasonably well approximated with the

pure modified-Blasius model for air or N₂O-O₂ (50/50), but the combined model differs from the pure models for He-O₂ (80/20) at these higher flow rates. It is suggested that the use of the modified-Blasius equation for analytical predictions in the first 5 generations of the conducting airways, in conjunction with the Pedley model in the more distal airways, provides an improvement for pressure drop prediction in the lungs of 4- to 8-year-old children.

The research in this thesis proposes improvements to models for pressure drop and airway resistance in the branching airways of children. In general, this was done by determining that a modified-Blasius model best describes pressure drop in the central airways of children, and subsequently determining how such a model may be used in conjunction with a disturbed laminar flow model such as the (Pedley et al., 1970) model to make pressure drop predictions across the entire tracheobronchial tree. It is intended that these results will be beneficial to other researchers involved in developing airway resistance models.

4.2 Assumptions, Limitations and Future Work

This work has provided further insight into the flow behavior and resultant pressure drop in the conducting airways of children. In vitro methods have been used successfully by many researchers to study flow effects in replicas of human airways (Borojeni et al., 2015; Garcia et al., 2009; Golshahi et al., 2011; Storey-Bishoff et al., 2008). The applicability of the in vitro methods used in this work requires the justification of certain simplifying assumptions. One consideration for validation of the flow behaviour is surface roughness. An ideal replica would have negligible roughness to replicate the conditions of the lung. Surface roughness in replicas used by Xi et al. (2012) was less than 0.1 mm and was argued to be negligible. The models used by Tavernini et al. (2018) which were produced in a fashion identical to those

used in this work (same 3D-printer model and material) had much lower roughness (1.9 μm). This indicates that surface roughness can be considered negligible in these experiments, thereby adequately representing physical geometries. The experimental results also involved a simplification of breathing rates by using a constant inspiratory flow rather than a physical tidal breathing pattern, based on the assumption that any transient behaviour of the flow can be considered negligible. The importance of the transient terms in the Navier-Stokes equations relative to the convective terms are denoted by the Strouhal number. Finlay (2001) analysed breathing in adults at flow rates of 18–60 L/min and found that the Strouhal numbers throughout all generations of the central airways were amply high to justify neglecting transient effects. Gases used for the measurements were all done at conditions of room temperature, which ranged between 23.1°C and 25.2°C and relative humidity less than 50%. These results are not anticipated to differ greatly from those of the same gases at fully saturated body temperature. Changes in air density between these conditions are calculated to be small (1.206 kg/m³ vs. 1.11 kg/m³) which would affect pressure drop results by approximately less than 5%. Likewise, air dynamic viscosity changes by less than 1% when relative humidity increases from 0 to 100% at 25°C (Kestin and Whitelaw, 1964), whereas increasing temperature from 25°C to 37°C increases viscosity by less than 4% (Katz et al., 2011a).

The in vitro methods presented here have proved an effective way to better understand flow behaviour in the respiratory system. There are yet many aspects related to this work of which further investigation would be beneficial. The results from Chapter 2 show that the behavior in the first few generations of airway replicas are well represented by a modified-Blasius equation with some constant value coefficient. The average value of coefficients from all subjects was found, and applied to the model as a constant coefficient, C . When calculating

pressure drop analytically for all replicas using this constant-coefficient modified-Blasius model, the results did not accurately predict absolute value pressure drop in these airways. An attempt was made to find a correlation between physical properties of subjects and C , such as diameter, height and age. However, none of the known physical properties of the subjects produced any strong correlation. Further work could focus on finding correlations for other physical properties that were unknown in this case.

Another area of interest would be applying the same analysis in this thesis to replicas of adult subjects, which were not included in this study. It would be valuable to understand whether the modified-Blasius formulation were also a valid model for adult airways. Additionally, an analysis of an approximate transition generation for an adult age range could also be done, similar to the work presented here.

To complement the experimental results, another useful approach would be that of computational fluid dynamics (CFD) simulations. By performing simulations on the geometries of the replicas studied here, more insight into the actual behavior in certain branches of the airway and at certain generations would be available. Ideally, obtaining data for each of these subjects comparable to that of Calmet et al. (2016) or Xi et al. (2008) where any turbulent effects convected downstream into the branching airways would be visible.

4.3 Chapter Citations

Borojeni, A. A., Noga, M. L., Martin, A. R., & Finlay, W. H. (2015). Validation of airway resistance models for predicting pressure loss through anatomically realistic conducting airway replicas of adults and children. *Journal of Biomechanics*, 48(10), 1988-1996. doi:10.1016/j.jbiomech.2015.03.035

- Calmet, H., Gambaruto, A. M., Bates, A. J., Vázquez, M., Houzeaux, G., & Doorly, D. J. (2016). Large-scale CFD simulations of the transitional and turbulent regime for the large human airways during rapid inhalation. *Computers in Biology and Medicine*, 69, 166-180. doi:<https://doi.org/10.1016/j.compbiomed.2015.12.003>
- Finlay, W. H. (2001). *The Mechanics of Inhaled Pharmaceutical Aerosols*.
- Garcia, G. J. M., Tewksbury, E. W., Wong, B. A., & Kimbell, J. S. (2009). Interindividual Variability in Nasal Filtration as a Function of Nasal Cavity Geometry. *Journal of Aerosol Medicine and Pulmonary Drug Delivery*, 22(2), 139-156. doi:10.1089/jamp.2008.0713
- Golshahi, L., Noga, M. L., Thompson, R. B., & Finlay, W. H. (2011). In vitro deposition measurement of inhaled micrometer-sized particles in extrathoracic airways of children and adolescents during nose breathing. *Journal of Aerosol Science*, 42(7), 474-488. doi:10.1016/j.jaerosci.2011.04.002
- Katz, I., Caillibotte, G., Martin, A. R., & Arpentinier, P. (2011a). Property value estimation for inhaled therapeutic binary gas mixtures: He, Xe, N(2)O, and N(2)with O(2). *Medical Gas Research*, 1, 28-28. doi:10.1186/2045-9912-1-28
- Kestin, J., & Whitelaw, J. H. (1964). The viscosity of dry and humid air. *International Journal of Heat and Mass Transfer*, 7(11), 1245-1255. doi:[https://doi.org/10.1016/0017-9310\(64\)90066-3](https://doi.org/10.1016/0017-9310(64)90066-3)
- Pedley, T. J., Schroter, R. C., & Sudlow, M. F. (1970). Energy losses and pressure drop in models of human airways. *Respiration Physiology*, 9(October 1969), 371-386. doi:10.1016/0034-5687(70)90093-9
- Slutsky, A. S., Berdine, G. G., & Drazen, J. M. (1980). Steady flow in a model of human central airways. *J Appl Physiol Respir Environ Exerc Physiol*, 49(3), 417-423.

- Storey-Bishoff, J., Noga, M., & Finlay, W. H. (2008). Deposition of micrometer-sized aerosol particles in infant nasal airway replicas. *Journal of Aerosol Science*, *39*(12), 1055-1065. doi:10.1016/j.jaerosci.2008.07.011
- Tavernini, S., Church, T. K., Lewis, D. A., Martin, A. R., & Finlay, W. H. (2018). Scaling an idealized infant nasal airway geometry to mimic inertial filtration of neonatal nasal airways. *Journal of Aerosol Science*, *118*, 14-21. doi:<https://doi.org/10.1016/j.jaerosci.2017.12.004>
- Xi, J., Berlinski, A., Zhou, Y., Greenberg, B., & Ou, X. (2012). Breathing Resistance and Ultrafine Particle Deposition in Nasal–Laryngeal Airways of a Newborn, an Infant, a Child, and an Adult. *Annals of Biomedical Engineering*, *40*(12), 2579-2595. doi:10.1007/s10439-012-0603-7
- Xi, J., Longest, P. W., & Martonen, T. B. (2008). Effects of the laryngeal jet on nano-and microparticle transport and deposition in an approximate model of the upper tracheobronchial airways. *Journal of Applied Physiology*, *104*(6), 1761-1777.

Bibliography

- Agah, J., Baghani, R., Tali, S., Hossein, S., & Tabarraei, Y. (2014). Effects of continuous use of Entonox in comparison with intermittent method on obstetric outcomes: a randomized clinical trial. *Journal of pregnancy*, 2014.
- Amirav, I., Borojeni, A. A. T., Halamish, A., Newhouse, M. T., & Golshahi, L. (2015). Nasal Versus Oral Aerosol Delivery to the "Lungs" in Infants and Toddlers. *Pediatric pulmonology*, 50(3), 276-283. doi:10.1002/ppul.22999
- Blasius, H. (1911). The similarity law in friction processes. *Physikalische Zeitschrift*, 12, 1175-1177.
- Borojeni, A. A., Noga, M. L., Martin, A. R., & Finlay, W. H. (2015). Validation of airway resistance models for predicting pressure loss through anatomically realistic conducting airway replicas of adults and children. *Journal of Biomechanics*, 48(10), 1988-1996. doi:10.1016/j.jbiomech.2015.03.035
- Borojeni, A. A. T., Noga, M. L., Vehring, R., & Finlay, W. H. (2014). Measurements of total aerosol deposition in intrathoracic conducting airway replicas of children. *Journal of Aerosol Science*, 73, 39-47. doi:10.1016/j.jaerosci.2014.03.005
- Calmet, H., Gambaruto, A. M., Bates, A. J., Vázquez, M., Houzeaux, G., & Doorly, D. J. (2016). Large-scale CFD simulations of the transitional and turbulent regime for the large human airways during rapid inhalation. *Computers in Biology and Medicine*, 69, 166-180. doi:<https://doi.org/10.1016/j.compbimed.2015.12.003>
- Cambonie, G., Milési, C., Fournier-Favre, S., Counil, F., Jaber, S., Picaud, J.-C., & Matecki, S. (2006). Clinical effects of heliox administration for acute bronchiolitis in young infants. *Chest*, 129(3), 676-682.

- Cheng, Y. S., Smith, S. M., Yeh, H. C., Kim, D. B., Cheng, K. H., & Swift, D. L. (1995). Deposition of ultrafine aerosols and thoron progeny in replicas of nasal airways of young children. *Aerosol Science and Technology*, 23(4), 541-552. doi:10.1080/02786829508965336
- Cohen, B. S., Sussman, R. G., & Lippmann, M. (1990). Ultrafine Particle Deposition in a Human Tracheobronchial Cast. *Aerosol Science and Technology*, 12(4), 1082-1091. doi:10.1080/02786829008959418
- Cohen, B. S., Sussman, R. G., & Lippmann, M. (1993). Factors affecting distribution of airflow in a human tracheobronchial cast. *Respiration Physiology*, 93(3), 261-278. doi:[https://doi.org/10.1016/0034-5687\(93\)90073-J](https://doi.org/10.1016/0034-5687(93)90073-J)
- Crawford, D. J. (1982). Identifying critical human subpopulations by age groups: radioactivity and the lung. *Physics in Medicine & Biology*, 27(4), 539.
- Damanhuri, N. S., Docherty, P. D., Chiew, Y. S., van Drunen, E. J., Desai, T., & Chase, J. G. (2014). A patient-specific airway branching model for mechanically ventilated patients. *Computational and mathematical methods in medicine*, 2014.
- Darquenne, C. (2012). Aerosol deposition in health and disease. *Journal of Aerosol Medicine and Pulmonary Drug Delivery*, 25(3), 140-147.
- Darquenne, C., & Prisk, G. K. (2004). Aerosol deposition in the human respiratory tract breathing air and 80: 20 heliox. *Journal of Aerosol Medicine*, 17(3), 278-285.
- Dekker, E. (1961). Transition between laminar and turbulent flow in human trachea. *Journal of Applied Physiology*, 16(6), 1060-1064.
- Douglas, R. B., Brown, P., Knight, K., Mills, G., & Wilson, G. (1974). Letter: Effects of entonox on respiratory function. *British Medical Journal*, 2(5913), 277-277.

- Duncan, P. G. (1979). Efficacy of helium — oxygen mixtures in the management of severe viral and post-intubation croup. *Canadian Anaesthetists' Society Journal*, 26(3), 206-212. doi:10.1007/bf03006983
- Faddy, S. C., & Garlick, S. R. (2005). A systematic review of the safety of analgesia with 50% nitrous oxide: can lay responders use analgesic gases in the prehospital setting? *Emergency Medicine Journal*, 22(12), 901.
- Ferkol, T., & Schraufnagel, D. (2014). The Global Burden of Respiratory Disease. *Annals of the American Thoracic Society*, 11(3), 404-406. doi:10.1513/AnnalsATS.201311-405PS
- Finlay, W. H. (2001). *The Mechanics of Inhaled Pharmaceutical Aerosols*.
- Finlay, W. H., Lange, C. F., King, M., & Speert, D. P. (2000). Lung delivery of aerosolized dextran. *Am J Respir Crit Care Med*, 161(1), 91-97. doi:10.1164/ajrccm.161.1.9812094
- Frazier, M. D., & Cheifetz, I. M. (2010). The Role of Heliox in Paediatric Respiratory Disease. *Paediatric Respiratory Reviews*, 11(1), 46-53. doi:10.1016/j.prrv.2009.10.008
- Garcia, G. J. M., Tewksbury, E. W., Wong, B. A., & Kimbell, J. S. (2009). Interindividual Variability in Nasal Filtration as a Function of Nasal Cavity Geometry. *Journal of Aerosol Medicine and Pulmonary Drug Delivery*, 22(2), 139-156. doi:10.1089/jamp.2008.0713
- Gemci, T., Ponyavin, V., Chen, Y., Chen, H., & Collins, R. (2008). Computational model of airflow in upper 17 generations of human respiratory tract. *Journal of Biomechanics*, 41(9), 2047-2054. doi:10.1016/j.jbiomech.2007.12.019
- Golshahi, L., Noga, M. L., Thompson, R. B., & Finlay, W. H. (2011). In vitro deposition measurement of inhaled micrometer-sized particles in extrathoracic airways of children and adolescents during nose breathing. *Journal of Aerosol Science*, 42(7), 474-488. doi:10.1016/j.jaerosci.2011.04.002

- Gouinaud, L., Katz, I., Martin, A., Hazebroucq, J., Texereau, J., & Caillibotte, G. (2015). Inhalation pressure distributions for medical gas mixtures calculated in an infant airway morphology model. *Computer Methods in Biomechanics and Biomedical Engineering*, 18(12), 1358-1366. doi:10.1080/10255842.2014.903932
- Haefeli-Bleuer, B., & Weibel, E. R. (1988). Morphometry of the human pulmonary acinus. *The Anatomical Record*, 220(4), 401-414.
- Hardin, J. C., & Patterson, J. L. (1979). Monitoring the state of the human airways by analysis of respiratory sound. *Acta Astronautica*, 6(9), 1137-1151. doi:[https://doi.org/10.1016/0094-5765\(79\)90061-4](https://doi.org/10.1016/0094-5765(79)90061-4)
- Hofmann, W., Martonen, T., & Graham, R. (1989). Predicted deposition of nonhygroscopic aerosols in the human lung as a function of subject age. *Journal of Aerosol Medicine*, 2(1), 49-68.
- Holroyd, I. (2008). Conscious sedation in pediatric dentistry. A short review of the current UK guidelines and the technique of inhalational sedation with nitrous oxide. *Pediatric anaesthesia*, 18(1), 13-17.
- Katz, I., Caillibotte, G., Martin, A. R., & Arpentinier, P. (2011a). Property value estimation for inhaled therapeutic binary gas mixtures: He, Xe, N₂O, and N₂ with O₂. *Medical Gas Research*, 1, 28-28. doi:10.1186/2045-9912-1-28
- Katz, I. M., Martin, A. R., Feng, C.-H., Majoral, C., Caillibotte, G., Marx, T., . . . Daviet, C. (2012). Airway pressure distribution during xenon anesthesia: the insufflation phase at constant flow (volume controlled mode). *Appl Cardiopulm Pathophysiol*, 16(5).
- Katz, I. M., Martin, A. R., Muller, P. A., Terzibachi, K., Feng, C. H., Caillibotte, G., . . . Texereau, J. (2011b). The ventilation distribution of helium-oxygen mixtures and the role of inertial losses in the presence of heterogeneous airway obstructions. *Journal of Biomechanics*, 44(6), 1137-1143. doi:10.1016/j.jbiomech.2011.01.022

- Kestin, J., & Whitelaw, J. H. (1964). The viscosity of dry and humid air. *International Journal of Heat and Mass Transfer*, 7(11), 1245-1255. doi:[https://doi.org/10.1016/0017-9310\(64\)90066-3](https://doi.org/10.1016/0017-9310(64)90066-3)
- Koullapis, P. G., Nicolaou, L., & Kassinos, S. C. (2018). In silico assessment of mouth-throat effects on regional deposition in the upper tracheobronchial airways. *Journal of Aerosol Science*, 117, 164-188. doi:10.1016/j.jaerosci.2017.12.001
- Kudukis, T. M., Manthous, C. A., Schmidt, G. A., Hall, J. B., & Wylam, M. E. (1997). Inhaled helium-oxygen revisited: effect of inhaled helium-oxygen during the treatment of status asthmaticus in children. *The Journal of pediatrics*, 130(2), 217-224.
- Lawrence, I., & Lin, K. (1989). A concordance correlation coefficient to evaluate reproducibility. *Biometrics*, 255-268.
- Lin, C.-L., Tawhai, M. H., McLennan, G., & Hoffman, E. A. (2007). Characteristics of the turbulent laryngeal jet and its effect on airflow in the human intra-thoracic airways. *Respiratory physiology & neurobiology*, 157(2), 295-309.
- Litwin, P. D., Reis Dib, A. L., Chen, J., Noga, M., Finlay, W. H., & Martin, A. R. (2017). Theoretical and experimental evaluation of the effects of an argon gas mixture on the pressure drop through adult tracheobronchial airway replicas. *Journal of Biomechanics*, 58, 217-221. doi:<https://doi.org/10.1016/j.jbiomech.2017.04.002>
- Longest, P. W., Vinchurkar, S., & Martonen, T. (2006). Transport and deposition of respiratory aerosols in models of childhood asthma. *Journal of Aerosol Science*, 37(10), 1234-1257. doi:10.1016/j.jaerosci.2006.01.011
- Lyratzopoulos, G., & Blain, K. (2003). Inhalation sedation with nitrous oxide as an alternative to dental general anaesthesia for children. *Journal of Public Health*, 25(4), 303-312.

- Martonen, T. B., Zhang, Z., & Lessmann, R. C. (1993). Fluid Dynamics of the Human Larynx and Upper Tracheobronchial Airways. *Aerosol Science and Technology*, 19(2), 133-156. doi:10.1080/02786829308959627
- Olson, D. E., Dart, G. A., & Filley, G. F. (1970). Pressure drop and fluid flow regime of air inspired into the human lung. *Journal of Applied Physiology*, 28(4), 482-494. doi:10.1152/jappl.1970.28.4.482
- Olson, D. E., Sudlow, M. F., Horsfield, K., & Filley, G. F. (1973). Convective patterns of flow during inspiration. *Archives of internal medicine*, 131(1), 51-57.
- Owen, P. (1969). Turbulent flow and particle deposition in the trachea. *Circulatory and Respiratory Mass Transport*, 236-252.
- Pedersen, R. S., Bayat, A., Steen, N. P., & Jacobsson, M.-L. B. (2013). Nitrous oxide provides safe and effective analgesia for minor paediatric procedures—a systematic review. *children*, 9, 11.
- Pedley, T. J., Schroter, R. C., & Sudlow, M. F. (1970). Energy losses and pressure drop in models of human airways. *Respiration Physiology*, 9(October 1969), 371-386. doi:10.1016/0034-5687(70)90093-9
- Phalen, R. F., Oldham, M. J., Beaucage, C. B., Crocker, T. T., & Mortensen, J. (1985). Postnatal enlargement of human tracheobronchial airways and implications for particle deposition. *The Anatomical Record*, 212(4), 368-380.
- Phillips, C. G., Kaye, S. R., & Schroter, R. C. (1994). A diameter-based reconstruction of the branching pattern of the human bronchial tree Part I. Description and application. *Respiration Physiology*, 98(2), 193-217. doi:[https://doi.org/10.1016/0034-5687\(94\)00042-5](https://doi.org/10.1016/0034-5687(94)00042-5)

- Piva, J. P., Barreto, S. S. M., Zelmanovitz, F., Amantéa, S., & Cox, P. (2002). Heliox versus oxygen for nebulized aerosol therapy in children with lower airway obstruction. *Pediatric Critical Care Medicine*, 3(1), 6-10.
- Pozin, N., Montesantos, S., Katz, I., Pichelin, M., Grandmont, C., & Vignon-Clementel, I. (2017). Calculated ventilation and effort distribution as a measure of respiratory disease and Heliox effectiveness. *J Biomech*, 60, 100-109. doi:10.1016/j.jbiomech.2017.06.009
- Reid, L. (1977). 1976 Edward BD Neuhauser lecture: the lung: growth and remodeling in health and disease. *American Journal of Roentgenology*, 129(5), 777-788.
- Slutsky, A. S., Berdine, G. G., & Drazen, J. M. (1980). Steady flow in a model of human central airways. *J Appl Physiol Respir Environ Exerc Physiol*, 49(3), 417-423.
- Storey-Bishoff, J., Noga, M., & Finlay, W. H. (2008). Deposition of micrometer-sized aerosol particles in infant nasal airway replicas. *Journal of Aerosol Science*, 39(12), 1055-1065. doi:10.1016/j.jaerosci.2008.07.011
- Swan, A. J., Clark, A. R., & Tawhai, M. H. (2012). A computational model of the topographic distribution of ventilation in healthy human lungs. *Journal of Theoretical Biology*, 300, 222-231.
- Taussig, L. M., Harris, T. R., & Lebowitz, M. D. (1977). Lung function in infants and young children: functional residual capacity, tidal volume, and respiratory rate. *American Review of Respiratory Disease*, 116(2), 233-239.
- Tavernini, S., Church, T. K., Lewis, D. A., Martin, A. R., & Finlay, W. H. (2018). Scaling an idealized infant nasal airway geometry to mimic inertial filtration of neonatal nasal airways. *Journal of Aerosol Science*, 118, 14-21. doi:<https://doi.org/10.1016/j.jaerosci.2017.12.004>

- Tgavalekos, N. T., Musch, G., Harris, R., Melo, M. V., Winkler, T., Schroeder, T., . . . Venegas, J. (2007). Relationship between airway narrowing, patchy ventilation and lung mechanics in asthmatics. *European Respiratory Journal*, *29*(6), 1174-1181.
- Valli, G., Paoletti, P., Savi, D., Martolini, D., & Palange, P. (2016). Clinical use of Heliox in asthma and COPD. *Monaldi archives for chest disease*, *67*(3).
- van Ertbruggen, C., Hirsch, C., & Paiva, M. (2005). Anatomically based three-dimensional model of airways to simulate flow and particle transport using computational fluid dynamics. *J. Appl. Physiol.*, *98*(3), 970-980. doi:10.1152/jappphysiol.00795.2004.
- Weibel, E. R. (1963). Geometric and Dimensional Airway Models of Conductive, Transitory and Respiratory Zones of the Human Lung. In (pp. 136-142). Berlin, Heidelberg: Springer Berlin Heidelberg.
- White, F. M. (2016). *Fluid Mechanics* (8 ed.): McGraw-Hill, New York.
- Wongviriyawong, C., Harris, R. S., Greenblatt, E., Winkler, T., & Venegas, J. G. (2012). Peripheral resistance: a link between global airflow obstruction and regional ventilation distribution. *Journal of Applied Physiology*, *114*(4), 504-514.
- Xi, J., Berlinski, A., Zhou, Y., Greenberg, B., & Ou, X. (2012). Breathing Resistance and Ultrafine Particle Deposition in Nasal–Laryngeal Airways of a Newborn, an Infant, a Child, and an Adult. *Annals of Biomedical Engineering*, *40*(12), 2579-2595. doi:10.1007/s10439-012-0603-7
- Xi, J., Longest, P. W., & Martonen, T. B. (2008). Effects of the laryngeal jet on nano-and microparticle transport and deposition in an approximate model of the upper tracheobronchial airways. *Journal of Applied Physiology*, *104*(6), 1761-1777.
- Xu, G. B., & Yu, C. P. (1986). Effects of Age on Deposition of Inhaled Aerosols in the Human Lung. *Aerosol Science and Technology*, *5*(3), 349-357. doi:10.1080/02786828608959099

Zhou, Y., Guo, M., Xi, J., Irshad, H., & Cheng, Y.-S. (2014). Nasal deposition in infants and children. *Journal of Aerosol Medicine and Pulmonary Drug Delivery*, 27(2), 110-116. doi:10.1089/jamp.2013.1039

Appendix – MATLAB Code

Chapter 2 Code

Main function

```
function [T, S, F, cAvg, N_QNOM, cNames] = MANUSCRIPT_I_CALCS()

%% SCRIPT SETUP: Setup script, arrange spot to save figures
N_QNOM = 4;    % how many different q-nominal values were tested

% ERROR FUNCTION FOR ACCUMANDAVERAGE
AVG_FUN      = @mean;
ERR_FUN      = @stderr;
PDRROP_NAME  = 'PDrop';
Q_NAME       = 'Qstp';
ATT_NAME     = 'att';
DET_NAME     = 'det';
ATTFLAG_NAME = 'attFlag';

AVG_NAME = func2str(AVG_FUN);
ERR_NAME = func2str(ERR_FUN);

% TABLE T
T_SRCFILE = 'EXPERIMENT_DATA.csv';
T_CRITERIA = {'fluidFlag', 'subNum', 'QNom', 'attFlag'};
T_VALUES   = {PDRROP_NAME, Q_NAME};
T_ACCUMFUN = {AVG_FUN, ERR_FUN};

% TABLE H
H_SRCFILE = 'HELIUX_FLOWRATE_CONVERT.csv';
H_CRITERIA = 'alicatHeliumReading';
H_VALUES   = {'actualHelioxFlowRate', 'tsiAirReading'};
H_ACCUMFUN = T_ACCUMFUN;

% TABLE E
E_SRCFILE = 'PDRROP_EMPTY.csv';
E_CRITERIA = {'fluidFlag', 'QNom'};
E_VALUES   = T_VALUES;
E_ACCUMFUN = T_ACCUMFUN;

% TABLE S
S_SRCFILE = 'SUBJECT_VALUES.csv';
S_LOOKUP  = 'subNum';
S_PROPERTIES = {'diam', 'length', 'areaAttach'};

% TABLE F
F_SRCFILE = 'FLUID_VALUES.csv';
F_LOOKUP  = 'fluidFlag';
F_PROPERTIES = {'fluidName', 'mu', 'rho', 'K_SE'};

% INITIAL GUESS FOR C:
INIT_GUESS_C = 2.5;

%% HELIUX CONVERSION DATA IMPORT
% accumulate and average the heliox Alicat-TSI flow rate conversion data
```

```

H = import_sourcedatafile(H_SRCFILE);
H = accumanddofun(H, H_VALUES, H_CRITERIA, H_ACCUMFUN);

%% IMPORT DATA FOR EXPERIMENT READINGS AND CORRECT (T)
T = import_sourcedatafile(T_SRCFILE);
T = correcthelioxflowrates(T, H, Q_NAME);
T = do_computenominalq(T, N_QNOM);
[T, T_VALUES] = accumanddofun(T, T_VALUES, T_CRITERIA, T_ACCUMFUN);
T = joinattachdetachpoints...
    (T, T_VALUES, T_CRITERIA, ATTFLAG_NAME, ATT_NAME, DET_NAME);

%% IMPORT EMPTY READINGS:
E = import_sourcedatafile(E_SRCFILE);
E = correcthelioxflowrates(E, H, Q_NAME);
E = do_computenominalq(E, N_QNOM);
E = accumanddofun(E, E_VALUES, E_CRITERIA, E_ACCUMFUN);

emptyairfun = createdropemptyfun(E, 1);
emptyhelfun = createdropemptyfun(E, 2);
pdropemptywrapper = @(q,ff) calcpdropempty(q,ff,emptyairfun, emptyhelfun);

%% ADD FLUID-SPECIFIC VARIABLES TO T (FROM F)
F = import_sourcedatafile(F_SRCFILE);
T = do_addvaluestotable(T, F, F_LOOKUP, F_PROPERTIES);

%% ADD SUBJECT-SPECIFIC VARIABLES TO T (diam, height, length).
S = import_sourcedatafile(S_SRCFILE);
T = do_addvaluestotable(T, S, S_LOOKUP, S_PROPERTIES);

%% CALCULATING PDROP DIST & NT from ATT & DET

getheadname = @(varName, funName, attName) [varName, '_', funName, '_', attName];

pDropAtt    = T.(getheadname(PDROP_NAME, AVG_NAME, ATT_NAME));
pDropDet    = T.(getheadname(PDROP_NAME, AVG_NAME, DET_NAME));
pDropErrAtt = T.(getheadname(PDROP_NAME, ERR_NAME, ATT_NAME));
pDropErrDet = T.(getheadname(PDROP_NAME, ERR_NAME, DET_NAME));
qAtt        = T.(getheadname(Q_NAME, AVG_NAME, ATT_NAME));
qDet        = T.(getheadname(Q_NAME, AVG_NAME, DET_NAME));
qErrAtt     = T.(getheadname(Q_NAME, ERR_NAME, ATT_NAME));
qErrDet     = T.(getheadname(Q_NAME, ERR_NAME, DET_NAME));

% FLOW RATE AVERAGE - BETWEEN THE ATTACHED AND DETACHED READINGS
T.Qavg = mean([qAtt, qDet], 2);

% SUDDEN EXPANSION TERM (AT ATTACHMENT POINT)
% correct for the sudden expansion (detached) value
% currently using just this Qstp but it should be the
% actual velocity (volumetric) values probably)
Q_m3s      = litre2mcube(T.Qavg);
A_m2       = T.areaAttach;
T.velAttPt = flow2vel(Q_m3s, A_m2); % flow velocity at the attachment point
P_SE       = (1/2) .* (T.rho) .* (T.K_SE) .* (T.velAttPt).^2;

% EMPTY CHAMBER PDROP
P_Empty = arrayfun(pdropemptywrapper, T.Qavg, T.fluidFlag);

```

```

% Distal and NT pressure drop
T.PDropDIST = pDropAtt - pDropDet + P_SE; % DeltaP_DIST (Distal airway pressure drop)
T.PDropNT   = pDropDet - P_SE - P_Empty; % DeltaP_NT (Nose-throat airway pressure
drop)

% ERROR PROPAGATION (ROOT SUM OF SQUARES)
T.errQ      = rssq([qErrAtt, qErrDet],2);
T.errPDropDIST = rssq([pDropErrAtt, pDropErrDet],2);
T.errPDropNT   = rssq(pDropErrDet,2); % ! assumes no error from empty chamber

%% CALCULATE RE AND CF
T.Re = flow2Re(litre2mcube(T.Qavg), T.diam, T.rho, T.mu); % Re

calcfwrapper = @(pDrop, pDropErr) calccf(pDrop, pDropErr, T.Qavg, T.errQ, T.diam,
T.rho);
[T.CF_DIST, T.errCF_DIST] = calcfwrapper(T.PDropDIST, T.errPDropDIST);
[T.CF_NT, T.errCF_NT]     = calcfwrapper(T.PDropNT, T.errPDropNT);

%% CALCULATE BLASIUS C COEFS
cNames = {'blasiusIdealC', 'blasiusAvgC'};

cIdealArray = computeblasiusidealC(T, S.subNum, INIT_GUESS_C); % subject-specific

cAvg = mean(cIdealArray);
cAvgArray = repmat(cAvg, size(cIdealArray)); % subject-independent

S.(cNames{1}) = cIdealArray;
S.(cNames{2}) = cAvgArray;

%% CALC BLASIUS PDRAP
T = do_addvaluestotable(T, S, S_LOOKUP, cNames); % add Blasius C values to table T
T = do_pdropblasius(T, cNames); % calculate analytical pDrop values

%% CLEAN UP
delNames = {'PDrop_mean_att'
'PDrop_stderr_att'
'Qstp_mean_att'
'Qstp_stderr_att'
'PDrop_mean_det'
'PDrop_stderr_det'
'Qstp_mean_det'
'Qstp_stderr_det'
'K_SE'
'areaAttach'
'velAttPt'
'blasiusIdealC'
'blasiusAvgC'};

T(:,delNames) = [];
end

% subfunctions
function [cF, cFerr] = calccf(deltaP, deltaPerr, Q_lpm, Qerr, diam, rho)
% Calculate friction coefficient (Slutsky, 1980) and error

cF = calc_cf_from_pdrop(deltaP, Q_lpm, diam, rho);
cFerr = calccferror(deltaP, deltaPerr, Q_lpm, Qerr, cF);
end

```

```

function cFerr = calccferror(deltaP, deltaPerr, Q, Qerr, cF)
    % calculate error of CF values

    pp = (deltaPerr ./ deltaP);
    qq = (Qerr ./ Q);

    cFerr = cF .* rssq([pp,qq,qq], 2);
end

```

Experimental data

```

function PDropEmpty = calcpdropempty(Q, fluidFlag, emptyairfun, emptyhelfun)
    % Returns values of pressure drop for empty in vitro chamber measurements
    % which are the pressure losses due to the exit tube.

    switch fluidFlag
        case 1
            PDropEmpty = emptyairfun(Q);
        case 2
            PDropEmpty = emptyhelfun(Q);
    end
end

function calcpdropemptyfun = createpdropemptyfun(E, fluidFlag)
    % Returns values of pressure drop for empty in vitro chamber measurements
    % which are the pressure losses due to the exit tube.

    iFluid = (E.fluidFlag == fluidFlag);
    Efluid = E(iFluid,:);

    Qslpm = Efluid.Qstp_mean;
    PDrop = Efluid.PDrop_mean;

    [a,b] = powerfit(Qslpm, PDrop);
    calcpdropemptyfun = @(q) a.*q.^b;
endfunction T = do_addvaluestotable(T, K, lookupName, propNameList)
% add values from a source table to a larger table with repeated values
% (similar to an Excel index-match function combination)

assert(~isnumeric(propNameList), 'propNames must be strings or string arrays');

if ~iscellstr(propNameList)
    propNameList = cellstr(propNameList);
end

lookup = @(propName) addvaluetotable(T, K, lookupName, propName);

for j = 1:length(propNameList)
    propName = propNameList{j};
    T.(propName) = lookup(propName);
end

```

```

end

function p = addvaluetotable(TbBig, TbSmall, lookupName, returnName)
    p = arrayfun(@(dummy) TbSmall.(returnName)(TbSmall.(lookupName)==dummy),
    TbBig.(lookupName));
    endfunction [T, valueNames, criteriaNames] = joinattachdetachpoints(...
    tbUnique, valueNames, criteriaNames, attFlagName, attName, detName)
    % Split the main table into "attached" and "detached" readings then recombine them,
    % matching each row where the criteria is the same (subNum, fluidFlag, QNom)

    idAtt = ['_' attName]; %att';
    idDet = ['_' detName]; %det';

    % Split into two tables ("attached" and "detached")
    tbAttach = tbUnique(tbUnique.attFlag==1, :);
    tbDetach = tbUnique(tbUnique.attFlag==0, :);
    assert(height(tbAttach) == height(tbDetach), 'tables do not match');

    % Remove the attFlag
    tbAttach.attFlag = [];
    tbDetach.attFlag = [];
    criteriaNames(strcmp(criteriaNames, attFlagName)) = [];

    % Append an identifier for attached or detached to each "value" reading (i.e. Q and
    Pdrop)

    valueNamesAtt = strcat(valueNames, idAtt);
    valueNamesDet = strcat(valueNames, idDet);

    tbAttach.Properties.VariableNames(valueNames) = valueNamesAtt;
    tbDetach.Properties.VariableNames(valueNames) = valueNamesDet;

    % Join the two tables back together
    valueNames = [valueNamesAtt, valueNamesDet];
    T = join(tbAttach, tbDetach);

end

```

Analytical Data

PRESSURE DROP MODELS

```

function [pDropPedley] = calcpdroppedley(Q_mcube, D_m, L_m, rho_kgm3, mu_Pas)

    Re = flow2Re(Q_mcube, D_m, rho_kgm3, mu_Pas);
    C = 1.85;
    Z = C/4/sqrt(2) .* (Re .* D_m ./ L_m).^(1/2);
    PdropHagenPois = 128*mu_Pas/pi .* L_m .* Q_mcube ./ D_m.^4;

    Z(Z < 1) = 1; % set all Z lower than 1 to 1 (gives pure Hagen-Poiseuille)

    pDropPedley = Z .* PdropHagenPois;

```

```

end

function [pDropModPed] = calcpdropmodpedley(Q_mcube, D_m, L_m, rho_kgm3, mu_Pas, gen)
% modified Pedley (1970) model (a.k.a. van Ertbruggen (2005) model) for pressure drop

    gamma = gammamodpedley(gen);
    A_m2 = diam2area(D_m);
    Re = flow2Re(Q_mcube, D_m, rho_kgm3, mu_Pas);
    U = flow2vel(Q_mcube, A_m2);
    pDropModPed = gamma.*(Re.*D_m./L_m).^(1/2).*32.*mu_Pas.*L_m.*U./D_m.^2;
end
function [gamma] = gammamodpedley(gen)
% gamma coefficient is a function of generation

    gammaVals = [0.162 0.239 0.244 0.295 0.175 0.303 0.356 0.566];
    for i=1:numel(gen)
        if gen(i)<=7
            gamma(i,1) = gammaVals(gen(i)+1);
        else
            gamma(i,1) = max(gammaVals); % ASSUMPTION: default for gen 8+
        end
    end
end
end

function pDrop = calcpdropblasius(Q_mcube, D_m, L_m, rho_kgm3, mu_Pas, blasiusC)
% Calculate pressure drop with the turbulent Blasius model
% where the coefficient C can be varied (originally C = 0.316)

%% f calculation
alpha = 0.25;
Re = flow2Re(Q_mcube, D_m, rho_kgm3, mu_Pas);
f = blasiusC .* (Re + eps).^(-alpha);

%% Velocity calculation
A_m2 = diam2area(D_m);
V = flow2vel(Q_mcube, A_m2);

pDrop = f .* (L_m./D_m) .* (1/2) .* (V.^2) .* rho_kgm3;

%% Alternative (simplified) expression
% pDrop = blasiusC*L_m.*rho_kgm3.^(3/4).*mu_Pas.^(1/4).*D_m.^(-4.75).*Q_mcube.^1.75;
end

```

ITERATIVE ANALYTICAL SOLUTION FOR BRANCHING (DISTAL) AIRWAYS PRESSURE DROP

```

function pDropFinal = computepdropdistal(subNum, qIn_litre, rho, mu, blasiusC, modelType)
% Compute distal (i.e. branching) airway pressure drop for a given subject using an
% iterative solution method

%% CONVERGENCE CONSTANTS
PATH_PDROP_RANGE_MAX = 1e-8;

%% AIRWAY DATA IMPORT: import data from Borojeni text file for the subject
[nameVec, diamVec, lenVec] = importairwaytextfile(subNum);

%% ALTER GEOMETRY: Remove distal airway extensions & shorten trachea (match NEW models)
[nameVec, diamVec, lenVec] = alterairwaygeometry(subNum, nameVec, diamVec, lenVec);

```

```

%% DEFINE GENERATIONS, DAUGHTERS, PATHS
genVec    = computegen(nameVec);
iDauVec   = calddaughterindex(nameVec);
iPathList = calcpathindexsets(nameVec);

%% PRESSURE DROP MODEL: Pressure drop and airway resistance model selection
switch modelType
case 'Pedley'
    calcmodepdrop = @(Q) calcpdroppedley(Q, diamVec, lenVec, rho, mu);
case 'ModPedley'
    calcmodepdrop = @(Q) calcpdropmodpedley(Q, diamVec, lenVec, rho, mu, genVec);
case 'Blasius'
    calcmodepdrop = @(Q) calcpdropblasius(Q, diamVec, lenVec, rho, mu, blasiusC);
end

%% ITERATIVE SOLVER: Pressure drop algorithm
qVec      = initqvec(nameVec, genVec, iDauVec, litre2mcube(qIn_litre)); % Q vector
init
reqVec    = zeros(size(qVec));
pDropVec  = calcmodepdrop(qVec);

P_DROP_TRACHEA = pDropVec(genVec==0);
calcrange_normalized = @(pathpdrop) range(pathpdrop) / P_DROP_TRACHEA;
pDropPathRange = 1;

while pDropPathRange > PATH_PDROP_RANGE_MAX

    % CALCULATE R VALUES
    rVec = pDropVec ./ qVec.^2 / rho;

    % CALCULATE Req VALUES (from distal to proximal airways)
    for gen = max(genVec):-1:0
        iValsAtGen = find(genVec'==gen);
        for p = iValsAtGen
            iDaught = iDauVec{p};
            reqDau = reqVec(iDaught);
            switch numel(iDaught)
                case 0, reqDau = [0, 0]; % outlet: 0 daughters
                case 1, reqDau(2) = Inf; % only 1 branch (rare case)
            end
            reqVec(p) = rVec(p) + (reqDau(1)^-0.5 + reqDau(2)^-0.5)^-2;
        end
    end

    % CALCULATE Q VALUES (from proximal to distal airways)
    for gen = 0:max(genVec)
        for p = find(genVec'==gen)
            iDaught = iDauVec{p};
            switch numel(iDaught)
                case 2
                    reqDau = reqVec(iDaught);
                    qVec(iDaught(1)) = qVec(p)*(reqDau(2)^0.5 / (reqDau(1)^0.5 + reqDau(2)^0.5));
                    qVec(iDaught(2)) = qVec(p) - qVec(iDaught(1));
                case 1
                    qVec(iDaught) = qVec(p);
            end
        end
    end
end

```

```

    end

    % CALCULATE PRESSURE ACROSS EACH PATH
    pDropVec      = calcmodeIpdrop(qVec);
    pDropPathList = calcpathpdrop(iPathList, pDropVec);

    % UPDATE CONVERGENCE CRITERIA TEST VALUE
    pDropPathRange = calcrange_normalized(pDropPathList);

end

% OUTPUT TOTAL DISTAL PRESSURE DROP
pDropFinal = mean(pDropPathList);

end

function [QinitVec] = initqvec(nameVec, genVec, iDauVec, Qin)
% Initialize flow values in each branch evenly divided at each bifurcation

QinitVec = zeros(numel(nameVec), 1);
QinitVec(1) = Qin;
for gen = 0:max(genVec)-1
    for p = find(genVec'==gen)
        iDaught = iDauVec{p};
        QinitVec(iDaught) = QinitVec(p)/numel(iDaught);
    end
end

end

function [pDropList] = calcpathpdrop(iPathList, pDropVec)

% pressure drop across each path
nPaths = length(iPathList);
pDropList = zeros(size(iPathList));
for j=1:nPaths
    pDropList(j) = sum(pDropVec(iPathList{j}));
end

end

function [nameVec, diamVec, lenVec] = importairwaytextfile(subNum)
% import airway dimension data for each generation of a given replica (subject)

txtFileName = ['Sub' num2str(subNum) '.txt'];

% Import data from file
fileID = fopen(txtFileName);
C = textscan(fileID, '%s %f %f');
fclose(fileID);

% Split raw data
rawNameVec = C{:,1};
rawLenVec  = C{:,2};
rawDiamVec = C{:,3};

% Format raw data
nameVec = trimDigit(rawNameVec); % remove leading numbers from names
lenVec  = rawLenVec/1000;        % convert lengths from mm to m

```

```

diamVec = rawDiamVec/1000;          % convert diameters from mm to m

end
function [nameVec] = trimDigit(rawNameVec) % Cut digits
    nameVec = regexprep(rawNameVec, '\d', '');
end

function [nameVec, diamVec, lenVec] = alterairwaygeometry(subNum, nameVec, diamVec,
lenVec)
    % Remove the distal airway extensions to match NEW models
    % New models have no extensions at outlets unlike Borojeni replicas which were added
    % for CFD simulation purposes, but are not included in these replicas.

    % Remove 10mm from all outlets (with a few exceptions which need only 2mm, 5mm removed)
    lenVec = removeextensions(nameVec, lenVec, subNum);

    % Shorten trachea length to match NEW models
    lenVec(strcmp(nameVec, 't')) = replacetrachealength(subNum);

end

function [lenVecCorr] = removeextensions(nameVec, lenVec, subNum)

    %% LONG EXTENSION REMOVAL (10 mm DEFAULTS)
    generalExtensionLength = 10 / 1000; % (10 mm) general length of MOST of the extensions
    iOut = isoutlet(nameVec);
    lenVec(iOut) = lenVec(iOut) - generalExtensionLength;      % Remove 10mm from all
outlets

    %% SHORT EXTENSION REMOVAL
    shortNameList = {};
    shortLenList = [];

    switch subNum
        case 2
            shortNameList = {'aaaaaaa'};
            shortLenList = [ 5 ];
        case 3 % 'aab' is short despite not being in <10mm category
            shortNameList = {'babaa', 'abab', 'aab'};
            shortLenList = [ 2 , 5 , 5 ];
        case 5 % 'abaab' 'bbba' are not <10mm but are short, bbba is not defined
            shortNameList = {'abaab', 'abaaa', 'aabb', 'babab', 'bbba'};
            shortLenList = [ 5 5 5 2.5 5 ];
        case 6 % potentially: abba, ababaa
            shortNameList = {'bbbababb', 'aaaa', 'aabb', 'aababab', 'abba', 'abaa',
'ababbb'};
            shortLenList = [ 5 5 5 5 0 5 0];
        case 9
            shortNameList = {'aaaba', 'aaabb', 'abaa', 'aababb', 'aaaabb'};
            shortLenList = [ 5 1 2 3 5 ];
        case 10 % 'abaaabbaa' length is unknown; not included here
            shortNameList = {'babaa', 'abaaabbb', 'abaaabbaa'};
            shortLenList = [ 0.5 5 0 ];
        case 11 % Might need to include: abaabbaaa; considered negligible here
            shortNameList = {'babbbab', 'abaabbaaa', 'abaabbb', 'babbbbaa'};
            shortLenList = [ 4.5 7.2 8.0 4.7 ];
        case 12

```

```

        shortNameList = {'baaabaab'};
        shortLenList = 2 ;
    case 13 % Some value between 2.3 and 5 mm
        shortNameList = {'aabbbb'};
        shortLenList = 3.5 ;
    case 14 % This is intentionally blank
        shortNameList = {};
        shortLenList = [];
end

%% SUBTRACT LENGTH OF SHORT EXTENSIONS
if ~isempty(shortNameList) % might update this to use ismember?
    for k = 1:length(shortNameList)
        iShorty = strcmp(nameVec, shortNameList{k});
        lenVec(iShorty) = lenVec(iShorty) + (generalExtensionLength -
shortLenList(k)/1000);
    end
end

lenVecCorr = lenVec;

end

function trachLen = replacetrachealength(subNum)
%% LENGTHS OF TRACHEAS IN NEW MODEL
subNumList = [ 2 3 5 6 9 10 11 12 13 14 ];
trachLenList = [ 17 14 14 17 17 15 17 14 20 17 ]/1000; % new models trach. len.

trachLen = trachLenList(subNumList==subNum);

end

function [daughterIndexVec] = calddaughterindex(nameVec)
% gets indices of the daughter of a given branch

parentNames = computeparentname(nameVec);
[~, parentIndex] = ismember(parentNames, nameVec);

d = accumarray(parentIndex(:), 1:numel(parentIndex), ...
    [numel(parentIndex) 1], @(x){x.'}');

genNum = computegen(nameVec); % Remove self-ref from the 0 gen daughter list

d{genNum==0}(d{genNum==0}==find(genNum==0))=[];

daughterIndexVec = d';

end

function [iPathList, sPathList] = calcpathindexsets(nameVec)
% Calculate indices for each branch that is an outlet

iOutList = find(isoutlet(nameVec));
nPaths = length(iOutList);

% Compile list of path indices for paths from inlet to every outlet
iPathList = cell(size(iOutList));
for j = 1:nPaths

```

```

    iOutlet = iOutList(j);
    iPathList{j} = iOutlet; %initialize
    name = nameVec{iOutlet};
    for k = 1:length(name)+1
        iPathList{j}(k) = find(strcmp(nameVec, name));
        name = computeparentname(name);
    end
    iPathList{j} = fliplr(iPathList{j});
end

% Show corresponding strings names for each path (optional)
sPathList = cell(size(iOutList));
for j = 1:nPaths
    names = nameVec(iPathList{j});
    sPathList{j} = strjoin(names);
end

end

function [genVec] = computegen(nameVec)
% compute the generation of a given airway branch

    genVec = computeresult(@length, nameVec);

end

function [parentNameVec] = computeparentname(nameVec) % Parent name
%% GIVES PARENT NAME OF ANY BRANCH
%% INPUT: BRANCH NAME (e.g. 'aabb')
%% OUTPUT: PARENT NAME (e.g. 'aab')

    parentNameVec = regexprep(nameVec, '.$', '');

end

function [outletIndexVec] = isoutlet(nameVec)
%% Finds all outlets in a list of distal airways names
%% INPUT: cell array of branch names (i.e. {'' 'a' 'b' 'ba' 'baa'})
%% OUTPUT: logical array of outlets (i.e. [0 1 0 0 1])

    dIndex = calcddaughterindex(nameVec); % Find indices of branch's daughters
    outletIndexVec = computeresult(@isempty, dIndex); % If no daughters exist, it's an
outlet

end

function [result] = computeresult(funName, values)
% Returns result of a function and handles the input values

if iscell(values)
    tempResult = cellfun(funName, values, 'uniformoutput', false);
    if ~ischar(cell2mat(tempResult))
        result = cell2mat(tempResult);
    elseif iscellstr(tempResult)
        result = tempResult;
    end
elseif ischar(values)
    result = funName(values);
end

```

```

else
    result = [];
end
end

```

Compute ideal coefficient for modified-Blasius equation

```

function blasiusIdealC = computeblasiusidealC(T, subNumVec, initGuessC)
% PURPOSE: Calculate ideal Blasius "C" coefficient, based on experimental data
% INPUT:   Experimental data table, subject numbers (i.e. 2, 3, [2 5 6], [2 3 5 6 ...])
% OUTPUT:  Ideal Blasius "C" coefficients -- corresponding to subject numbers
% METHOD:   Solves Lin Concordance Coefficient equation -- optimizes it to 1
% BLASIUS:  $f = C Re^{-0.25}$ 
% REF.:    - White, Fluid Mechanics, Chapter 6
%          - Lin (1990)

% get data points for this particular subject only
% (flow rate, distal pressure drop, fluid name)
assert(isnumeric(subNumVec), 'subNumVec is not numeric');
assert(istable(T), 'tbExp is not a table');
assert(min(size(subNumVec))==1, 'subnum must be an integer or 1D array of int');
assert(all(ismember(subNumVec, unique(T.subNum))), 'input subnum not valid');

SOLVER_OPTIONS = optimoptions('fsolve','Display','off');
SOLVER_INIT_GUESS_C = initGuessC;

blasiusIdealC = zeros(size(subNumVec)); % force output to be same shape as input
for k = 1:length(subNumVec)

    subNum = subNumVec(k);
    iSubNum = T.subNum == subNum;

    QAVGS      = T.Qavg(iSubNum);
    PDROPEXPS  = T.PDropDIST(iSubNum);
    RHO        = T.rho(iSubNum);
    MU         = T.mu(iSubNum);

    % For the given subject, try to solve for the slope of linear fitting analytical vs.
    % experimental pressure drop to be 1 (i.e. linoptimal - 1 = 0).

    func_to_zero = @(blasiusC) linoptimal(subNum, PDROPEXPS, QAVGS, RHO, MU, blasiusC) -
1;
    blasiusIdealC(k) = fsolve(func_to_zero, SOLVER_INIT_GUESS_C, SOLVER_OPTIONS);

end

end

function linCcc = linoptimal(subNum, pDropExp, Qavg, rho, mu, blasiusC)
% function for optimizing Lin's concordance coefficient iteratively

funblas = @(q, rho, mu) computepdropdistal(subNum, q, rho, mu, blasiusC, 'Blasius');

pAnalytic = arrayfun(funblas, Qavg, rho, mu); % analytical (Blasius) p drop

```

```

linCcc = calclinconcord(pDropExp, pAnalytic);
end

```

Chapter 3 Code

```

% MAIN SCRIPT FOR CHAPTER 3
addpath(genpath('FUNCTIONS'));
addpath(genpath('SOURCE_DATA'));

set_figures_defaults;

[T, S, F, C_AVG, N_QNOM, cNames] = MANUSCRIPT_I_CALCS(); % retrieve values from Chap. 2

DimsByAge = import_all_finlay_lung_dimensions(...
    {'FINLAY_AGE4.csv', 'FINLAY_AGE8.csv', 'FINLAY_ADULT.csv'},...
    {'age4' , 'age8', 'adult'});

SourceData.DimsByAge = DimsByAge;
SourceData.F         = F;
SourceData.C_AVG     = C_AVG;

Ggen    = make_genvals_table(SourceData, {'age4', 'age8'}, [1 2 3], 0:0.1:65);
Gsum    = make_gensums_table(Ggen);
Gmix    = make_genmixmodel_table(Ggen, 6);

```

Import airway dimensions from Finlay et al. (2000)

```

function DimsByAge = import_all_finlay_lung_dimensions(fileNames, varNames)
% Import tables from excel file with Finlay lung dimensions

fileNames = cellstr(fileNames);
varNames  = cellstr(varNames);

numFileNames = numel(fileNames);
numVarNames  = numel(varNames);

assert(numFileNames==numVarNames, 'fileNames and varNames must be same size');

for i = 1:numFileNames

    name = fileNames{i};
    var  = varNames{i};

    DimsByAge.(var) = import_each_finlay_lung_dimension(name);

end

end

function AgeTable_m = import_each_finlay_lung_dimension(fileName)
% Import tables from excel file with Finlay lung dimensions (in meters)

```

```

% Import CSV airway dimensions data file
assert(ischar(fileName), 'filename must be a string');
AgeTable_cm = import_sourcedatafile(fileName);

% Convert dimensions from cm to m
assert(containsheaders(AgeTable_cm, {'genNum', 'length_cm', 'diam_cm'}), ...
    'imported file does not contain required dimensions (genNum, length_cm, diam_cm)');

AgeStruct_m.genNum = AgeTable_cm.genNum;           % convert cm to m
AgeStruct_m.length = AgeTable_cm.length_cm / 100;
AgeStruct_m.diam    = AgeTable_cm.diam_cm / 100;

% Convert to output table format
AgeTable_m = struct2table(AgeStruct_m);

end

```

Calculate and tabulate pressure values for each flow rate, age, and gas type

TABLE OF GENERATIONAL PRESSURE DROP VALUES

```

function Ggen = make_genvals_table(SourceData, ageList, fluidList, qNomList)
% Create master data table with flow, pressure drop and entry length analysis based on
% age, fluid type, and flow rate

% Unpack SourceData
DimsByAge = SourceData.DimsByAge;
F         = SourceData.F;
C_AVG    = SourceData.C_AVG;

ageList = cellstr(ageList); % for looping elements
Ggen = table;
for age = ageList
    G = DimsByAge.(age{:});
    G.age = repmat(age, height(G), 1);

    for fluid = fluidList
        MU = fluidmu(F, fluid);
        RHO = fluidrho(F, fluid);
        calc_modblas = @(q,diam,len) calcpdropblasius(q,diam,len,RHO,MU,C_AVG);
        calc_pedley = @(q,diam,len) calcpdroppedley(q,diam,len,RHO,MU);
        G.fluid = repmat(fluid, height(G), 1);
        G.rho = repmat(RHO, height(G), 1);
        G.mu = repmat(MU, height(G), 1);

        for qNom = qNomList
            Q_MCUBE = litre2mcube(qNom);
            calc_generation_flow = @(gen) Q_MCUBE ./ (2.^ gen);
            calc_reynolds_num = @(q,diam) flow2Re(q,diam,RHO,MU);
            calc_velocity = @(q,diam) q./(pi/4 * diam.^2);
            G.qNom = repmat(qNom, height(G), 1);

            G.qMcube = calc_generation_flow(G.genNum); % Flow
            G.Re = calc_reynolds_num(G.qMcube, G.diam);
            G.vel = calc_velocity(G.qMcube, G.diam);
            G.pDropModBlas = calc_modblas(G.qMcube, G.diam, G.length); % pDrop
        end
    end
end

```

```

    G.pDropPedley      = calc_pedley(G.qMcube, G.diam, G.length);
    G.entryLengthLaminar = calc_entry_length(G.Re, G.diam, 'laminar'); % entrylen
    G.ratioLtole       = G.length ./ G.entryLengthLaminar;

    Ggen = [Ggen; G];          % Stack current slice onto main table

    end
  end
end

% Rearrange table so that age, fluid, qNom and genNum columns are listed first
allVars = Ggen.Properties.VariableNames;
firstVars = {'age', 'fluid', 'qNom', 'genNum'};
lastVars = allVars(~ismember(allVars,firstVars));

Ggen = [Ggen(:, firstVars), Ggen(:, lastVars)];

End

TABLE OF TOTAL TRACHEOBRONCHIAL PRESSURE DROP VALUES

function Gsum = make_gensums_table(Ggen)
% Create table of only total pressure drop values, square-velocity differences and
% elevation differences (energy equation) based on model switch generation

% Energy equation is  $\Delta P_{(2-1)} = ( P + (\alpha \cdot \rho \cdot v^2 / 2) + (\rho \cdot g \cdot z) )_{(2-1)}$ 
% i.e.  $\Delta P_{(2-1)} = (P_2 - P_1) + (\alpha \cdot \rho / 2) \cdot (v_2^2 - v_1^2) + (\rho \cdot g) \cdot (z_2 - z_1)$ 
% i.e.  $\Delta P_{(2-1)} = (\Delta P) + (\alpha \cdot \rho / 2) \cdot (\Delta v^2) + (\rho \cdot g) \cdot (\Delta z)$ 

ALPHA = 1; % velocity term constant
g = 9.81; % gravitational constant

iiGroups = findgroups( Ggen(:, {'age', 'fluid', 'qNom'}) );

Gsum = table;

for i = 1:max(iiGroups)

    iiThisGroup = find(i == iiGroups); % find seems to speed up performance here somehow
    ThisG = Ggen(iiThisGroup,:);
    colSize = [height(ThisG), 1];

    RHO = ThisG.rho(1);

    % Calculate DeltaP term, ie. total path pressure drop given genModelSwitch = genNum
    [ThisG.pDrop0to23, ThisG.pDrop0, ThisG.pDrop1to23] = compute_pdrop0to23(ThisG);
    ThisG.ratioPdrop0vs1to23 = ThisG.pDrop0 ./ ThisG.pDrop1to23;

    % Append values to table
    Gsum = [Gsum; ThisG];

end

origVars = varnames(Ggen);
currVars = varnames(Gsum);
addedVars = currVars(~ismember(currVars, origVars));
keepVars = {'age', 'fluid', 'qNom', 'genNum', 'rho', 'mu'};
useVars = [keepVars, addedVars];
Gsum = Gsum(:, useVars); % eliminate a few headers not applicable to this table

```

```

Gsum.Properties.VariableNames{'genNum'} = 'genModelSwitch';

% add other vars
TbDiams = unique(slicetablecols(slicetablerows(Ggen,'genNum',0),'age','diam'));
Gsum.diamTrachea = zeros(height(Gsum),1);
for age = {'age4' 'age8'}
    Gsum.diamTrachea( ismember(Gsum.age, age{:}) ) =
TbDiams.diam(ismember(TbDiams.age,age{:}));
end
    Gsum.reTrachea =
calc_reynoldsnum_litresinput(Gsum.qNom,Gsum.diamTrachea,Gsum.rho,Gsum.mu);

end

function pDropMixModel = compute_pdropmixmodel(G, genModelSwitch)

iiUseModBlas = G.genNum < genModelSwitch;
iiUsePedley = ~iiUseModBlas;
pDropMixModel = [G.pDropModBlas(iiUseModBlas); ...
                G.pDropPedley(iiUsePedley)];

end

function [pDrop0to23, pDrop0, pDrop1to23] = compute_pdrop0to23(G)
% compute total pressure drop on single path from gen 0 to 23 with a combination of
% turbulent flows and laminar flows

colSize = [height(G), 1];

pDrop0to23 = zeros(colSize);
pDrop0      = zeros(colSize);
pDrop1to23 = zeros(colSize);

for i = 1:height(G)
    genModelSwitch = G.genNum(i);
    pDropMixModel = compute_pdropmixmodel(G, genModelSwitch);

    % create arrays
    pDrop0to23(i) = sum(pDropMixModel);
    pDrop0(i)     = pDropMixModel(G.genNum==0);
    pDrop1to23(i) = pDrop0to23(i) - pDrop0(i);
end

end

TABLE OF MIXED-MODEL PRESSURE DROP VALUES

function Gmix = make_genmixmodel_table(Ggen, genModelSwitch)
% Create table of generational and cumulative pressure drop values
% where they are mixed according to a change of model (from modified-Blasius
% to Pedley at genModelSwitch

iiGroups = findgroups( Ggen(:,{'age', 'fluid', 'qNom'}) );

mixModelName = ['pDropMixedModel' 'SwitchGen' num2str(genModelSwitch)];
mixModelCumulatName = ['pDropMixedModelCumulat' 'SwitchGen' num2str(genModelSwitch)];
Ggen.(mixModelName) = zeros(height(Ggen),1);
Ggen.(mixModelCumulatName) = zeros(height(Ggen),1);

```

```

for i = 1:max(iiGroups)

    iiThisGroup = find(i == iiGroups); % find seems to speed up performance here somehow
    ThisG = Ggen(iiThisGroup,:);

    v1 = [ThisG.pDropModBlas(ThisG.genNum < genModelSwitch); ...
          ThisG.pDropPedley(ThisG.genNum >= genModelSwitch)];

    v2 = cumsum(v1);

    Ggen(iiThisGroup, mixModelName) = num2cell(v1);
    Ggen(iiThisGroup, mixModelCumulatName) = num2cell(v2);

end

Gmix = Ggen;

end

```

Calls to plot each figure

```

%% FIG 3.1
makefullfig(slicetablerows(Ggen, 'qNom', [5 15]), ...
    'groupingVars', {'age', 'qNom', 'fluid'}, ...
    'headersXY', {'genNum', 'Re'}, ...
    'panelRows', 'fluid',...
    'legendLoc', 'northeast',...
    'labelFontSize', 15,...
    'legendFontSize', 12);

%% FIG 3.2
makefullfig(slicetablerows(Gsum, 'qNom', [5 20 60]), ...
    'groupingVars', {'age', 'qNom', 'fluid'}, ...
    'headersXY', {'genModelSwitch', 'pDrop0to23'}, ...
    'panelRows', 'qNom', ...
    'panelCols', 'age', ...
    'legendLoc', 'southeast', ...
    'XLim', [0 23])

%% FIG 3.3
Gsum_genmaxpdropvsqnom = create_table(Gsum);

makefullfig(Gsum_genmaxpdropvsqnom, ...
    'groupingVars', {'age', 'fluid'}, ...
    'headersXY', {'qNom', 'genNumMaxPdrop'}, ...
    'legendLoc', 'northwest', ...
    'panelRows', 'age', ...
    'XLim' , [0 65],...
    'labelFontSize', 15,...
    'legendFontSize', 12);

function Gsum_genmaxpdropvsqnom = create_table(Gsum)
% create table for Fig plotting
groupingVars = {'age', 'fluid', 'qNom'};
inputVars = {'pDrop0to23'};

```

```

for i = 1:numel(groupingVars)
    v = groupingVars{i};
    grps(:,i) = findgroups(Gsum.(v));
end
[~,~,Ig] = unique(grps,'rows');
for j = 1:max(Ig)
    Wslice = Gsum(Ig==j,:);
    [~, Im(j)] = max(Wslice.pDrop0to23);
    genNumMaxPdrop(j,1) = Wslice.genModelSwitch(Im(j));
    qNom(j,1) = Wslice.qNom(Im(j));
    age{j,1} = Wslice.age{Im(j)};
    fluid(j,1) = Wslice.fluid(Im(j));
end
Gsum_genmaxpdropvsqnom = table(age, fluid, qNom, genNumMaxPdrop);
end

%% FIG 3.4
makefullfig(slicetablerows(Ggen, 'qNom', [5 15]), ...
    'groupingVars', {'age', 'qNom', 'fluid'}, ...
    'headersXY', {'genNum', 'ratioLtoLe'}, ...
    'panelRows', 'qNom', ...
    'panelCols', 'age', ...
    'stylePref', 'points', ...
    'legendLoc', 'northwest', ...
    'XLim', [0 12], ...
    'YLim', [0 2], ...
    'refLine', [0 1]);

%% FIG 3.5
Ggen_genmaxlengthratiovsqnom = ttt(Ggen);

makefullfig(Ggen_genmaxlengthratiovsqnom, ...
    'groupingVars', {'age', 'fluid'}, ...
    'headersXY', {'qNom', 'genLtoLeRatioCrossover'}, ...
    'panelRows', 'age', ...
    'legendLoc', 'southeast', ...
    'XLim', [0 65], ...
    'YLim', 'MatchAll', ...
    'labelFontSize', 15,...
    'legendFontSize', 12);

function Ggen_genmaxlengthratiovsqnom = ttt(Ggen)
[a,~,I] = unique(Ggen(:, {'age', 'fluid', 'qNom'}), 'rows');
genLtoLeRatioCrossover = zeros(max(I),1);
for j = 1:max(I)
    Slice = Ggen(I==j,:);
    genLtoLeRatioCrossover(j) = min(Slice.genNum(Slice.ratioLtoLe >= 1));
end
Ggen_genmaxlengthratiovsqnom = [a, table(genLtoLeRatioCrossover)];
end

%% FIG 3.6 AND 3.7
Gsum_pdroptotalvsqnom = combine_table(Gsum, 6);

makefullfig(Gsum_pdroptotalvsqnom, ...

```

```

'groupingVars', {'age', 'fluid', 'genModelSwitch'}, ...
'headersXY', {'qNom', 'pDrop0to23'}, ...
'panelRows', 'fluid', ...
'panelCols', 'age', ...
'legendLoc', 'northwest',...
'Position', [0 0 0.45 0.91], ...
'legendFontSize', 10);

function Gsum_pdroptotalvsqnom = combine_table(Gsum, GEN_SWITCH)
    X1 = slicetablerows(Gsum, 'age', 'age4', 'genModelSwitch', [0 GEN_SWITCH 22]);
    X2 = slicetablerows(Gsum, 'age', 'age8', 'genModelSwitch', [0 GEN_SWITCH 23]);
    Gsum_pdroptotalvsqnom = [X1;X2];
end

%% FIG 3.8
makefullfig(slicetablerows(Gmix, 'qNom', 14), ...
'groupingVars', {'age', 'qNom', 'fluid'}, ...
'headersXY', {'genNum', 'pDropMixedModelSwitchGen6',
'pDropMixedModelCumulatSwitchGen6'}, ...
'panelRows', 'fluid', ...
'panelCols', 'age', ...
'plotType', {'bar', 'line'}, ...
'stylePref', {'lines', 'points'}, ...
'legendLoc', 'northeast', ...
'XLim', [-1 23], ...
'YLim', 'MatchAll',...
'labelFontSize', 16);

%% FIG 3.9
PctDiffTable = main(Gsum_special, 6, 'pDrop0to23');
plotfig(PctDiffTable, 'pDrop0to23');

function PctDiffTable = main(Gsum, GEN_SWITCH, pDropVar)
% create percent differences table (both fluid and GT differences combined)
Gsum_x = slicetablecols(Gsum,'age','fluid','qNom','genModelSwitch', pDropVar);

f1 = calc_pctdiff_then_unstack_F(Gsum_x, GEN_SWITCH, [1 2], pDropVar);
f2 = calc_pctdiff_then_unstack_F(Gsum_x, GEN_SWITCH, [1 3], pDropVar);
ggg = calc_pctdiff_then_unstack_G(Gsum_x, [GEN_SWITCH 10], pDropVar);

PctDiffTable = jointtablemulti(f1,f2,ggg);
end
function FF3 = calc_pctdiff_then_unstack_F(Gsum, GEN_SWITCH, fluidPair, pDropVar)
% calculate the pct diffs and unstack the table (comparing fluid)
FF1 = slicetablerows(Gsum, 'genModelSwitch', GEN_SWITCH);
FF2 = create_pct_diff_table(FF1, pDropVar, 'fluid', fluidPair);
vA = num2str(fluidPair(1));
vB = num2str(fluidPair(2));
FF3 = unstack_renamecols_with_varnames(FF2, ['pctdiff_fluid' vB 'vs' vA],
'genModelSwitch');
end
function GG3 = calc_pctdiff_then_unstack_G(Gsum, genPair, pDropVar)
% calculate the pct diffs and unstack the table (comparing GT)
GG2 = create_pct_diff_table(Gsum, pDropVar, 'genModelSwitch', genPair);
vA = num2str(genPair(1));
vB = num2str(genPair(2));
GG3 = unstack_renamecols_with_varnames(GG2, ['pctdiff_genModelSwitch' vB 'vs' vA],
'fluid');

```

```

end
function TablePctDiff = create_pct_diff_table(Gsum, valVar, indVar, comparePair)
    % create table of percent differences

    GsumSlice = slicetablerows(Gsum, indVar, comparePair);

    GsumSlice.(indVar) = regexprep(cellstr(num2str(GsumSlice.(indVar))), '\s*(\d+)',
[indVar '$1']);

    gu = unstack(GsumSlice, valVar, indVar);

    vA = num2str(comparePair(1));
    vB = num2str(comparePair(2));
    xA = [indVar vA];
    xB = [indVar vB];

    pctChange = (gu.(xB) - gu.(xA)) ./ gu.(xA) * 100;
    gu.(['pctdiff_' indVar vB 'vs' vA]) = pctChange;    %calc_percent_diff(gu.(xA),
gu.(xB));

    gu.(xA) = [];
    gu.(xB) = [];

    TablePctDiff = gu;

end
% PLOTS
function plotfig(PctDiffTable, pDropVar)
    % plot entire figure

    figure('name', pDropVar);

    fluidPctDiffs = ...
        {'pctdiff_fluid2vs1_genModelSwitch6', ...
        'pctdiff_fluid3vs1_genModelSwitch6'};

    genSwitchPctDiffs = ...
        {'pctdiff_genModelSwitch10vs6_fluid1', ...
        'pctdiff_genModelSwitch10vs6_fluid2', ...
        'pctdiff_genModelSwitch10vs6_fluid3'};

    % Plot panels
    subplot(2,2,1); hold on; plotpanel(PctDiffTable, 'age4', fluidPctDiffs);
    subplot(2,2,2); hold on; plotpanel(PctDiffTable, 'age4', genSwitchPctDiffs);
    subplot(2,2,3); hold on; plotpanel(PctDiffTable, 'age8', fluidPctDiffs);
    subplot(2,2,4); hold on; plotpanel(PctDiffTable, 'age8', genSwitchPctDiffs);

    axArr = findall(gcf,'type','axes');
    for i = 1:numel(axArr)
        ax = axArr(i);
        r=refline(ax, 0,0); set(r,'linewidth',0.5);
    end
end
function plotpanel(PctDiffTable, age, yVarArr)
    % plot a one panel on the subplot

    Table = slicetablerows(PctDiffTable, 'age', age);

```

```

legendEntries = yVarArr;
legendEntries = regexp(legendEntries, 'pctdiff_genModelSwitch.*_fluid(\d+)', 'Fluid
$1');
legendEntries = regexp(legendEntries, 'pctdiff_fluid(\d+)vs(\d+)_.*', 'Fluid $1 \:
Fluid $2');

quickplot = @(yVar,d,l) ...
    plot( Table.qNom, Table.(yVar), 'DisplayName', d, 'LineStyle', l);

lineStyles = {'-', '--', ':'};
for i = 1:numel(yVarArr)
    quickplot(yVarArr{i}, legendEntries{i}, lineStyles{i});
end

end

```

General Sub-functions

Fluid flow and properties

```

function [A_m2] = diam2area(D_meter)
    % Calculates area of a circle given diameter
    A_m2 = pi.*D_meter.^2./4;
endfunction [Re] = flow2Re(Q_mcube, D_meter, rho_kgpm3, mu_pas)
    % Converts flow rate to Reynolds number
    A = diam2area(D_meter);
    U = flow2vel(Q_mcube, A);
    Re = rho_kgpm3.*U.*D_meter./mu_pas;
end
function [U] = flow2vel(Q_mcube, A_m2)
    % Convert flow rate and circular area to velocity
    U = Q_mcube./A_m2;
end
function [Q_mcube] = litre2mcube(Q_lpm)
    % Converts Q from L/min to m3/s
    Q_mcube = Q_lpm / 60 / 1000;
end
function rho = fluidrho(F, fluidFlag)
    % Get density value for a fluid
    rho = fluidproplookup(F, 'rho', fluidFlag);
end
function mu = fluidmu(F, fluidFlag)
    % Get viscosity value for a fluid
    mu = fluidproplookup(F, 'mu', fluidFlag);
end
function name = fluidname(F, fluidFlag)
    % Get name of a fluid
    name = F.fluidName{F.fluidFlag==fluidFlag};
end

```

Data manipulation

```
function Slice = slicetablerows(T, varargin)
% Gets a slice of rows of a certain table based on using ismember() function
% Essentially short-hand for T( ismember(T.var1, [a b]) & ismember(T.var2, [c d]), :)
% etc.
% USE EXAMPLES:
%   slicetablerows(Xmaster, 'age', 'age4')
%   slicetablerows(Xmaster, 'age', 'age4', 'fluid', [1 2])

p = inputParser;

assert(istable(T), 'first argument must be a table');
varNames = T.Properties.VariableNames;

for i = 1:numel(varNames)
    v = varNames{i};
    defaultVal = []; % default slice removes nothing (empty)
    addParameter(p, v, defaultVal); % all table headers are added as parameters
end

parse(p, varargin{:});

paramsWithInputs = p.Parameters(~ismember(p.Parameters, p.UsingDefaults));

if isempty(paramsWithInputs) % no requested slices
    Slice = T; return;
end

for i = 1:numel(paramsWithInputs) % loop through only parameters that received inputs
    v = paramsWithInputs{i}; % varName
    m = p.Results(v); % input given (members wanted for slice under varName)

    if ischar(m)
        isMemberArr(:,i) = ismember(T.(v), m); % boolean column from ismember (strings)
    else
        isMemberArr(:,i) = ismembertol(T.(v), m); % boolean column from ismembertol
    end
end

keepRows = all(isMemberArr, 2); % combine all boolean columns into one
Slice = T( keepRows, :); % slice table rows

end

function TableWithNewVar = operatetablecols(Table, var1, var2, operation, varargin)
% Calculate an operation (*/+/-) with two table variables and append it to the table
% e.g. calctablevarsratio(T, 'length', 'diam', '+'); makes 'sumlengthanddiam' column
% calctablevarsratio(T, 'length', 'diam', '/', 'myratio'); makes 'myratio'
column
% varargin is optional varname for the ratio being defined

% validate table input
assert(istable(Table), 'first argument must be a table');
tableVarNames = varnames(Table);
```

```

% validate varname inputs
assert(ismember(var1, tableVarNames), 'var1 must match a header in table');
assert(ismember(var2, tableVarNames), 'var2 must match a header in table');
assert(ismember(operation, {'+', '-', '/', '*', 'mean'}), 'operation must be +, -, /, *
or mean');

% validate varargin inputs (optional varname for the ratio)
if isempty(varargin)
    % no varname specified
    switch operation
        % set default variable name
        case '+', defaultVarName = [var1 'PLUS' var2];
        case '-', defaultVarName = [var1 'MINUS' var2];
        case '*', defaultVarName = [var1 'MULTBY' var2];
        case '/', defaultVarName = [var1 'DIVBY' var2];
        case 'mean', defaultVarName = ['MEAN'];
    end
    newVarName = defaultVarName;
else
    assert(numel(varargin)==1, 'only one optional input (new varname) is allowed');
    assert(ischar(varargin{1}), 'optional argument must be a string for new ratio
value');
    newVarName = varargin{1};
end

% get column data and validate
data1 = Table.(var1);
data2 = Table.(var2);
assert(isnumeric(data1) & isnumeric(data2), 'both columns must contain numeric data');

% calculate operation between the columns
switch operation
    case '+', newData = data1 + data2;
    case '-', newData = data1 - data2;
    case '*', newData = data1 .* data2;
    case '/', newData = data1 ./ data2;
    case 'mean', newData = mean([data1, data2],2);
end

% add ratio column to table
Table.(newVarName) = newData;

% output assignment
TableWithNewVar = Table;

end

function Slice = slicetablecols(Table, varargin)
% Keeps only requested columns of a table based on variable header names
% Essentially short-hand for Table(:, {'var1', 'var2', 'var5', ...})
% USE EXAMPLES:
% slicetablecols(Table, 'age', 'fluid', 'qNom')
% slicetablecols(Table, 'age', 'fluid')

% extract input data
keepVars = varargin;
tableVarNames = varnames(Table);

```

```

% validate input
assert(istable(Table), 'first argument must be a table');
assert(iscellstr(keepVars), 'optional inputs must be strings');
assert(all(ismember(keepVars, tableVarNames)), 'optional inputs must be headers in
table');

if ~isempty(keepVars)
    Slice = Table(:, keepVars);
else
    Slice = Table;
end
end

function TableNewNames = renametablevars(Table, varargin)
% Rename variable names in table with value-pair inputs
% Example: renametablevars(T, 'fluidFlag', 'fluid', 'QNom', 'qNom',...);

p = inputParser;

assert(istable(Table), 'first argument must be a table');
varNames = varnames(Table);

for i = 1:numel(varNames)
    v = varNames{i};
    defaultVal = v; % default changed name is the original name (no change)
    addParameter(p, v, defaultVal, @ischar); % all table headers are added as parameters
end

parse(p, varargin{:});

paramsWithInputs = p.Parameters(~ismember(p.Parameters, p.UsingDefaults));

if isempty(paramsWithInputs) % no requested slices
    TableNewNames = Table; return;
end

for i = 1:numel(paramsWithInputs) % loop through only parameters that received inputs
    v = paramsWithInputs{i}; % varName
    newV = p.Results.(v); % input given (members wanted for slice under varName)
    Table.Properties.VariableNames(v) = {newV};
end

TableNewNames = Table;

end

% (This function is very similar to slicetablerows in implementation)

```

Data plotting

MAIN PLOTTING FUNCTION SET

```

function fig = makefullfig(Table, varargin)%PlotParams, DICTS)
% Function for making subplots for any figure in Chapter 3

% Input parsing

```

```

parsedInputs = parse_plot_inputs(Table, varargin);

% Regexp dictionaries
DICTS.LEGEND = build_legend_regexp_prep_dict();
DICTS.LABELS = build_label_regexp_prep_dict();

% Create figure
fig = figure;

% Break up table into panel-specific tables
InputTable = parsedInputs.Results.Table;
panelRows = parsedInputs.Results.panelRows;
panelCols = parsedInputs.Results.panelCols;
SubPlotCell = organize_tablecell(InputTable, 'panelRows', panelRows, 'panelCols',
panelCols);

% Plot everything by panels
subplot_tablecell_internal(SubPlotCell, parsedInputs);

% Set legend locations for all panels
set_for_entire_fig('legend', 'location', parsedInputs.Results.legendLoc);

% Set axes limits
if ~isempty(parsedInputs.Results.XLim)
    set_for_entire_fig('axes', 'XLim', parsedInputs.Results.XLim);
end

yLimInput = parsedInputs.Results.YLim;
numYaxes = numel(parsedInputs.Results.headersXY) - 1;
if ~isempty(yLimInput)
    if isnumeric(yLimInput)
        set_for_entire_fig('axes', 'YLim', yLimInput); % user gives input as [0 30] for ex.

    elseif strcmpi(yLimInput, 'MatchAll') % make all subplot y axes match each other
        if numYaxes==1 % one y-axis
            set_all_subplot_ylim_to_match(fig, 1)
        elseif numYaxes==2 % two y-axes
            set_all_subplot_ylim_to_match(fig, [1 2])
        end

    end
end

% Add reference line if requested
refLineValues = parsedInputs.Results.refLine;
if ~isempty(refLineValues)
    ax = findall(gcf, 'type', 'axes');
    for i=1:numel(ax)
        set(refline(ax(i), refLineValues(1), refLineValues(2)), 'Color', 'k', 'LineWidth', 1.2)
    end
end

inputPosition = parsedInputs.Results.Position;
if ~isempty(inputPosition)
    set(gcf, 'Position', inputPosition);
end

labelsXY = parsedInputs.Results.labelsXY;

```

```

% Default regexp of label text
if ~isempty(labelsXY)
    set_all_xlabel(labelsXY{1});
    set_all_ylabel(labelsXY{2});
else
    regexp_figure_strings(gcf, 'text', DICTS); % set defaults listed in dictionary
end

% Default regexp of all legend entries and title
regexp_figure_strings(gcf, 'legend', DICTS);

% Default font sizes (if the figure defaults aren't handling it)
set(findall(gcf, 'type', 'legend'), 'fontSize', parsedInputs.Results.legendFontSize);
set(findall(gcf, 'type', 'text'), 'fontSize', parsedInputs.Results.labelFontSize)

end
function parsedInputs = parse_plot_inputs(Table, vararginList)
% Parse function inputs and assign default values

inputIsAlreadyParsed = numel(vararginList)==1 && isa(vararginList{1}, 'inputParser');

if inputIsAlreadyParsed
    parsedInputs = vararginList{1}; % if input is already inputParser results
else
    p = inputParser;
    addRequired(p, 'Table');
    addParameter(p, 'groupingVars', {});
    addParameter(p, 'headersXY', {});
    addParameter(p, 'errVar', {});
    addParameter(p, 'plotType', 'line');
    addParameter(p, 'stylePref', 'lines');
    addParameter(p, 'panelRows', []);
    addParameter(p, 'panelCols', []);
    addParameter(p, 'legendLoc', 'northwest');
    addParameter(p, 'XLim', [], @(x) isnumeric(x) & numel(x)==2);
    addParameter(p, 'YLim', [], @(x) (isnumeric(x) & numel(x)==2) |
strcmpr(x, 'MatchAll'));
    addParameter(p, 'refLine', [], @(x) isnumeric(x) & numel(x)==2);
    addParameter(p, 'Position', [], @(x) isnumeric(x) & numel(x)==4);
    addParameter(p, 'labelsXY', [], @(x) iscellstr(x) & numel(x)==2);
    addParameter(p, 'labelFontSize', 13, @(x) isnumeric(x));
    addParameter(p, 'legendFontSize', 11, @(x) isnumeric(x));
    parse(p, Table, vararginList{:});
    parsedInputs = p;
end

end
function TableCell = organize_tablecell(X, varargin)
% Organize data for each subplot panel into a table, packed into a cell

p = inputParser;
addParameter(p, 'panelRows', []);
addParameter(p, 'panelCols', []);
parse(p, varargin{:})

panelRows = p.Results.panelRows;
panelCols = p.Results.panelCols;

```

```

horizList = assign_list_values(X, panelCols);
vertList  = assign_list_values(X, panelRows);

for i = 1:numel(vertList)
    for j = 1:numel(horizList)

        vertVal = vertList(i);
        horizVal = horizList(j);

        if ~isempty(panelRows) && isempty(panelCols)
            TableCell{i,1} = X(ismember(X.(panelRows), vertVal),:);

        elseif isempty(panelRows) && ~isempty(panelCols)
            TableCell{1,j} = X(ismember(X.(panelCols), horizVal),:);

        elseif ~isempty(panelCols) && ~isempty(panelRows)
            TableCell{i,j} = X(...
                ismember(X.(panelCols), horizVal) & ...
                ismember(X.(panelRows), vertVal) ,:);

        elseif isempty(panelCols) && isempty(panelRows)
            TableCell{1,1} = X;

        end

    end

end

end

function someList = assign_list_values(X, someVars)
    % assign list values in table cell

    if ~isempty(someVars)
        someList = unique(X.(someVars));
    else
        someList = 1;
    end

end

function subplot_tablecell_internal(TableCell, varargin)
    % make subplots based on table locations in tablecell

    % Input parsing
    parsedInputs = parse_plot_inputs(TableCell, varargin);

    headersXY    = parsedInputs.Results.headersXY;
    groupingVars = parsedInputs.Results.groupingVars;
    errVar       = parsedInputs.Results.errVar;
    plotType     = parsedInputs.Results.plotType;
    stylePref    = parsedInputs.Results.stylePref;

    NI = size(TableCell,1);
    NJ = size(TableCell,2);

    for i = 1:NI
        for j = 1:NJ

```

```

        p = NJ*(i-1) + j; % numbers 1 2 3; 4 5 6; ...
        subplot(NI,NJ,p); hold on;
        title(titleletter(p))
        plot_series_collection(TableCell{i,j}, headersXY, groupingVars, errVar, plotType,
stylePref)

    end
end
end
function plot_series_collection(DataTable, headersXY, groupingVars, errVar, plotType,
stylePref)
% Plot total pressure drop across single path vs. starting laminar model generation
% Before laminar start gen - modified-Blasius model is used
% From laminar start gen to end (gen 23) - laminar Pedley model is used

plotType = cellstr(plotType);

switch numel(headersXY)
    case 2, numAxesY = 1;
    case 3, numAxesY = 2;
    otherwise, error('headersXY can only have 2 or 3 elements');
end

allHeaders = DataTable.Properties.VariableNames;
assert( all(ismember(groupingVars, allHeaders)), 'groupname header does not exist');

% Find which grouping vars are constant and which are variable
constantGroupingVars = find_constant_grouping_vars(DataTable, groupingVars);
if isempty(constantGroupingVars)
    variableGroupingVars = groupingVars;
else
    variableGroupingVars = groupingVars(~ismember(groupingVars, constantGroupingVars));
    constantGroupingVarsPaired = pair_constant_grouping_vars_with_values(DataTable,
constantGroupingVars);
end

% DataTable(:, variableGroupingVars)

[uVariableVars, ~, idx] = unique(DataTable(:, variableGroupingVars), 'rows'); %
groupingVars here could be variableGroupingVars if needed

uVariableVarGroups = column_groups(uVariableVars);

stylePref = cellstr(stylePref);

for i = 1:numel(stylePref)
    LineAttributesByGroup{i} = create_styles_table_by_group(uVariableVarGroups,
stylePref{i});
end

for i = 1:max(idx) % Loop over each unique row index and slice out the specified rows.

    Slice = DataTable( idx == i, : );

    for yax = 1:numAxesY
        x = Slice.(headersXY{1});

```

```

y = Slice.(headersXY{yax+1});
thisPlotType = plotType{yax};

PlotOptions = make_styles_struct(LineAttributesByGroup{yax}(i,:), thisPlotType);

if numAxesY==2
    switch yax
        case 1, yyaxis left;
        case 2, yyaxis right;
    end
end

switch thisPlotType
    case {'plot', 'line'}
        p = plot(x,y);
    case 'bar'
        p = bar(x,y);
    case 'errorbar'
        err = Slice.(errVar);
        p = errorbar(x,y,err);
end
hold on;
p = format_plot_styles(p, PlotOptions.Styles);
% p = plot_single_series(x, y, PlotOptions); hold on;

if isempty(variableGroupingVars)
    seriesName = strjoin(constantGroupingVarsPaired, ', ');
else
    for j = 1:numel(variableGroupingVars)
        headerVals(j) = string(Slice{1, variableGroupingVars{j}});
    end
    seriesName = char(strjoin(strcat(variableGroupingVars, {' = '}), headerVals), ',
');
end

p.DisplayName = seriesName;

end
end

if numAxesY==1
xlabel(headersXY{1});
ylabel(headersXY{2});
elseif numAxesY==2
    yyaxis left;
    xlabel(headersXY{1});
    ylabel(headersXY{2});
    yyaxis right;
    ylabel(headersXY{3});
end

if isempty(variableGroupingVars) || isempty(constantGroupingVars)
    legTitle = '';
else
    legTitle = strjoin(constantGroupingVarsPaired, ', ');
end

% xlabel(X_LABEL);

```

```

% ylabel(Y_LABEL);
title(legend('show'), legTitle);

end
function PlotOptions = make_styles_struct(LineAttributesByGroupThisRow, plotType)
% create a struct of styles for each plots series

PlotOptions.plotType = plotType;

switch plotType
case 'bar'
    PlotOptions.Styles.FaceColor = 'w';
otherwise % for lines or points
    if isempty(LineAttributesByGroupThisRow) % no unique groups so one plot only
        PlotOptions = defaultlineplotoptions;
    else
        styleAspect = LineAttributesByGroupThisRow.Properties.VariableNames;
        for j = 1:numel(styleAspect)
            s = styleAspect{j};
            Styles.(s) = LineAttributesByGroupThisRow.(s){:}; % {:}
        end
        PlotOptions.Styles = Styles;
    end
end
PlotOptions.plotType = plotType;
end

end
function constantGroupingVarsPaired = pair_constant_grouping_vars_with_values(DataTable,
constantGroupingVars)
% find which grouping variables are constant across the entire table

for i = 1:numel(constantGroupingVars)

    headerName = constantGroupingVars{i};

    constVal = DataTable.(headerName)(1);

    if iscellstr(constVal) || ischar(constVal)
        constantValString = char(constVal);
    elseif isnumeric(constVal)
        constantValString = num2str(constVal);
    else
        error('uncertain value type for headerName');
    end

    constantGroupingVarsPaired{i} = [headerName ' = ' constantValString];

end

end
function GroupsTable = column_groups(DataTable)
% get the groups of the table based on the grouping columns

varNameList = DataTable.Properties.VariableNames;
groupNameList = strcat(varNameList, '_groups');

GroupsTable = cell2table(cell(size(DataTable)), 'VariableNames', groupNameList);

```

```

for i = 1:numel(varNameList)

    varName    = varNameList{i};
    groupName  = groupNameList{i};

    GroupsTable.(groupName) = findgroups(DataTable.(varName));

end

end
function GroupsLinestyles = create_styles_table_by_group(uVariableGroupsTable, stylePref)
% Assign specific line styles to each series

StyleOrder.LineStyle = repmat({'-', ':', '--', '-.'}, 1, 10)';
StyleOrder.Marker     = repmat({'o', 'x', '^', 's', '*', '+', 'd', '>', '<' }, 1, 10)';
StyleOrder.Color      = repmat({'k', 'b', 'r', 'y', 'g', 'c', 'm'}, 1, 10)';

switch stylePref
case {'LineStyle', 'lines'}
    lineStyleOrder = {'LineStyle', 'Marker', 'Color'};
case {'Marker', 'points'}
    lineStyleOrder = {'Marker', 'LineStyle', 'Color'};
case {'Color', 'color'}
    lineStyleOrder = {'Color', 'LineStyle', 'Marker'};
otherwise
    lineStyleOrder = {'LineStyle', 'Marker', 'Color'};
end

groupNameList = uVariableGroupsTable.Properties.VariableNames;

numVars = width(uVariableGroupsTable);
lineStyleList = lineStyleOrder(1:numVars);

GroupsLinestyles = cell2table(cell(size(uVariableGroupsTable)), 'VariableNames',
lineStyleList);

for i = 1:numel(lineStyleList)

    s = StyleOrder.(lineStyleList{i});
    GroupsLinestyles.(lineStyleList{i}) = s(uVariableGroupsTable.(groupNameList{i}));

end

end

function constantGroupingVars = find_constant_grouping_vars(DataTable, groupingVars)
% which grouping vars in table have only one (constant) value in the table

constantGroupingVars = [];
counter = 1;

groupingVars = cellstr(groupingVars);
for i = 1:numel(groupingVars)
    groupingVarName = groupingVars{i};
    columnVals      = DataTable.(groupingVarName);

```

```

columnGroups    = findgroups(columnVals);

if range(columnGroups)==0    % i.e. all elements in column are the same
    constantGroupingVars{counter} = groupingVarName;
    counter = counter + 1;
end

end

end

function hPlot = format_plot_styles(hPlot, Styles)
% format the plot based on the line styles assigned

styleNameList = fieldnames(Styles);
for i = 1:numel(styleNameList)
    styleName = styleNameList{i};
    styleVal  = Styles.(styleName);
    set(hPlot, styleName, styleVal);
end

end

function PlotOptions = defaultlineplotoptions()
% Create default line styles (hard-coded values)

PlotOptions.plotType = 'line';
PlotOptions.Styles.LineStyle = '-';
PlotOptions.Styles.LineWidth = 1.2;
PlotOptions.Styles.Marker    = 'o';
PlotOptions.Styles.MarkerSize = 5;
PlotOptions.Styles.MarkerFaceColor = 'k';

end

function dictLeg = build_legend_regexprep_dict()
% dictionary of replacement values for axes legends

dictLeg = containers.Map;

dictLeg('age = age4') = 'Age 4';
dictLeg('age = age8') = 'Age 8';
dictLeg('age = adult') = 'Adult';
dictLeg('fluid = 1')   = 'Air';
dictLeg('fluid = 2')   = regexprep('escape', 'He-\mathrm{O}_2$ (80/20)');
dictLeg('fluid = 3')   = regexprep('escape', '$\mathrm{N}_2$-\mathrm{O}_2$
(50/50)');
dictLeg('qNom = (\d+)') = '$1 L/min';
dictLeg('genModelSwitch = 0') = '$G_T = 0$';
dictLeg('genModelSwitch = 22') = '$G_T = \infty$'; % 22 is last gen. for age 4
dictLeg('genModelSwitch = 23') = '$G_T = \infty$'; % 23 is last gen. for age 8
dictLeg('genModelSwitch = ([1-9]|1[0-9]|2[0-1])$') = '$G_T = $1$';
end

function dictLab = build_label_regexprep_dict()
% dictionary for replacement values of axes labels

dictLab = containers.Map;

dictLab('genNum')      = 'Generation';
dictLab('length')     = 'Length (m)';
dictLab('diam')       = 'Diameter (m)';

```

```

dictLab('age')           = 'Age';
dictLab('fluid')        = 'Fluid';
dictLab('qNom')         = 'Nominal flow rate (L/min)';
dictLab('qMcube')       = 'Flow rate (m^3/s)';
dictLab('Re')           = 'Reynolds number';
dictLab('entryLengthLaminar') = 'Laminar entry length (m)';
dictLab('ratioLtoLe')   = '$L/L_e$ ratio';
dictLab('pDropModBlas') = 'Generational Pressure drop, Modified-Blasius model (Pa)';
dictLab('pDropPedley')  = 'Generational Pressure drop, Pedley model (Pa)';
dictLab('genModelSwitch') = 'Model transition generation, $G_T$';
dictLab('genLtoLeRatioCrossover') = 'First airway generation when $L > L_e$';
dictLab('pDrop0to23')   = 'Total path pressure drop (Pa)';
dictLab('genNumMaxPdrop') = 'Generation of max. total pressure drop';
dictLab('mean_PDdropNT') = 'Average experimental $\Delta P_{NT}$ (Pa)';
dictLab('pDropMixedModelSwitchGen([1-9]|1[0-9]|2[0-3])$') ...
    = 'Generational $\Delta P$ (Pa)';
dictLab('pDropMixedModelCumulatSwitchGen([1-9]|1[0-9]|2[0-3])$') ...
    = 'Cumulative $\Delta P$ (Pa)';
dictLab('pctDiffGenSwitch') ...
    = regexptranslate('escape', ['$\Delta P_{total}$ Difference (%)']);
end
function set_all_xlabels(xLabelString)
    % set all xlabels to a value
    ax = findall(gcf,'type','axes');

    for i = 1:numel(ax)
        ax(i).XLabel.String = xLabelString;
    end
end
function set_all_ylabels(yLabelString)
    % set all ylabels to a value
    ax = findall(gcf,'type','axes');

    for i = 1:numel(ax)
        ax(i).YLabel.String = yLabelString;
    end
end
function set_for_entire_fig(internalObjectName, attributeName, value, varargin)
    % Set any attribute of object on a figure universally

    if isempty(varargin)
        fig = gcf;
    elseif isobject(varargin)
        fig = varargin;
    else
        error('invalid varargin object');
    end

    objArr = findall(fig, 'type', internalObjectName);
    arrayfun(@(x) set(x, attributeName, value), objArr);
end
function regexprep_figure_strings(fig, findType, DICTS)

    % Replace all raw legend names with formatted descriptions
    % such as 'fluid = 1' replaces to 'Air'

    assert(ismember(get(fig,'type'),{'figure'}), 'must be a figure object');

```

```

assert(ismember(findType, {'legend', 'text'}), 'must be either legend or text')

arr = findall(fig, 'type', findType);

switch findType
    case 'legend'
        DICT_OBJ = DICTS.LEGEND;
        keyRegexAppend = ''; % no end of line $ - can have lists ('Age 4, 20 L/min,...')

        case 'text'
            DICT_OBJ = DICTS.LABELS;
            keyRegexAppend = '$'; % add end of line $ - must match entire label only
        end
    end

% for each legend object: check the regular exp. dictionary to replace legend names
for i = 1:numel(arr)
    for v = keys(DICT_OBJ)
        key = v{:};

        arr(i).String = regexprep(arr(i).String, [key, keyRegexAppend], DICT_OBJ(key));

        % if the legend has a title
        if strcmp(findType, 'legend') && ~isempty(arr(i).Title.String)
            arr(i).Title.String = regexprep(arr(i).Title.String, key, DICT_OBJ(key));
        end
    end
end
end
end
function titleLabel = titleletter(i)
% Get 'letter label' for any subplot.
% example: input 5 gives '(e)'

    letters = ('a':'z');
    titleLabel = ['(' letters(i) ')'];
end
function set_all_subplot_ylim_to_match(fig, yAxisInd)
% After a figure of subplots is created, this function sets all the y-axes of
% each subplot to the same value (maximum of the others) and sets the minimum to zero
% fig = figure handle
% yAxisInd = number of y axes (1 or 2)

assert(all(ismember(yAxisInd,[1 2])), 'ok axis vals: 1 2'); % 1 and/or 2 only
yAxisInd = reshape(yAxisInd, [1 length(yAxisInd)]); % force horizontal

ax = findall(fig, 'type', 'axes');

maxLimits = arrayfun(@(yAx) ...
    find_largest_ylim_of_subplots_for_an_axis(ax, yAx), yAxisInd);

arrayfun(@(yAx, maxLim) ...
    apply_largest_ylim_to_all_subplots_of_one_axis(ax, yAx, maxLim), yAxisInd, maxLimits);

end

function maxLimit = find_largest_ylim_of_subplots_for_an_axis(ax, yAxisNum)
% find max of all subplots' current y-limits

    limitCell = arrayfun(@(x) x.YAxis(yAxisNum).Limits, ax, 'uni', 0);

```

```

    limitArr = cell2mat(limitCell);
    maxLimit = max(limitArr(:));

end

function apply_largest_ylim_to_all_subplots_of_one_axis(ax, yAxisNum, maxLimit)
% Assign same y-limit to all subplots

    for i = 1:length(ax)
        ax(i).YAxis(yAxisNum).Limits = [0 maxLimit];
    end

end

% SET DEFAULTS FOR ALL FIGURES
function set_figures_defaults()
% Pre-set all defaults for figures made for manuscript

    set_default('Figure', 'Color', 'w');
    set_default('Figure', 'Units', 'normalized');
    set_default('Figure', 'Position', [0 0 0.40 0.92]);
    set_default('Axes' , 'ColorOrder', [0 0 0]);
    set_default('Text' , 'Interpreter', 'Latex');
    set_default('Legend', 'Interpreter', 'Latex');
    set_default('Text' , 'FontSize', 20);
    set_default('Legend', 'FontSize', 12);
    set_default('Line' , 'LineWidth', 1.2);
    set_default('Axes' , 'XColor', 'k');
    set_default('Axes' , 'YColor', 'k');
    set_default('Axes' , 'ZColor', 'k');
    set_default('Legend', 'EdgeColor', 'k');

end

```